University of Alberta

# On Forecasting Severe Storms in Alberta Using Environmental Sounding Data

by

**Maxwell L. Dupilka** ©

A thesis submitted to the Faculty of Graduate Studies and Research in partial fulfillment

of the requirements for the degree of

**Doctor of Philosophy**

Department of Earth & Atmospheric Sciences

Edmonton, Alberta

Spring 2006

Library and
Archives Canada

Published Heritage
Branch

395 Wellington Street
Ottawa ON K1A 0N4
Canada

Bibliothèque et
Archives Canada

Direction du
Patrimoine de l'édition

395, rue Wellington
Ottawa ON K1A 0N4
Canada

*Your file Votre référence*
*ISBN: 0-494-13966-8*
*Our file Notre référence*
*ISBN: 0-494-13966-8*

NOTICE:
The author has granted a non-exclusive license allowing Library and Archives Canada to reproduce, publish, archive, preserve, conserve, communicate to the public by telecommunication or on the Internet, loan, distribute and sell theses worldwide, for commercial or non-commercial purposes, in microform, paper, electronic and/or any other formats.

The author retains copyright ownership and moral rights in this thesis. Neither the thesis nor substantial extracts from it may be printed or otherwise reproduced without the author's permission.

AVIS:
L'auteur a accordé une licence non exclusive permettant à la Bibliothèque et Archives Canada de reproduire, publier, archiver, sauvegarder, conserver, transmettre au public par télécommunication ou par l'Internet, prêter, distribuer et vendre des thèses partout dans le monde, à des fins commerciales ou autres, sur support microforme, papier, électronique et/ou autres formats.

L'auteur conserve la propriété du droit d'auteur et des droits moraux qui protège cette thèse. Ni la thèse ni des extraits substantiels de celle-ci ne doivent être imprimés ou autrement reproduits sans son autorisation.

In compliance with the Canadian Privacy Act some supporting forms may have been removed from this thesis.

While these forms may be included in the document page count, their removal does not represent any loss of content from the thesis.

Conformément à la loi canadienne sur la protection de la vie privée, quelques formulaires secondaires ont été enlevés de cette thèse.

Bien que ces formulaires aient inclus dans la pagination, il n'y aura aucun contenu manquant.

Canada

# Dedication

To my dad and mom,
who always encouraged me to pursue a doctoral degree.

## Abstract

Thermodynamic and dynamic parameters computed from observed sounding data are examined to determine whether they can aid in forecasting the potential for severe weather in Alberta. The primary focus is to investigate which sounding parameters can provide probabilistic guidance to distinguish between Significant Tornadoes (F2 to F4), Weak Tornadoes (F0 and F1), and Non-Tornado severe hail storms (≥ 3 cm diameter hail but no reported tornado). The observational data set contains 87 thunderstorm events from 1967 to 2000 within 200 km of Stony Plain, Alberta. Three tornadic thunderstorms with F-scale ratings of F3 and F4 are examined in more detail. A secondary focus is to determine whether sounding data can be used to predict 24 hour snowfall amounts (specifically amounts ≥ 10 cm). Snowfall data covered all of Alberta east of the mountains from October 1990 to April 1993. The major findings were:

a) Significant Tornadoes tended to have stronger environmental bulk wind shear values than Weak Tornadoes or Non-Tornado storms, with a shear magnitude in the 900-500 mb layer exceeding 3 $m\ s^{-1}\ km^{-1}$. Combining the 900-500 mb shear with the 900-800 mb shear increased the probabilistic guidance for the likelihood of Significant Tornado occurrence.

b) Values of storm-relative helicity showed skill in distinguishing Significant Tornadoes from both Weak Tornadoes and Non-Tornadoes. Significant Tornadoes tended to occur with 0-3 km storm-relative helicity >140 $m^2\ s^{-2}$ whereas Weak Tornadoes were typically formed with values between 30 and 150 $m^2\ s^{-2}$.

c) The amount of precipitable water showed statistically significant differences between Significant Tornadoes and the other two groups. Significant Tornadoes had values exceeding 21 mm. Combining precipitable water values with the 900-500 mb shear increased the probabilistic guidance for the potential of Significant Tornadoes.

d) Values of thermal buoyancy, storm convergence, and height of the lifted condensation level provided no skill in discriminating between the three storm categories.

e) The Edmonton tornado case, unlike the Holden and Pine Lake cases, did not feature a prominent synoptic scale moisture front.

f) Observed snowfall amounts showed a roughly linear dependence on the 850 mb temperature, supporting a moisture conservation theory.

# Preface

During the past several decades there has been significant advancement in the knowledge of the physics and prediction of severe storms both in summer and winter. As computing power has steadily increased, numerical weather prediction models have taken great strides toward more accurate forecasts of synoptic scale events such as the spatial and temporal distribution of precipitation. However, operationally accurate predictions of meso-scale events such as thunderstorms are still beyond the capability of numerical weather models. I was a forecaster with the Meteorological Service of Canada for nearly 20 years before re-entering the University of Alberta. As such, I am aware of the shortcomings of numerical models and the critical need of forecasters for additional tools to aid in the prediction of severe weather events. There still does not exist a complete understanding and modeling of the processes involved with tornadogenesis. Numerical models generally under-predict large snowfall amounts. My motivation for this research stems from many frustrating times as a forecaster wishing there were additional knowledge and techniques to better assess the potential for severe storm development, be it tornadoes or snowstorms. The forecasting aids most useful in an operational setting should be fairly easy to apply in an environment that is often hectic and under stringent time deadlines. In many cases the forecaster has only minutes to decide whether a warning for a severe event, such as a tornado, should be issued. Readers do not need knowledge of the workings of a weather office however, those who do have operational forecasting experience will likely have significant appreciation for my motivation for this research.

The reader of this thesis is expected to have learned the basic ideas about weather systems as they are presented in many textbooks of general meteorology. An understanding of the concepts of convective development, such as parcel theory, and the interaction of meso-scale with synoptic scale events is a necessary prerequisite. The emphasis of this thesis is on physical concepts and their applications rather than extensive mathematical derivations. Nevertheless, it is assumed the reader has mastered the fundamentals of classical physics and has a thorough knowledge of elementary differential and integral calculus. Knowledge of mathematical descriptions of atmospheric processes, as expressed by the equations of motion, hydrostatic balance, mass continuity, and elementary thermodynamics, is necessary for a successful understanding of this thesis. Readers are expected to be familiar with the basic concepts of synoptic weather charts, including the display and contouring of data.

## Table of Contents

Chapter I Introduction 1

1. Research topic 1
2. Forecasting techniques for predicting severe weather 3
3. Development of understanding of severe storm formation in Alberta – a historical review 7
4. Review of Alberta tornado parameters 11
5. Predicting heavy snowfall in Alberta 16
6. Statement of originality 17
7. Statement of the research problems 19

References 24

Chapter II Rawinsonde Data and Convective Instability 32

1. Rawinsonde network 32
2. Radiosonde sensors 33
3. Wind profile 37
4. Thermodynamic diagrams 37
5. Convective Available Potential Energy (CAPE) 40

References 44

Chapter III Forecasting Tornadic Thunderstorms in Alberta using Environmental Sounding Data. Part I: Wind Shear and Buoyancy 49

Abstract 49

1. Introduction 51

2. Observations 56

3. Calculation of sounding parameters 59

4. Environmental wind shear 60

    a. Bulk shear 60

    b. Bulk shear ratio 62

    c. Directional shear 65

5. Most Unstable CAPE and Bulk Richardson Number 66

6. Assessing the risk for Significant Tornadoes 67

7. Conclusion and discussion 70

Acknowledgements 72

References 73

Chapter IV Forecasting Tornadic Thunderstorms in Alberta using Environmental Sounding Data. Part II: Helicity, Precipitable Water, and Storm Convergence 87

Abstract 87

1. Introduction 89

2. Storm-Relative Helicity (SRH) 94

3. Humidity parameters 96

4. Storm Convergence and Normalized MUCAPE 99

5. Identifying the likelihood of Severe Tornado events 104

6. Conclusions 106

Acknowledgements 109

References 110

Chapter V An Examination of Three Severe Convective Storms that Produced Significant Tornadoes in Central Alberta 123

Abstract 123

1. Introduction 125

2. Synoptic-scale storm environment 129

3. Sounding analysis 133

4. Dryline analysis 140

5. Storm tracks 145

6. Conclusions and implications for forecasting 146

Acknowledgements 149

Authors 150

References 151

Chapter VI On Predicting Maximum Snowfall Amounts in Alberta 166

Abstract 166

1. Introduction 168

2. Theory of maximum snow accumulation 171

3. Testing of theory with Alberta observations 174

4. Comparison with ECMWF model QPF 179

5. Discussion 183

6. Conclusions 185

Acknowledgements 187

References 188

Chapter VII Conclusions and Discussion 196

1. Summary 196

2. Implications for forecasting 199

3. Recommendations for further research 205

References 208

APPENDIX A Defining a Tornado 209

References 214

APPENDIX B Tornado Classification Scale 216

References 218

APPENDIX C Storm Convergence Method 219

References 225

APPENDIX D A Day in the Life of a Severe Weather Forecaster 226

References 232

# List of Tables

Chapter II

Table 1. Range, accuracy and precision of various rawinsonde measurements..........36

Table 2. Sounding data at Stony Plain Alberta for 0000 UTC 01 August 1987 .........38

Chapter III

Table 1. Percent occurrence of ST, WT, and NT events for 900-800 and 900-500 mb (SHR8*, SHR5*) shear threshold pairs. Shear is in m $s^{-1}$ $km^{-1}$.....................69

Chapter IV

Table 1. Percent occurrence of ST, WT, and NT events for 900-500 mb shear (SHR5*) and Precipitable Water (PW*) threshold pairs. SHR5* is in m s-1 km-1 and PW* is in mm...........................................................................106

Chapter V

Table 1. A comparison between the Edmonton, Holden, and Pine Lake Tornadoes. The parameters are taken from the 0000 UTC proximity soundings and are described in the text...........................................................................130

Chapter VI

Table 1. Values of $a$ and $b$ for the prediction for different values of cloud top pressure $p_1$ (mb) for $p_0 = 850$ mb and $q_{s1} = 0.2$ g $kg^{-1}$............................................174

Table 2. Comparison of statistical skill scores of three methods to forecast 24 hour maximum snowfall amounts ≥ 10 cm. The techniques are: the predicted snowfall (TT) based on the snowfall-temperature relationship Eq. (10), the wet-bulb potential temperature (WBPT) method using Eq. (11), and the 24 hour maximum snowfall accumulation snowfall using the ECMWF model. ..........182

Chapter VII

Table 1. Suggested thresholds associated with severe weather events in Alberta. ...203

APPENDIX B

Table 1. The Fujita Tornado Damage Scale, referred to as the F-Scale, classifies tornadoes based on the resulting damage. ..........217

## List of Figures

Chapter I

Fig. 1 Average annual number of tornadoes per 10.000 km2 in Canada. (Adapted from Newark 1984). ....................30

Fig. 2 Illustrations of crosswise (top) and streamwise (bottom) vorticity. The circular rings indicate the direction of rotation. The storm updraft is indicated by the vertical arrow. The environmental vertical wind profile is indicated by the arrows in the top left corner of each image. Crosswise vorticity is perpendicular to the unidirectional environmental flow. Directional change of wind with height results in parallel components of vorticity and environmental flow. (Adapted from Doswell 2000). ....................31

Chapter II

Fig. 1. Schematic of a sonde with balloon, parachute, and train. (From Wright 1997)..46

Fig. 2. Map of western Canada and northwest U.S. showing the upper air reporting stations: Fort Nelson (YYE), Prince George (YXS), Vernon (WVK), Port Hardy (YZT), Fort Smith (YSM), Stony Plain (WSE), Quillayute (UIL), Spokane (GEG), Salem (SLE), Medford (MFR), Boise (BOI), Great Falls (GTF), and Glasgow (GGW). ....................47

Fig. 3. Skew T-log p diagram for the WSE 01 August 1987 0000 UTC sounding. The plot on the right is the temperature (°C) and the plot on the left is the dewpoint (°C). The curved line on the far right is the best level parcel ascent curve. The shaded area indicates the CAPE. Winds are plotted along the right side in m $s^{-1}$. Half barbs denote 5 m $s^{-1}$ and full barbs denote 10 m $s^{-1}$. ....................................48

Chapter III

Fig. 1. Outline of Alberta showing the locations of the upper air station at Stony Plain (WSE) and the cities of Edmonton and Calgary. The circle marks the 200 km radius from WSE. ....................................78

Fig. 2. Frequency of tornadoes in F-scale categories. The bars show the frequency for the study cases in central Alberta during the period from 1967 – 2000. The total number of cases is 74. The value above each bar indicates the number of study cases in that F group. The dots and line shows the frequency of events in Canada during the period from 1950 to 1998. ....................................79

Fig. 3. Box and whiskers plots of bulk shear (SHR) values for Non-Tornado (NT) and tornado (WT, ST) cases in the layers 900-800, 900-700, 900-600, and 900-500 mb. Gray boxes denote 25th to 75th percentiles, with a heavy solid horizontal bar at the median value. The vertical lines (whiskers) extend to the maximum and minimum values ....................................80

Fig. 4. Box and whisker plots of $\beta$ = SHR8/SHR5 for Non-Tornado (NT) and tornado (WT, ST) cases. ....................................81

Fig. 5. Frequency of occurrence of $\beta$ for the combined set of cases in the study (NT, WT, and ST). ....................................82

Fig. 6. Box and whiskers plots of INIS values for Non-Tornado (NT) and tornado (WT, ST) cases in the layers 900-800, 900-700, 900-600, and 900-500 mb. ....83

Fig. 7. Box and whiskers plots of MUCAPE for Non-Tornado (NT) and tornado (WT, ST) cases........................................................................................................84

Fig. 8. Box and whiskers plots of Bulk Richardson Number (BRN) for Non-Tornado (NT) and tornado (WT, ST) cases. .................................................................85

Fig. 9. Scatter plot of SHR8 versus SHR5 for the 87 Alberta storms categorized into NT (diamonds), WT (squares) and ST (dots) cases. The solid (dashed) line marks the 77% (100%) threshold for ST events................................................86

Chapter IV

Fig. 1. Box and whiskers plots of SRH estimated via the Bunkers et al. (2000) storm motion algorithm for NT, and WT and ST tornado cases. a) shows SRH in the 0-1 km AGL layer; b) shows SRH in the 0-3 km AGL layer. Gray boxes denote 25th to 75th percentiles, with a heavy solid horizontal bar at the median value. The vertical lines (whiskers) extend to the maximum and minimum values....114

Fig. 2. Scatter plot of 0-3 km SRH versus SHR5 for the 87 Alberta storms categorized into NT (diamonds), WT (squares) and ST (dots) cases. .................................115

Fig. 3. Box and whiskers plot of the Most Unstable Lifting Condensation Level (MULCL) for Non-Tornado (NT) and tornado (WT, ST) cases. ......................116

Fig. 4. Box and whiskers plot of Precipitable Water (PW) for Non-Tornado (NT) and tornado (WT, ST) cases. ........................................................................117

Fig. 5. Scatter plot of Precipitable Water (PW) versus Tropospheric Humidity (TH) for the 87 Alberta storms categorized into NT (diamonds), WT (squares) and ST (dots) cases. ....118

Fig. 6. Box and whiskers plot of Tropospheric Humidity (TH) ratio for Non-Tornado (NT) and tornado (WT, ST) cases. ....119

Fig. 7. Box and whiskers plots of average Storm Convergence (C) for Non-Tornado (NT) and tornado (WT, ST) cases: a) C50 in the layer LFC to 50 mb above the LFC; b) C100 in the layer LFC to 100 mb above the LFC. ....120

Fig. 8. Box and whiskers plot of Normalized Most Unstable CAPE (NMUCAPE) for Non-Tornado (NT) and tornado (WT, ST) cases. ....121

Fig. 9. Scatter plot of PW versus SHR5 for the 87 Alberta storms categorized into NT (diamonds), WT (squares) and ST (dots) cases. The solid (dashed) line marks the 77% (100%) threshold for ST events. ....122

Chapter V

Fig. 1. Location of surface weather observing stations (dots) within the province of Alberta. The squares show the sites of the Edmonton, Holden, and Pine Lake storms. The circles show the cities of Red Deer (YQF) and Calgary (YYC). The location Stony Plain (WSE) upper air station is marked by the star. ....156

Fig. 2. 500 mb and 850 mb height contour maps at 0000 UTC for the Edmonton tornado (top panel), Holden tornado (middle panel) and Pine Lake tornado (bottom). Geo-potential heights (solid) are contoured every 60 m, isotherms (dashed) are contoured every 5°C. ....157

Fig. 3. Vertical profile of the 12-h temperature change (ΔT ) from 1200 UTC to 0000 UTC for the three tornado cases. ......158

Fig. 4. Adjusted Skew T-log p diagrams for the Edmonton tornado (top panel), the Holden tornado (middle panel), and the Pine Lake tornado (bottom panel) for a), c), and e) 1200 UTC (morning of the events); b), d), and f) 0000 UTC (evening of the events). Wind vectors (in m s-1) are shown at selected pressure levels at the right of each sounding. ......159

Fig. 5 Vertical soundings at 0000 UTC of a) wet-bulb potential temperature (θw in °C), b) vapor mixing ratio (q in g kg-1) for the Edmonton, Holden, and Pine Lake storms. ......160

Fig. 6. Contour analysis of surface dewpoint temperatures for the Pine Lake storm from 1300 UTC 14 July 2000 to 0200 UTC 15 July 2000. Contours are drawn every 2 °C, with shading for Td > 12 °C. Dots show dewpoint observations, the star shows the Pine Lake storm site, and the cross marks the storm. ......162

Fig. 7. Hourly evolution of the surface dewpoint field for the Edmonton storm from 18 UTC to 23 UTC 31 July 1987. Contours are drawn every 2 °C, with shading for Td > 12 °C. The star marks the city of Edmonton. ......163

Fig. 8. Evolution of surface dewpoint temperatures (in °C) recorded at Edmonton (solid), Red Deer (short dashed), and Calgary (long dashed) airports for the a) Edmonton, b) Holden, and c) Pine Lake storm events. The shaded zones indicate the approximate duration of each tornado. ......164

Fig. 9. Thunderstorm tracks plotted every hour for the Edmonton storm (1900 UTC 31 July 1987 to 0000 UTC 01 August 1987), the Holden storm (0100 UTC 30 July

1993 to 0400 UTC 30 July 1993), and the Pine Lake storm (2000 UTC 14 July 3000 to 0200 UTC 15 July 2000). The three circles mark the locations of the tornado sites (see Fig. 1)........165

Chapter VI

Fig. 1. Outline of Alberta with the locations of the snowfall reporting sites used in this study. ........191

Fig. 2. Snowfall observations compared with 850 mb temperature values from upwind site. a) Measurements of maximum 24 hour snowfall S plotted versus temperature T0 at 850 mb. The triangles denote the observations and the dashed line shows the optimal regression line. The solid line shows the theoretical prediction based on Eq. (10); b) Average and maximum S values plotted against T0 at 850 mb; c) Percentage frequency of cases when S ≥ 10 cm plotted against T0 at 850 mb........192

Fig. 3. Skew-T sounding observed at Stony Plain (50 km west of Edmonton, Alberta) at 1200 UTC, November 25, 1990, depicting temperature and dewpoint profiles. Horizontal lines are isobars (mb), straight lines skewed to the right are isotherms (oC), thin curved lines skewed to the left are dry adiabats (oC), thicker curved lines are moist adiabats (oC), and dashed lines are mixing ratio (g kg-1). ........193

Fig. 4. Snowfall observations compared with 700 wet-bulb potential temperature values from upwind site. a) S plotted versus 700 mb wet-bulb potential temperature (WBPT) at 700 mb in oC. The triangles denote the observations and the solid line shows the optimal regression line Eq. (11); b) Average and maximum S plotted against WBPT at 700 mb; c) Percentage frequency of cases when S ≥ 10 cm plotted against WBPT at 700 mb..........194

Fig. 5. Comparison of forecasting techniques for Alberta snowfall. a) Predicted snowfall amounts (TT) based on snowfall-temperature relationship Eq. (10) plotted against observed maximum 24 hour snowfall (S); b) Predicted 24 hour snowfall amount from the ECMWF model plotted against observed maximum 24 hour snowfall (S). ..........195

APPENDIX D

Fig. 1. Miller diagram at 0000 UTC 30 July 1993 showing the jet cores at 500mb, 700mb,and 850mb (arrows), the 500mb trough (double dashed line), the 700mb thermal axis (dotted line), the surface dryline (open semi-circle front), and 500 mb ridge axes (wavy lines). The shaded area denotes a greater potential for severe convective development. ..........233

Fig. 2. 1.5 km CAPPI image from the Stony Plain (WSE) radar at 2030 UTC 29 July 1993 (the afternoon of the Holden tornado event) The range rings are spaced every 40 km. The colors represent either rainfall rates (mm/hr) or reflectivity (dBZ). The arrow points to the Holden site. The storm which may develop into the tornadic storm is circled. ..........234

Fig. 3. 1.5 km CAPPI image from the Stony Plain (WSE) radar at 0230 UTC 30 July 1993 (about 2 hours before the Holden tornado event). ..........235

# Chapter I

# Introduction

## 1. Research topic

Forecasting the weather remains challenging, particularly predicting severe weather events which cause significant property damage, fatalities or otherwise dramatically impact the lives of people. Providing timely warnings of severe weather events throughout the year is a mandate for public weather offices such as the Meteorological Service of Canada (MSC). In the summer months, in Alberta, high impact weather most often occurs in the form of thunderstorms causing large hail, strong winds and occasionally tornadoes. During the fall, winter and spring Alberta's severe weather often takes the form of heavy snowfalls (> 10 cm in 24 hours). As the population of Alberta continues to increase and expand into presently rural areas, the need for timely weather warnings for severe thunderstorms which may produce tornadoes and warnings for high snowfall amounts will become increasingly important. In addition to public safety concerns associated with severe weather there is also a need to provide private enterprise sectors with the most accurate weather warnings possible. For example, the aviation sector is critically dependent upon accurate forecasts of thunderstorm and potential tornado activity. Snowfall prediction is crucial for proper highway maintenance and will become increasingly critical a growing population puts more demand on consistent road access. Forecasting aids, specific to the geographical location and complexities of the varying terrain Alberta, are becoming essential in order to help maintain and improve prediction of severe weather in this region.

A forecasting approach, presently being explored throughout Canada and the United States, centers on providing *probabilistic* rather than *deterministic* forecasts. With a probabilistic prediction a forecaster would provide an estimate of the likelihood of an event rather than only indicating whether that event will or will not occur. An example of everyday use is the Probability of Precipitation forecast in which the probability of rain for a given day is indicated in percentage terms. The probability of an event might be assessed by comparing given environmental flow patterns and thermodynamic variables to climatological or historical outcomes occurring under similar conditions. If an event has occurred only under a relatively confined set of environmental conditions and these conditions are realized, the forecast probability is likely much greater than if an event had occurred over a very broad range of environmental conditions.

When assessing the potential for severe weather events, forecasters consider three critical aspects:

1) the location or spatial extent [what area will the event encompass];
2) the temporal extent [over what time period is the event expected to occur];
3) the intensity [will the event reach defined severe warning criteria and if so what is the degree of severity likely to be].

This research is concentrated on the third aspect, probabilistic determination of the potential for a severe weather event (tornado or heavy snow) to occur and the degree of severity which may be realized. The main focus of this thesis is directed toward severe convective storms producing tornadoes in Alberta. This component of the research will be introduced in Section 4. The goal of this study is to provide forecasters with additional knowledge and tools to assess the potential for thunderstorms in Alberta to become tornadic and, additionally, the intensity of resultant tornadoes. In this manner, a forecaster can make a probabilistic prediction for the likelihood of tornadoes. It is important to emphasize that this research does not attempt to provide a means to predict whether a thunderstorm will develop and that the potential for tornado development is *conditional* upon the prior existence of a thunderstorm. In essence this research attempts to provide tools for the forecaster to answer the question: "Given that a thunderstorm is expected to occur, is there a potential for the thunderstorm to become tornadic and what is the likely intensity of the tornado?" A secondary aspect of this thesis is to investigate the use of sounding data to predict the potential for heavy snowfall in Alberta (introduced in Section 5). Similar to tornado probability, this part of the study develops tools which may aid forecasters in making probabilistic predictions for heavy snowfall. Similar to the tornado study, the potential for heavy snowfall is *conditional* upon the development of the storm which will produce the snow. This component of the thesis research develops a tool for the forecaster to answer the question: "Given that a snowfall event is expected to occur, how much snow is likely and is there a potential for heavy snowfall?"

## 2. Forecasting techniques for predicting severe weather

Forecasters use several techniques for making longer range (more than 6 hours) predictions. These include: numerical weather prediction models, conceptual models which rely on correlating synoptic and meso-scale patterns with similar weather events, and ingredients based approaches which examine various parameters that are physically related to storm development.

With ever increasing computational resources numerical weather prediction models, which simulate synoptic scale processes, have been steadily improving in horizontal resolution and now operate with a horizontal grid spacing of about 15 km. However, even this scale does not approach that needed for modeling of thunderstorm updrafts and downdrafts which would require a horizontal resolution of about 100 m. Modeling of tornadoes with diameters on the order of 100 m is not possible with these operational numerical models. The development of meso-scale computer models capable of realistic simulations of tornadic storms (Schlesinger 1975, Klemp and Wilhelmson 1978) and tornadoes (Rotunno 1979) provided a means to evaluate the physical processes which yield tornadoes. The sophistication of these models has continued to grow so that now it is possible to produce tornado-like vortices within a numerical model of a thunderstorm (Orf and Wilhelmson 2004). Unfortunately, these fine-scale tornado simulation models require several hours of computing time on super computers and are thus, not feasible in an operational forecast environment. In addition, the need for reliable initial data far outstretches the current operational data collection network.

Conceptual models in meteorology allow us to integrate a large number of physical parameters related to a common event, such as a thunderstorm outbreak, into one overall "pattern". Conceptual models are generally developed by taking a large number of observations of parameters related to similar weather events and combining them in such a way as to best describe the most likely scenario. Since conceptual models describe the most probable occurrence, they can often fail for extreme cases. Smith and Yau (1993a,b) developed a synoptic scale conceptual model for severe convective outbreaks in Alberta (discussed in the next section). This model allows forecasters to recognize weather patterns and physical parameters which are often conducive to the development of severe thunderstorms. Lemon and Doswell (1979) developed a conceptual model of a supercell thunderstorm which included such features as a rear flanked downdraft, a surface gust front structure resembling a mid-latitude cyclone, a hook shaped radar reflectivity region surrounding a cyclonically rotating updraft, and a tornado, if present, that occurred in the vertical velocity gradient between the updraft and the rear flanked downdraft. This model has undergone little modification since its presentation over 25 years ago and is still used widely by operational forecasters. Conceptual models can be very useful for allowing the forecaster to make fairly quick assessments for the potential of severe convective activity. However, these models can also be dangerous if the forecaster uses them in a dogmatic fashion and rejects outcomes which may not precisely fit the model. In order to make a more detailed assessment of the potential for severe thunderstorms and possible tornadoes, a forecaster must have a sound knowledge of the physical processes involved as well as the inherent uncertainties of existing theories.

To make a more refined assessment of thunderstorm and tornado development, forecasters could employ an ingredients-based approach which examines various physical parameters related to storm development and tornadogenesis. These storm parameters usually include the amount of vertical shear in the horizontal wind, thermal buoyancy, atmospheric humidity, storm-relative helicity, among others (e.g. Colquhoun and Shepherd 1989; Brooks et al. 1994; Rasmussen and Blanchard 1998; Thompson et al. 2003). Using an ingredients method allows the forecaster to examine each physical variable to determine whether its contribution could affect the probability of the development under question.

This thesis research investigates the use of the ingredients-based approach to aid in deciding the potential for tornadic thunderstorms and the intensity of tornadoes in a probabilistic manner. This study uses the method of examining various environmental sounding parameters associated with tornadic events to determine if these parameters can be used to distinguish between non-tornadic and tornadic thunderstorms and also to discriminate between the intensity of tornadoes. Certain parameters have been established through theoretical and numerical modeling as being important in supercell formation [e.g. the bulk Richardson number (Weisman and Klemp 1982), buoyancy, vertical wind shear]. The approach of using environmental proximity soundings to assess parameters related to meso-scale supercells and tornadoes has been widely used. Pioneering research was done by Darkow and Fowler (1971) to examine the role of wind shear to distinguish severe storms. Rasmussen and Wilhelmson (1983) examined shear and buoyancy. Rasmussen and Blanchard (1998) developed a sounding climatology of supercell and tornado parameters. Monteverdi et al. (2003) investigated buoyancy and wind shear for California tornadic storms. Thompson et al. (2003) used numerical model generated soundings to calculate various parameters (including shear, helicity, and buoyancy) which could be used to distinguish between non-tornadic storms, weak tornadoes, and significant tornadoes. Davies (2004) investigated the use of sounding calculated buoyancy parameters to distinguish between non-tornadic and tornadic storms. Research in this area continues, supporting a long range goal, outlined by Brooks et al. (1994), to explore whether environmental parameters can be used to help discriminate between environments of tornadic thunderstorms and non-tornadic severe thunderstorms. This approach provides the operational forecaster with additional tools to assess the potential for tornadic storm development. In addition, those performing numerical modeling and theoretical studies need to have data that indicate whether or not they are exploring physically relevant parameters and parameter ranges.

## 3. Development of understanding of severe storm formation in Alberta – a historical review

The research findings presented in this thesis have to be seen in the context of our current understanding of severe convective storms forming in central Alberta. Starting with the Alberta Hail Project in the late 1960's there have been a number of important milestones is refining our knowledge of Alberta storms. It seems instructive to highlight the major research findings in their chronological order.

1959: Douglas and Hitschfeld examined hailstorms in Alberta during the summer of 1957 through correlation of surface reported hail sizes with radar observations. They found higher storm tops and colder cloud top temperatures were closely correlated with larger hail sizes.

1961: Hage confirmed that lee cyclogenesis is common for Alberta. Lee cyclogenesis is a significant factor for the development of synoptic scale storms which can generate severe convective outbreaks, and also for the development of snow storms. It commences when an area of positive vorticity advection in advance of an upper low spreads over a baroclinic zone in the lee of the Rocky Mountains. Hage also suggested that the movement of the upper low may be influenced by a second upper low further upstream.

1972: Chisholm and Renick characterized the radar structure and behavior of single cell, multi-cell, and supercell storm types. They constructed qualitative storm vertical wind profiles associated with these three major storm types.

1976: Chung, Hage, and Reinelt analyzed the frequency of cyclone formation in the lee of the Rocky Mountains. As noted previously, cyclone formation is a factor in the development of synoptic scale storms which can produce severe convection or snow events. They found the greatest frequency was over southwestern Alberta. Cyclone intensification was found to occur further east of the initiation area under an eastward moving upper trough.

1984: Newark compiled a climatology of the frequency of occurrence of tornadoes throughout Canada. He showed that central Alberta is one of the most frequent regions for tornado activity with up to 4 tornadoes per 10,000 $km^2$ per year.

1984: Krauss and Marwitz analyzed an Alberta supercell using aircraft and radar to investigate the microphysical processes leading to precipitation. They found that fine-scale convective clouds within a supercell provide a viable source of hailstone embryos. They also presented a conceptual model of precipitation processes leading to the formation of hail.

1987: Wallace documented the 31 July 1987 Edmonton tornado including the weather conditions, track, and physical dimensions of the tornado at various stages. He also discussed the watches and warning issued by the weather office.

1993: Smith and Yau analyzed synoptic and meso-scale air flow patterns associated with severe convective storms in Alberta. They developed a conceptual model of the synoptic pattern and processes for the development of severe thunderstorms. The model includes a mountain-plain circulation which allows for the buildup and subsequent release of convective available potential energy.

1993: Reuter and Jacobsen showed convective storm intensity in Alberta is affected by the detail of the vertical wind profile. A concave profile (magnitude of the vertical shear decreases with height) implies more intensity while a convex profile (magnitude of the vertical shear increases with height) is associated with a less intense storm.

1995: Reuter and Aktary analyzed over 1400 balloon soundings in central Alberta to assess whether there were deep layers susceptible to convective or moist symmetric instability. They found that during the summer, 97% of the soundings were susceptible to convective instability During winter, 44% of the observed soundings indicated the potential for moist symmetric instability, and about half of the total snowfall amounts were associated with these symmetrically unstable soundings.

1995: Charlton, Kachman, and Wojtiw documented five Alberta hailstorms, three of which set records for Canada's most costly natural disasters.

1996: Reuter and Beaubien analyzed sounding data to investigate snowfall production in a long-lasting snowband over Alberta. The sounding data indicated that the snow band was caused by the release of moist symmetric instability.

1998: Smith, Reuter, and Yau investigate the frequency and duration of hail day episodes (hail size ≥ 33 mm) for 29 summers (June, July, August) in central Alberta. They found that severe hail episodes (one or more consecutive days of hail > 4 cm in diameter) occur on average 6.6 times over the summer period.

1998: Charlton, Kachman, and Wojtiw did an extensive documentation of the wind and hail damage associated with the 31 July 1987 Edmonton tornado. This included many photos of the damaged areas and images of the tornado at various stages.

2000: Joe and Dudley documented the damage and track of the 14 July 2000 Pine Lake tornado in central Alberta. The storm followed the typical pattern of a severe Alberta supercell with large hail and spawned an F3 tornado.

2002: Erfani, Methot, Goodson, Belair, Yeh, Cote, and Moffet used a fine scale version of the Global Environmental Multiscale model to simulate the initiation, development and structure of the 14 July 2000 Pine Lake tornado-producing supercell storm. The simulated evolution of the surface fields such as the dewpoint and winds closely resembled the synoptic observation of a strong gradient across central Alberta.

2002: Brimelow, Reuter, Poolman improved upon one of the few numerical hail models (HAILCAST). They found the magnitude of convective available potential energy significantly affects the size of hailstones.

2003: Hage compiled an extensive climatology of Alberta tornadoes from 1879 to 1984. This is the only published climatology of tornado events in Alberta.

## 4. Review of Alberta tornado parameters

The province of Alberta, whose boundaries extend from 49° to 60° N and 120° to 110° W, is situated in a meteorologically active area with the mean position of the jet stream across southern Alberta during the summer (Petterssen 1956). The Rocky Mountains, which extend about 2400 km from the Yukon to New Mexico, form a northwest-southeast barrier along the western border of Alberta. The plains to the east provide a striking contrast to the mountainous west. The combination of these two geographic features greatly aides in the development of synoptic storms throughout the year. During the summer months a significant influence of the mountains is to cause a subsidence inversion that acts as a capping lid for the build-up of Convective Available Potential Energy (CAPE). Central Alberta is highly susceptible to severe convection, having on average 52 days with hail fall each summer (Smith et al. 1998). Alberta thunderstorms that spawn tornadoes occur far less frequently but are nonetheless a significant component of thunderstorm climatology (Newark 1984). A high annual number of tornadoes per 10,000 $km^2$ in Canada (Fig. 1) covers a large portion of central Alberta. Hage (2003) compiled an extensive tornado climatology starting from 1879 and found that, on average, 10 tornadoes occur over Alberta each summer. Even though tornadic storms in central Alberta are generally associated with hail, less than 10% of Alberta hailstorms spawn tornadoes. Similar to other regions, most tornadoes in Alberta are rated at F0 or F1 [based on the Fujita damage scale (see Appendix B); Fujita 1981]. However, most of the structural damage, injuries, and fatalities come from the more severe F2, F3, and F4 tornadoes.

A number of storm parameters are known to be associated with the formation of severe thunderstorms. They include the presence of a large amount of Convective Available Potential Energy (CAPE), a build up of latent energy below a capping inversion, strong vertical shear of the horizontal wind for storm organization, and a trigger mechanism to release the latent energy. However, there still does not exist a complete understanding and physical model of tornadogenesis and there remains considerable uncertainty as to which factors may be necessary for the formation of tornadoes and which factors might affect the intensity of tornadoes. Rasmussen et al. (1994) discussed theories regarding tornadogenesis. Updrafts in supercell thunderstorms usually begin rotating in the mid-levels as a result of tilting by the updraft of low-level horizontal vorticity associated with strong environmental vertical wind shear (e.g. Klemp 1987). When the storm-relative winds veer significantly with height in the lowest few kilometers, the environmental vorticity has a large component in the same direction as the storm-relative wind (streamwise vorticity; Fig. 2). The updraft tilts this streamwise vorticity into the vertical to form the initial mid-level meso-cyclone (Davies-Jones 1984). For prolonged updraft rotation, the low-level storm-relative winds must be strong enough to prevent the storm's cold outflow from surging ahead of the storm and choking off the updraft from its low-level source of warm and moist air.

Numerical simulations suggest that the formation of a low-level meso-cyclone (i. e. near 2 km AGL) may be initially dependent on the formation of a rain-cooled downdraft (e.g. Rotunno and Klemp 1985; Davies-Jones and Brooks 1993). Once the low-level meso-cyclone is formed, its rotation may then be augmented by the mid-level rotation. Low-level rotation is suspected to develop first in evaporatively cooled subsiding air just behind the gust front on the left (when facing the rear of the thunderstorm) rear side of the meso-cyclone. Rapidly subsiding air that has been cooled by rain can acquire considerable horizontal vorticity generated by buoyancy differences between the coldest air within the downdraft and relatively warmer air near the fringe. Another possible mechanism for developing large amounts of horizontal vorticity may be the very strong horizontal wind shear which develops as a result of rapidly rising air on the edge of an updraft in relation to relatively small vertical motions outside of the updraft core. Horizontal shear vorticity along the edge of the updraft might form into a sheet of "vorticity rolls". Development of the downdraft will further enhance these vorticity rolls as well as bringing them downward to the surface. The subsiding air then spreads out as it hits the surface with some moving forward and becoming entrained into the right rear side of the main updraft. Within the updraft the vorticity is increased by intense vertical stretching. Since tornadoes typically form near the interface between the updraft and downdraft, the production and downward transport of cyclonic vorticity in the downdraft followed by a transport of this vorticity along the ground and into the side of the updraft may be a mechanism for tornadogenesis. Even though the mechanism described is plausible for many stronger tornadoes that may form in meso-cyclones, there still remains much uncertainty concerning the development of a low-level meso-cyclone and its relationship to tornadogenesis. An examination by Ziegler et al. (2001) of a Texas tornado during project VORTEX (Rasmussen et al. 1994) found the mid-level meso-cyclone underwent an initial stage of downward growth which was coupled with the development of a boundary layer vortex in proximity to the developing mid-level meso-cyclone. They hypothesized that a merger of the low-level and mid-level meso-cyclones may have contributed to further intensification and deepening of the circulation. Following the initial development of separate low-level and mid-level meso-cyclones, the meso-cyclone became continuous in the vertical prior to the development of a significant (F3) tornado. In addition it was also found both the tornado cyclone and meso-cyclone contracted in horizontal scale with convergent intensification.

The preceding discussion may apply to many of the stronger tornadoes developed from meso-cyclones but may not account for a broad number of generally weaker tornadoes that do not form from meso-cyclones. A possible mechanism for tornadoes which are not produced from meso-cyclones is horizontal shearing instability causing the vertical vorticity generated at a wind-shift line to form individual vortices, which are subsequently stretched upwards by convective updrafts passing over the vorticies (Wakimoto and Wilson 1989).

Despite much progress in the past 25 years, a definitive model of the tornado and tornadogenesis still does not exist. It remains uncertain whether tornadic storms develop in an environment markedly different from non-tornadic severe thunderstorms and whether the intensity of tornadic storms is related to the certain environmental parameters. A number of studies have examined the relationship between environmental sounding parameters and tornado development ( e.g. Brooks et al. 1994; Rasmussen and Blanchard 1998; Monteverdi et al. 2003; Thompson et al. 2003). These studies have shown that parameters such as wind shear and helicity appear to correlate well with the potential for tornadic development. Other parameters, such as CAPE, show varying amounts of correlation with some studies finding CAPE useful for discriminating between non-tornadic and tornadic storms while other studies find no such correlation. The large majority of research has concentrated on the tornadoes in the United States. In a recent study Rasmussen (2003) questions whether some environmental parameters which appear to distinguish between tornadic and non-tornadic storms are, in fact, merely separating different geographical characteristics of storms. For example, a study by Rasmussen and Blanchard (1998) found that the height of the Lifted Condensation Level (LCL) was able to discriminate between tornadic and non-tornadic storms occurring throughout the U.S. However, most tornadoes are spawned in the southeast U.S. where the proximity to the Gulf of Mexico provides high humidity and correspondingly low LCL values for *all* storms, not just tornadoes. In contrast, lower humidity in the high plains of the U.S. results in higher LCL values for all thunderstorms, with a large number of hailstorms occurring without tornadoes. Thus LCL values of tornadic storms for the whole U.S. will be strongly influenced by the overall lower values for tornadoes in the southeast U.S. This thesis research, being confined to a much smaller geographical area, may not be as subject to geographical characteristics which may unduly influence the overall results.

Three convective storms in Alberta which had the most intense tornadoes recorded during 1983-2003 were:

1. Edmonton; 31 July 1987 (F4) resulting in 27 deaths and 250 million dollars of property damage (Bullas and Wallace 1988). The detailed climatology of Alberta tornados compiled by Hage (2003) showed that the Edmonton tornado was the only case of an F4 tornado in Alberta during recorded history.
2. Holden; 29 July 1993 (F3) which destroyed several well constructed brick and mortar farm buildings (Knott and Taylor, 2000).
3. Pine Lake; 14 July 2000 (F3) causing 12 fatalities, more than 130 injuries and over 13 million dollars damage (Erfani et al. 2002).

The conceptual model of Smith and Yau (1993a,b) describes the typical summer time synoptic patterns and processes that lead to the initiation of severe convective outbreaks over Alberta. Smith and Yau (1993b) identified two stages leading to the formation of severe convective storms. Stage 1 is characterized by clear skies in subsiding air ahead of an approaching upper-level ridge. Stage 2 begins when the upper-level ridge moves eastward and an upper-level trough approaches resulting in a severe convective outbreak. This model is described in more detail in Chapter IV.

### 5. Predicting heavy snowfall in Alberta

In contrast to summer time convective storms, snowfall during the fall, winter and spring is a very important component of the climate in Alberta. Nearly one half of the annual precipitation for all of Alberta occurs in the form of snow (Reuter and Beaubien, 1996). A major task of a weather forecast office such as the Prairie and Northern Region Weather Office in Edmonton, Alberta is to predict snowfall amounts and provide timely warnings of heavy snowfall. Numerical Weather Prediction (NWP) models are skilful to resolve and track large-scale baroclinic disturbances, however model predictions of snowfall accumulations are often inaccurate, particularly for heavy snowfall (Kocin and Uccellini 1990; Aktary and Reuter 1993). The operational forecaster could benefit from techniques, complementary to NWP guidance, to assist in deciding whether or not the 24 hour accumulation of snow will exceed 10 cm. This thesis investigates the use of sounding data to predict heavy snowfall in Alberta. The goal is to provide tools for the forecaster to determine whether a snow storm in Alberta is capable of producing heavy snowfalls and the amount of snow that may occur.

## 6. Statement of originality

Most tornado research has concentrated on the United States with little attention directed towards Alberta. Consequently, forecasters for Alberta are left with the option of attempting to apply findings developed in the U.S. to predict tornadic storm development in their area. Clearly, the physics and dynamics of storm development should not vary from one location to another, i.e. the storm does not "know" whether it is in Texas or Alberta. However, as discussed earlier, there is increasing evidence that some of the parameters hypothesized to be associated with tornadogenesis may merely be distinguishing between characteristics of storms developing in different geographical locations. Prior to Hage's (2003) study, there had been no comprehensive climatology of tornadoes in Alberta. Hage documented the date, location, and detailed type of damage of many if not all recorded tornadoes occurring over Alberta from 1879 to 1984. This thesis is the first to exploit Hage's tornado climatology. After extensive consultation with Alberta forecasters, it was determined that additional knowledge and tools to aid in tornado prediction specific to Alberta would be an invaluable addition to help fulfill the Canadian weather service mandate to provide timely warnings of severe weather potential.

In Chapters III and IV various environmental parameters in Alberta are examined to determine their ability to distinguish between tornadic and non-tornadic storms and also the intensity of tornadic storms. Chapter III investigates vertical wind shear to determine a set of threshold values for low-level and deep-layer shear specific to the Alberta forecast situation. In addition an original use of the ratio of low-level to deep-layer shear is explored. Chapter IV introduces two original concepts for predicting tornadogenesis: 1) the application of a combination of precipitable water and tropospheric humidity (Bluestein and Jain 1985) to help determine the vertical moisture profile of the atmosphere and 2) storm convergence, calculated using the vertical gradient of CAPE, to estimate the amount of vorticity enhancement near the base of the cloud. The characteristics of a rear-flank downdraft within a supercell are often different for tornadic versus non-tornadic storms and may be influenced by the vertical moisture structure of the atmosphere (Markowski et al. 2002). A previously unexplored combination of precipitable water and tropospheric humidity may provide information concerning the vertical humidity structure which cannot be obtained by either sounding parameter alone. Storm convergence near the base of the thunderstorm might provide an estimation of the amount of vertical vorticity generation due to convergence and stretching in the updraft. Whereas other studies have examined the total CAPE, this research concentrates on the vertical gradient of CAPE near the cloud base to estimate the storm updraft and stretching near that region.

Chapter V of this thesis provides an original detailed examination of the three most intense tornadic storms in Alberta outlined previously. Even though the Edmonton tornado is the most severe tornadic storm recorded in Alberta, there has not been a peer reviewed documentation and examination of that event. Case studies comparing the similarities and differences of significant storm events such as these can provide valuable clues when forecasters may be faced with similar situations. In particular, the unique characteristics of surface moisture fields brought forward in this research may put forecasters on the alert to further investigate the potential for tornado development.

Chapter VI provides an original method for estimating maximum snowfall in Alberta by relating the snowfall amount to the saturated vapor mixing ratio at cloud base and cloud top levels. Numerical approximations are used to obtain a linear relationship between maximum snowfall and cloud base temperature. Further investigation is done to show that Quantitative Precipitation Forecast (QPF) amounts predicted by a numerical weather can be complemented and improved upon by the snowfall-temperature relationship.

## 7. Statement of the research problems

This thesis investigates, for central Alberta, whether observed environmental sounding parameters can be used to assess the potential for severe storm development.

The specific issues investigated in this research can be stated in terms of four related problems:

**Problem 1: Determining which sounding parameters can be used to forecast tornado probability.**

Which sounding parameters can distinguish between non-tornadic and tornadic storms in Alberta? Further, can these parameters discriminate between weak and significant tornadoes? Is using environmental proximity sounding data a viable and useful approach for examining thunderstorms? This thesis investigates the usual storm parameters including wind shear, buoyancy, helicity, and available humidity. In addition this thesis introduces a novel storm parameter referred to as near cloud base storm convergence and investigates its role in tornadogenesis.

**Problem 2: Developing threshold values for probabilistic forecasting**

Can threshold values for sounding parameters be established which will aid forecasters in assessing the probability for tornadic development and the intensity of tornadoes in Alberta? Does a combination of threshold values produce better guidance than a single parameter threshold? Are threshold values for Alberta storms different from those developed in other regions, such as the U. S.?

**Problem 3: Similarities and differences between tornadic storms**

What are the synoptic and meso-scale similarities and differences between the three most severe tornadic storms in Alberta in the past 25 years? Were there factors associated with these storms which appear contrary to conceptual models and thus emphasize the importance of an ingredients-based forecasting approach?

**Problem 4: Forecasting snowfall amounts using low-level temperature values.**

Can the 850 mb temperature within a developing synoptic system be used to predict snowfall amounts (specifically amounts > 10 cm in a 24 hour period)? Does this method provide additional precipitation guidance beyond that obtained from numerical models? Can a threshold value for 850 mb temperature be established which will aid forecasters in assessing the probability for heavy snowfalls of > 10 cm in a 24 hour period?

The approach taken in this thesis focuses on analyzing observed sounding data from Stony Plain and from other upper air reporting sites in western North America plus surface observations from the Environment Canada network in Alberta.

This thesis is written in "paper" format, and thereby abides by certain conventions. Each chapter is a self-contained unit with its own abstract, introduction, conclusions, and references. The numbers assigned to tables, figures, and equations refer to the current chapter. Chapters intended for journal submission are written in the format required by that journal.

Chapter II contains no original research and it is not intended for journal publication. Instead, it contains essential background material on the use of rawinsonde data; material which is scattered throughout technical notes and manuals and not easily available to the researcher. A discussion of the network of upper air sounding sites and the errors associated with rawinsonde measurements is presented. Also, a summary of the use of thermodynamic diagrams to display rawinsonde data is given. In addition, some concerns and problems associated with analyzing buoyancy are discussed.

Chapter III has been accepted for publication as a journal article in Weather and Forecasting, the technical journal for original advances in weather forecasting by the American Meteorological Society (AMS). This chapter investigates the use of various sounding based wind shear parameters to distinguish between thunderstorms that produce significant tornadoes, weak tornadoes or ones without tornadoes. The ratio of low-level shear to deep-layer bulk shear, and the directional shear are also investigated. The role of buoyancy, such as CAPE is also quantified.

Chapter IV (accepted for publication by Weather and Forecasting of the AMS) continues to investigate the use of storm sounding parameters to differentiate between significant tornadoes, weak tornadoes, and non-tornadic hail storms. A new storm parameter, referred to as storm convergence is introduced and its usefulness tested.

Chapter V (to be published in National Weather Digest) compares the three most intense tornadic storms in recent years for Alberta. Specifically, detailed case studies are made for the Edmonton, Holden, and Pine Lake storms. The role of the surface moisture front (dryline) is examined, as well as temperature changes to build up convective instability.

Chapter VI (published in Atmosphere Ocean) investigates the use of sounding data to predict heavy snowfall in Alberta. Specifically the research examines the use of 850 mb temperature values to predict maximum 24 hour snowfall amounts.

The final chapter of the thesis will synthesise the results, offer implementations for forecasting and make some suggestions for further research. Additional material is included in appendices. APPENDIX A discusses the vagaries and problems associated with defining a tornado and supercell. A new definition proposed by some tornado researchers is outlined. APPENDIX B gives the Fujita tornado damage scale commonly used to categorize tornadoes. APPENDIX C details the derivation of the storm convergence method introduced in Chapter IV. APPENDIX D contains an informal personalized account of the daily procedures that are commonly followed by a severe weather forecaster.

# References

Aktary, N., and G. W. Reuter, 1993: Observations of a snowband in a symmetrically unstable flow over Alberta. *Contrib. Atmos. Phys.*, **66**, 25-282.

Bluestein, H. B., and M. H. Jain, 1985: Formation of mesoscale lines of precipitation: Severe squall lines in Oklahoma during the spring. *J. Atmos. Sci.,* **42,** 1711-1732.

Brimelow, J. C., G. W. Reuter, and E. R. Poolman, 2002: Modeling the maximum hail size in Alberta thunderstorms. *Wea. and Forecasting*, **17**, 1048-1062.

Brooks, H., E., C. A. Doswell III, and J. Cooper, 1994: On the environment of tornadic and non-tornadic mesocyclones. *Wea. Forecasting*, **9**, 606-618.

Bullas, J. M., and A. F. Wallace, 1988: The Edmonton tornado, July 31, 1987. Preprints, *15th Conf. on Severe Local Storms*, Baltimore MD, Amer. Meteor. Soc., 437-443.

Charlton, R. B., B. M. Kachman, and L. Wojtiw, 1995: Urban hailstorms: a view from Alberta. *Natural Hazards*, **12**, 29-75.

_______, _______, and_______, 1998: The Edmonton tornado and hailstorm: A decade of research. *CMOS Bulletin*, **26**, 1-56.

Chisholm, A. J., and J. H. Renick, 1972: The kinematics of multicell and supercell Alberta hailstorms. Research Council of Alberta Hail Studies Report 72-2, 7 pp.

Chung, Y. S., K. D. Hage, and E. R. Reinelt, 1976: On lee cyclogenisis and airflow in the Canadian Rocky Mountains and East Asian mountains. *Mon. Wea. Rev.*, **104**, 879-891.

Colquhoun, J. R., and D. J. Shepherd, 1989: An objective basis for forecasting tornado intensity. *Wea. Forecasting*, **4**, 35-50.

Darkow, G. L., and M. G. Fowler, 1971: Tornado proximity wind sounding analysis. Preprints, *7th Conf. on Severe Local Storms*, Kansas City, Missouri, Amer. Meteor. Soc., 148-151.

Davies, J. M., 2004: Estimations of CIN and LFC associated with tornadic and nontornadic supercells. *Wea. Forecasting*, **19**, 714–726.

Davies-Jones, R. P., 1984: Streamwise vorticity: The origin of updraft rotation in supercell storms. *J. Atmos. Sci.*, **41**, 2991-3006.

_______, and H. E. Brooks, 1993: Mesocyclogenesis from a theoretical perspective. The Tornado: Its Structure, Dynamics, Prediction and Hazards. Geophys. Monogr., No. 79, Amer. Geophys. Union, pp. 105-114.

Doswell, C. A. III, cited 2000: A primer on vorticity for application in supercells and tornadoes. [Available online at http://www.cimms.ou.edu/~doswell/vorticity/vorticity_primer.html.]

Douglas, R. H., and W. Hitschfeld, 1959: Patterns of hailstorms in Alberta. *Quart. J. Roy. Meteor. Soc.*, **85**, 105-119.

Erfani A., A. Methot, R. Goodson, S. Belair, K. S. Yeh, J. Cote, and R. Moffet, 2002: Synoptic and mesoscale study of a severe convective outbreak with the nonhydrostatic Global Environmental Multiscale (GEM) model. *Met. Atmos. Physics, **82**, 31-53.*

Fujita, T. T., 1981: Tornadoes and downbursts in the context of generalized planetary scales. *J. Atmos. Sci.*, **38**, 1511-1534.

Hage, K. D., 1961: On summer cyclogenesis in the lee of the Rocky Mountains.*Bull. Amer. Meteor. Soc.*, **42**, 20-33.

_______, 2003: On destructive Canadian prairie windstorms and severe winters. *Natural Hazards*, **29**, 207-228.

Joe, P. and D. Dudley, 2000: A quick look at the Pine Lake storm. *CMOS Bulletin*, **28**, 172-180.

Klemp, J. B., and R.B. Wilhelmson, 1978: The simulation of three-dimensional convective storm dynamics. *J. Atmos. Sci.*, **35**, 1097-1110.

_______, 1987: Dynamics of tornadic thunderstorms. *Annu. Rev. Fluid Mech.*, **19**, 369-402.

Knott, S. J., and N. M. Taylor, 2000: Operational aspects of the Alberta weather outbreak of 29 July 1993. *Natl. Wea. Dig.*, **24**, 11-23.

Kocin, P.J., and L.W. Uccellini, 1990: Snowstorms along the northeastern coast of the United States:1995 to 1985. Meteor. Monographs, 22, Amer. Meteor. Soc., Boston, Mass., 280pp.

Krauss, T. W., and J. D. Marwitz, 1984: Precipitation processes within an Alberta supercell hailstorm. *J. Atmos. Sci.*, **41**, 1025-1033.

Lemon, L. R., and C. A. Doswell, 1979: Severe thunderstorm evolution and mesocyclone structure as related to tornadogenesis. *Mon. Wea. Rev.*, **107**, 1184–1197.

Markowski, P. M., J. M/. Strake, and E. N. Rasmussen, 2002: Direct surface thermodynamic observations within the rear-flank downdrafts of nontornadic and tornadic supercells. *Mon. Wea. Rev.*, **130**, 1692-1721.

Monteverdi, J. P., C. A. Doswell III, and G. S. Lipari, 2003: Shear parameter thresholds for forecasting tornadic thunderstorms in Northern and Central California. *Wea. Forecasting*, **18**, 357-370.

Newark, M. J., 1984: Canadian tornadoes, 1950-1979. *Atmos. Ocean*, **22**, 343-353.

Orf, L., and Wilhelmson, R., 2004: Evolution of tornado-like vortices in a numerically simulated supercell thunderstorm. Preprints, *22nd Conf. on Severe Local Storms*, Hyannis, MA, Amer.. Meteor. Soc., CD-ROM, 9.5.

Petterssen, S., 1956: *Weather Analysis and Forecasting.* 2nd ed. McGraw-Hill, New York, 428 pp.

Rasmussen, E. N., 2003: Refined supercell and tornado forecast parameters. *Wea. Forecasting*, **18**, 530–535.

_______, and D. O. Blanchard, 1998: A baseline climatology of sounding-derived supercell and tornado forecast parameters. *Wea. Forecasting*, **13**, 1148-1164.

_______, R. Davies-Jones, C. A. Doswell III, F. H. Carr, M. D. Eilts, D. R. MacGorman, J. M. Straka, and F. H. Carr, 1994: Verification of the Origins of Rotation in Tornadoes Experiment: VORTEX. *Bull. Amer. Met. Soc.*, **75**, 995–1006.

_______, and R. B. Wilhelmson, 1983: Relationships between storm characteristics and 1200 GMT hodographs, low level shear and stability. Preprints, 13th Conference on Severe Local Storms, Tulsa, OK., Amer. Meteor. Soc., 55-58.

Reuter, G. W., and O. Jacobsen 1993: Effects of variable wind shear on the mesoscale circulation forced by slab-symmetric diabatic heating. *Atmos. Ocean*, **31**, 451-469

_______, and N. Aktary, 1995: Convective and symmetric instabilities and their effect on precipitation: Seasonal variations in Central Alberta during 1990 and 1991. *Mon. Wea. Rev.*, **123**, 153-162.

_______, and R. Beaubien, 1996: Radar observations of snow formation in a warm pre-frontal snowband. *Atmos. Ocean*, **34**, 605-626.

Rotunno, R., 1979: A study of tornado-like vortex dynamics. *J. Atmos. Sci.*, **36**, 140-155.

_______, and J. B. Klemp, 1985: On the rotation and propagation of simulated supercell thunderstorms. *J. Atmos. Sci.*, **42**, 271-292.

Schlesinger, R.E., 1975: A three-dimensional numerical model of an isolated thunderstorm. Preliminary results. *J. Atmos. Sci.*, **32**, 835-850.

Smith, S. B., and M. K. Yau, 1993a: The causes of severe convective outbreaks in Alberta. Part I: A comparison of a severe outbreak with two nonsevere events. *Mon. Wea. Rev.*, **121**, 1099-1125.

_______, and _______, 1993b: The causes of severe convective outbreaks in Alberta. Part II: Conceptual and statistical analysis. *Mon. Wea. Rev.*, **121**, 1126-1133.

_______, G.W. Reuter, and M.K. Yau, 1998: The episodic occurrence of hail in central Alberta and the Highveld of South Africa. *Atmos. Ocean*, **36**, 169-178.

Thompson, R. L., R. Edwards, J. A. Hart, K. L. Elmore, and P. Markowski, 2003: Close proximity soundings within supercell environments obtained from the Rapid Update Cycle. *Wea. Forecasting*. **18**, 1243-1261.

Wakimoto, R. M., and J. W. Wilson, 1989: Non-supercell tornadoes. *Mon. Wea. Rev.*, **117**, 1113-1140.

Wallace, A. F., 1987: Track of the Edmonton tornado, July 31, 1987. Tech Note, Environment Canada, 22 pp. [Available from Meteorological Service of Canada, Environment Canada, 4999-98th Ave., Edmonton, AB T6B 2X3.].

Weisman, M. L., and J. B. Klemp, 1982: The dependence of numerically simulated convective storms on vertical wind shear and buoyancy. *Mon. Wea. Rev.*, **110**, 504-520.

Ziegler, C. L., E. N. Rasmussen, T. R. Shepherd, A. I. Watson, and J. M. Straka, 2001: The evolution of low-level rotation in the 29 May 1994 Newcastle–Graham, Texas, storm complex during VORTEX. *Mon. Wea. Rev.*, **129**, 1339-1368.

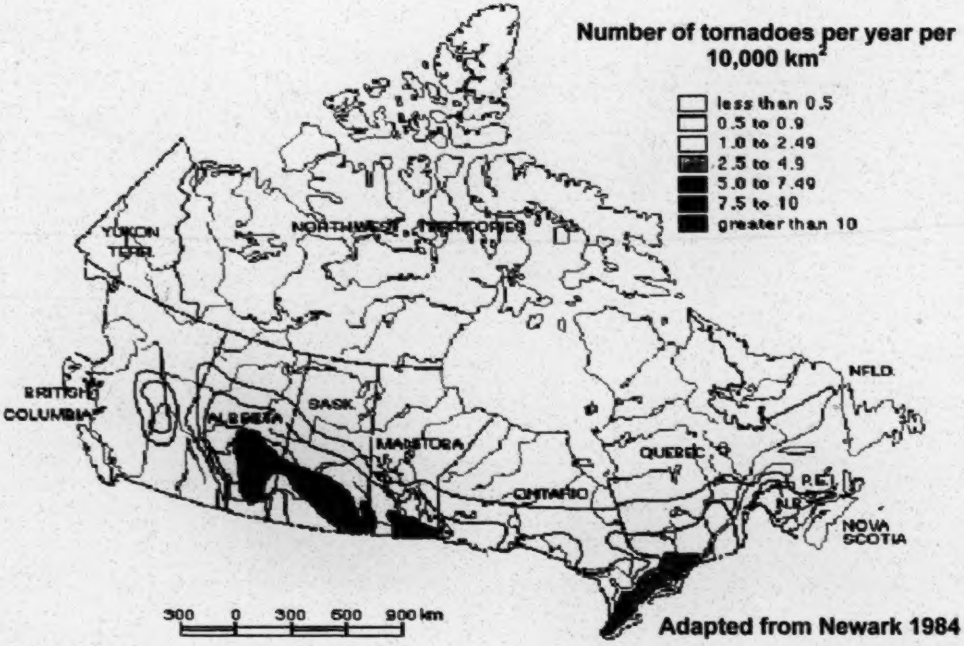
Number of tornadoes per year per 10,000 km²
less than 0.5
0.5 to 0.9
1.0 to 2.49
2.5 to 4.9
5.0 to 7.49
7.5 to 10
greater than 10
YUKON TERR.
NORTHWEST TERRITORIES
BRITISH COLUMBIA
ALBERTA
SASK.
MANITOBA
ONTARIO
QUEBEC
NFLD.
P.E.I.
N.B.
NOVA SCOTIA
300 0 300 600 900 km

Adapted from Newark 1984

Fig. 1 Average annual number of tornadoes per 10,000 km$^2$ in Canada. (Adapted from Newark 1984)

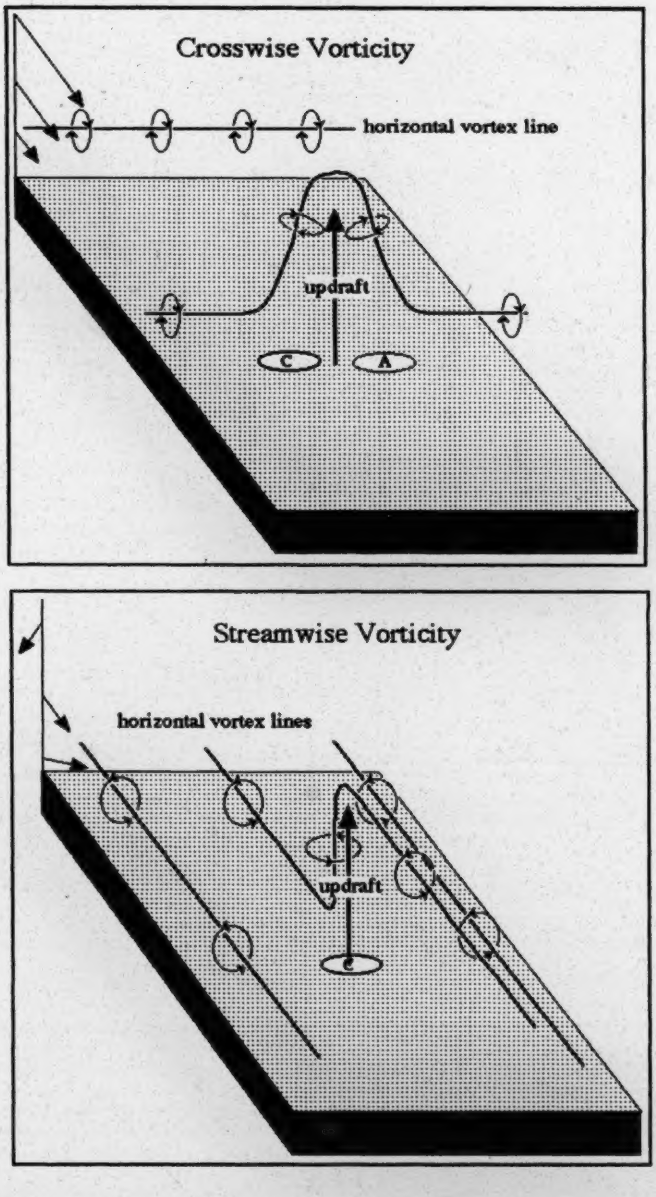
Crosswise Vorticity
horizontal vortex line
updraft
C
A
Streamwise Vorticity
horizontal vortex lines
updraft
C

Fig. 2 Illustrations of crosswise (top) and streamwise (bottom) vorticity. The circular rings indicate the direction of rotation. The storm updraft is indicated by the vertical arrow. The environmental vertical wind profile is indicated by the arrows in the top left corner of each image. Crosswise vorticity is perpendicular to the unidirectional environmental flow. Directional change of wind with height results in parallel components of vorticity and environmental flow. (Adapted from Doswell 2000)

# Chapter II

# Rawinsonde Data and Convective Instability

## 1. Rawinsonde network

The intensity and organization of convective storms depends largely on the vertical stratification of temperature, humidity, and wind. To assess the vertical profile of the atmosphere, meteorologists rely on balloon-sounding data.

A radiosonde measurement system consists of a helium-filled balloon with an instrument package (Fig. 1) which ascends from the earth's surface through the troposphere and beyond. During the course of its ascent, temperature and humidity are measured (Wright 1997). The sensors' information is transmitted to a ground receiving station where it is processed every few seconds. When wind information is processed by tracking the balloon's movement the instrument package is termed a *rawinsonde*. Thus, rawinsonde observations of the atmosphere describe the vertical profile of temperature, humidity, wind direction, and wind speed as a function of pressure (or height) from the surface to the altitude where the sounding is terminated. Other parameters (such as dewpoint, wind shear, and convective stability indices) can then be derived from a rawinsonde observation. The rawinsonde system consists of a balloon-borne radiosonde, receiving and tracking equipment, and computer systems for data processing.

Rawinsondes are released at designated World Meteorological Organization (WMO) stations throughout the world, often termed upper-air stations or sites. The WMO recommends a minimum upper-air station spacing of about 250 km over large land areas and 1000 km over sparsely populated and oceanic regions. Furthermore, upper air observations should be taken one-to-four times daily. In Canada and most other regions throughout the world rawinsonde observations are done daily at 0000 UTC (Coordinated Universal Time) and 1200 UTC. A map of the upper air stations in western Canada and the northwest U.S. is shown in Fig. 2. The WMO spatial requirement is often not followed in Canada where some neighboring observation sites in fairly highly populated regions are separated by 600 km or more (e.g. Stony Plain, Alberta to Prince George, BC).

Meteorological data are archived at standard and mandatory isobaric levels. The standard levels are selected at specified pressure levels: 1000, 925, 850, 700, 500, 400, 300, 250, 200, 150, 100, 70, 50, 30, 20, and 10 mb. Mandatory levels are defined as: the surface; the highest level achieved (termination level); one level between 110 and 100 mb; the tropopause; the bases and tops of temperature inversions and isothermal layers greater than 200 mb in thickness and at pressures greater than 300 mb; the bases and tops of all inversion layers with temperature changes of 2.5 °C or 20% relative humidity at pressures greater than 300 mb; levels delineating layers with missing or doubtful data.

## 2. Radiosonde sensors

The sensors mounted on a radiosonde measure pressure, temperature, and humidity throughout the whole range of flight conditions from launch to balloon burst. The pressure sensor is usually an evacuated aneroid cell, a part of which flexes with variations in pressure. The flex is proportional to the absolute pressure. The flex is then reported as a movement of a mechanical arm, as a capacitance, or as a voltage. The pressure cell is usually temperature-compensated to measure pressures at temperatures in the range from -90 °C to +50 °C. A hypsometer can be also used to measure the ambient atmospheric pressure. The hypsometer bases its measurement on the known boiling-point of a fluid at a specific external pressure. By keeping the fluid at its boiling-point and measuring its temperature, the ambient air pressure can be calculated. Some radiosondes do not use a pressure sensor. Instead, the pressure levels are computed from the hypsometric equation using height determined from radar together with the temperature and humidity measurements from the radiosondes.

The temperature sensor which measures the ambient air temperature is usually an electrical device whose resistance or capacitance varies proportionately with the change in temperature. The temperature sensor is exposed during flight to solar short-wave and infrared long-wave radiation which can introduce temperature measurement errors. Short-wave radiation affects the sensor through warming. Long-wave, however, may affect the sensor either by warming or cooling depending on the ambient air temperature and the temperature of bodies surrounding the sensor. Ground, clouds, or the radiosonde balloon act as long-wave radiation sources making it difficult to determine the radiation effect. Radiation effects on temperature sensors also differ in the troposphere and stratosphere owing to the different thermal lapse rate. In general, radiation effects are larger in the stratosphere, where sensors record too warm in the daytime and too cold at night. The differences can be up to a few tenths °C in the troposphere and 1 °C or more in the stratosphere.

The humidity sensor measures the ambient water vapor (humidity). In the past, physical sensors such as hair and goldbeaters skin were used. However, these had poor measurement accuracy or precision, slow response times and limited measurement ranges. Modern electrical sensors, such as the carbon element and the thin-film capacitance sensors are now widely used. Humidity sensors typically used on radiosondes measure relative humidity directly. The humidity sensor can be affected by liquid and frozen precipitation encountered below and in precipitating clouds. Sensors are placed in a duct within the radiosonde or otherwise protected to minimize this effect, but this placement can result in inadequate ventilation.

Common limitations to sensors include sensor lag and hysteresis. Sensor lag mainly affects temperature and humidity sensors. A sensor's time lag is the time that the sensor takes to respond to an instantaneous change in the ambient environment. As the balloon rises, a sensor's value can lag significantly behind the actual values of the atmospheric environment. For temperature sensors, typical lag time is on the order of seconds. For the humidity sensor the lag may range from seconds to minutes. A carbon element sensor may require one minute or more to stabilize to the new conditions when passing through steep humidity gradients at temperatures lower than -40°C. Hysteresis refers to the property of a sensor failing to reproduce the same values when cycling from an initial value to another value and then back again to the original value. For example, when a balloon enters and exits clouds, hysteresis of the carbon element sensor can cause a measurement error. The hysteresis effect in humidity sensors is particularly important due to the highly variable nature of the vertical humidity profile in the lower troposphere.

The range, accuracy, precision and resolution of the various radiosonde sensors is summarized in Table 1 (Wright 1997).

Table 1. Range, accuracy and precision of various rawinsonde measurements.

| Variable | Range | Accuracy | Precision | Resolution |
|---|---|---|---|---|
| Air Temperature | -90 to +50 °C | 0.5 °C | 0.40 °C for 1050-20 mb<br>1.00 °C < 20 mb | 0.1 °C |
| Relative Humidity | 1 to 100% | 5% | 2.5% for 100 - 30%<br>3.5% 29.9 - 1% | 1% |
| Wind Speed | 0 to 225 kt | 3 kt | 6 kt | 1 kt |
| Wind Direction | 360 ° | 5 ° | Varies with wind speed | 1 ° |
| Atmospheric Pressure | 1070 to 2 mb | 2.0 mb for P > 300 mb<br>1.5 mb for 300 < P < 50 mb<br>1.0 mb for P < 50 mb | 1.5 hPa | 0.1 mb for P > 50 mb<br>0.01 mb for P < 50 mb |
| Geopotential Height | 1070-500 mb<br>500-300 mb<br>300-100 mb<br>100-10 mb<br>10-3 mb | < 10 m<br>< 15 m<br>< 20 m<br>< 30 m<br>< 50 m | < 10 m<br>< 15 m<br>< 20 m<br>< 30 m<br>< 50 m | 1 m |

Air temperature has an error on the order of about 1% while humidity errors are about 5%. The data encoding electronics periodically sample the various sensors, then encode and transmit the sensor signals. The sampling rate for each measurement is chosen so that it provides a representative profile of the atmosphere. Present radiosonde sampling rates are in the 1 to 6 second range.

### 3. Wind profile

In the early days of wind measurements using rawinsondes, winds were measured by tracking the radiosonde balloon or pilot balloon (pibal) using an optical theodolite and an assumed rate of ascent for the balloon (Golden 1986). Rawinsondes now receive signals from fixed transmitting stations on the ground or from moving satellites in space. The rawinsonde then either retransmits the received signal to the ground subsystem or processes the signals into Doppler-shift velocities and then transmits. Balloon position and wind data are contained in or derived from this information. The range, accuracy, precision and resolution of the wind measurements are summarized in Table 1. Typical errors are within 5%.

### 4. Thermodynamic diagrams

Data obtained from a typical sounding is shown in Table 2. In order to study the vertical structure and various properties of the atmosphere above certain locations thermodynamic diagrams are used. Observed sounding data (temperature, dewpoint, relative humidity) at selected pressure levels are plotted on these diagrams. These data are considered as essentially vertical profiles.

Table 2. Sounding data at Stony Plain Alberta for 0000 UTC 01 August 1987

| Height (m-AGL) | Pressure (mb) | Temperature ($^oC$) | Dewpoint ($^oC$) | Relative Humidity (%) | Wind Direction (deg) | Wind Speed ($m\ s^{-1}$) |
|---|---|---|---|---|---|---|
| 0 | 914 | 24 | 19 | 74 | 63 | 5.1 |
| 135 | 900 | 23 | 18 | 73 | | |
| 145 | 899 | 23 | 18.1 | 74 | | |
| 342 | 879 | 22 | 18.3 | 80 | | |
| 471 | 866 | 21 | 12.4 | 58 | | |
| 632 | 850 | 19.9 | 11.9 | 60 | 103 | 8.8 |
| 1153 | 800 | 16.2 | 9.2 | 63 | 148 | 9.8 |
| 1654 | 754 | 12.7 | 6.7 | 67 | | |
| 2180 | 708 | 8 | 8 | 100 | | |
| 2274 | 700 | 7 | 7 | 100 | 194 | 20.1 |
| 2524 | 679 | 4.6 | 4.6 | 100 | | |
| 2805 | 656 | 3.4 | 0.8 | 83 | | |
| 2879 | 650 | 2.7 | 2 | 95 | | |
| 3523 | 600 | -1.9 | -2.2 | 98 | 182 | 22.7 |
| 3944 | 569 | -4.9 | -4.9 | 100 | | |
| 4055 | 561 | -5.8 | -13.8 | 53 | | |
| 4571 | 525 | -9.9 | -15.6 | 63 | | |
| 4840 | 507 | -10.6 | -33.6 | 13 | | |
| 4947 | 500 | -10.9 | -33.8 | 13 | 171 | 28.8 |
| 5276 | 479 | -11.5 | -33.6 | 14 | | |
| 6043 | 433 | -16 | -37.2 | 14 | | |
| 6597 | 402 | -21.2 | -31.7 | 38 | | |
| 6634 | 400 | -21.5 | -31.7 | 39 | 166 | 29.9 |
| 6877 | 387 | -23.1 | -31.7 | 45 | | |
| 7423 | 359 | -27.3 | -32.5 | 61 | | |
| 7606 | 350 | -26.5 | -30.9 | 66 | 162 | 26.8 |
| 7647 | 348 | -26.3 | -30.4 | 68 | | |
| 8542 | 307 | -32.9 | -39.4 | 52 | | |
| 8704 | 300 | -34 | -40.4 | 52 | 156 | 30.9 |
| 9563 | 265 | -39.6 | -45.8 | 52 | | |
| 9941 | 250 | -42.9 | m | | 144 | 41.7 |
| 10448 | 231 | -47.1 | m | | | |
| 11363 | 200 | -53.4 | m | | 134 | 39.6 |
| 11823 | 186 | -56.5 | m | | | |
| 11892 | 184 | -55.5 | m | | | |
| 12210 | 175 | -56.8 | m | | 144 | 34.5 |
| 12469 | 168 | -68.7 | m | | 285 | 31.9 |
| 12545 | 166 | -58 | m | | | |
| 12858 | 158 | -57.1 | m | | | |

|  |  |  |  |  |  |  |
|---|---|---|---|---|---|---|
| 13021 | 154 | -53 | m |  |  |  |
| 13187 | 150 | -51.8 | m |  | 181 | 26.8 |
| 13535 | 142 | -49.8 | m |  |  |  |
| 13950 | 133 | -51.4 | m |  |  |  |
| 14144 | 129 | -50.8 | m |  |  |  |
| 14343 | 125 | -51.8 | m |  | 198 | 18 |
| 14655 | 119 | -53 | m |  |  |  |
| 15510 | 104 | -53.1 | m |  |  |  |
| 15758 | 100 | -54.7 | m |  | 214 | 9.8 |

Thermodynamic diagrams consist of several different families of isolines or isopleths such as isobars, isotherms, isentropics or dry adiabats (lines of equal potential temperature) for dry air, saturated adiabats, equisaturated curves (e. g. constant mixing ratio), etc. The importance of these diagrams lies in their speed and convenience of usage for analyzing large amounts information. They allow the study of the vertical stability of the atmosphere and a number of atmospheric processes. Stability indices can be quickly calculated and easily displayed. The vertical structure also aids in indicating the types of air masses present. The uses of these diagrams dictate the choice of coordinates with many different diagrams having been developed for specific purposes. For weather forecasting purposes two types of thermodynamic diagrams in most often used; the tephigram and the Skew T-log $p$ diagram (e.g. Iribarne and Godson 1973).

The name "tephigram" comes from the letters $T$ (temperature) and $\phi$ (entropy). The coordinates of the tephigram are potential temperature ($\ln\theta$) and temperature ($T$). The coordinate $\ln\theta$ is proportional to the specific entropy and is labeled in units of $\theta$ (i.e. the vertical axis is a logarithmic scale of $\theta$). On the tephigram, isotherms and adiabats are straight lines. Isobars are logarithmic, however their curvature is very small over the range of meteorological usage. The Skew T-log $p$ diagram has coordinates of

-ln *p* and *T*. The angles between -ln *p* and *T*. axes depend on the scales used for the coordinate axes (a typical choice is 45°). Isobars and isotherms are straight lines.

## 5. Convective Available Potential Energy (CAPE)

Of special interest in the assessment for the likely severity of convection is the buoyant energy of an air parcel. Buoyant energy represents a conversion of potential energy to kinetic energy and is expected to occur whenever an unstable layer exists. Parcel theory (e.g. Rogers and Yau 1996) is used to estimate the vertical velocity of a convective element. Assumptions in elementary parcel theory are: the air parcel maintains its identity in the thermodynamic process; the parcel does not interact with or perturb its environment; the parcel has uniform properties throughout; and the parcel pressure instantly adjusts itself to the pressure of the surroundings. Under these assumptions we can obtain the following relations (e.g. Rogers and Yau 1996). The thermal buoyancy, *B*, of the parcel is given as:

$$B \equiv \frac{T - T'}{T'} \tag{1}$$

where $T$ is the parcel temperature and $T'$ is the ambient air temperature. The vertical velocity $w(z)$ of the parcel at height $z$ above the height of the level of free convection, $z_0$, can be calculated as:

$$w^2(z) = w_0^2 + 2g \int_{z_0}^{z} \frac{T - T'}{T'} dz \tag{2}$$

The Convective Available Potential Energy (CAPE) between levels $z_0$ and $z$ is defined as:

$$\mathrm{CAPE} \equiv g \int_{z_0}^{z} \frac{T - T'}{T'} dz \tag{3}$$

The CAPE represents the area on a thermodynamic diagram bounded by the process curve of parcel temperature and the ambient temperature profile from height $z_0$ to $z$. The area is proportional to the increase in kinetic energy of the buoyant parcel between the two levels. It is important to note that the vertical velocity derived from this simple parcel theory can be expected to be an upper limit for the following reasons:

1. Aerodynamic drag was neglected.
2. Mixing with ambient air was neglected.
3. Compensating forces of the surrounding air were neglected. These include non-hydrostatic pressure perturbations (e.g. Doswell and Markowski 2004).
4. The weight of condensed water (water drag) which is carried along with the rising parcel was neglected.

Figure 3 shows the Skew *T*-log *p* diagram for the Stony Plain Alberta (WSE) 0000 UTC 01 August 1987 sounding data (listed in Table 2). The temperature and dew points are the plotted lines on the diagram. The parcel ascent curve is shown to the far right and the shaded area indicates the positive CAPE. The calculation of CAPE depends on the values of temperature and dewpoint in the boundary layer, since these will determine the height of the Level of Free Convection (LFC). The choice of which values to use for the initial parcel temperature and dewpoint can be made in several different ways and there is no clear consensus within the convective storm research community as to which method is superior. Three different methods are commonly used:

1. *Surface-based method* which uses surface values for the initial parcel temperature and dewpoint.
2. *Parcel layer method* which estimates the parcel temperature and dewpoint by using average values of the temperature and mixing ratio in some defined boundary layer. The thickness of this boundary layer is often taken to be 100 mb, however this is as arbitrary choice as any other. Craven et al. (2002) showed that choosing a layer method of 100 mb depth gave calculated heights of the lifted condensation level which agreed better with observed cloud base heights than did the surface-based method.
3. *Most Unstable method* which uses the most unstable parcel in the lowest 300 mb (Doswell and Rasmussen 1994). This method essentially provides an upper limit. Choosing the most unstable parcel also has the advantage of being applicable when surface-based parcels or layers are clearly inappropriate, such as in nocturnal inversions. This method will generally give lower heights for the LFC and higher CAPE values than the other two methods.

Since there is no consensus as to which is "best" way to calculate CAPE, it is essential for researchers to clearly define the method they have used.

Still another complication in the calculation of CAPE is the choice of whether or not to use the *virtual* temperature in Eq. (2). Some algorithms used to calculate CAPE use the virtual temperature correction and some do not. Doswell and Rasmussen (1994) discuss the effect of neglecting the virtual temperature correction. It is well known that the virtual temperature $T_v$ is the proper temperature to use in the equation of state $p =$

$\rho RT_v$ (where $p$ is pressure, $\rho$ is air density, and $R$ is the gas constant for dry air) in order that the gas constant $R$ is indeed constant. The virtual temperature is defined as $T_v \equiv T(1+\varepsilon q)$ where $\varepsilon = 0.608$ when the specific humidity $q$ (approximately equal to the mixing ratio) is expressed in g g$^{-1}$. This definition allows the use of the gas constant for *dry* air ($R$ = 287 m$^2$ s$^{-2}$ K$^{-1}$) in the equation of state. The virtual temperature correction is always positive because adding water vapor to a parcel makes it less dense, which can be considered equivalent to warming the parcel. Since CAPE is related to the difference in density between a rising parcel and its environment and, since an accurate calculation of density requires the virtual temperature, the virtual correction should be applied when calculating CAPE. Using the virtual correction in Eq. (3) gives:

$$\text{CAPE} \equiv g\int_{z_0}^{z}\frac{T_v - T'_v}{T'_v}\,dz = R\int_{p}^{p_0}\left(T_v - T'_v\right)d\ln p \qquad (4)$$

For the sounding depicted in Fig. 3 the virtual temperature corrected CAPE for the most unstable parcel is about 2700 J kg$^{-1}$. Values above ~2500 J kg$^{-1}$ are often associated with severe thunderstorms (Rasmussen and Wilhelmson 1983).

To assess the convective potential at different locations on weather charts it is convenient to represent the stability (or instability) of the atmosphere as a number called an index of stability. Two common indices are the Lifted Index and the Showalter Index (e.g. Djurić 1994 pp. 84).

## References

Craven, J. P., R. E. Jewell, and H. E. Brooks, 2002: Comparison between observed convective cloud-base heights and lifting condensation level for two different lifted parcels. *Wea. and Forecasting*, **4**, 885–890.

Djurić, D. 1994: *Weather Analysis*. Prentice Hall Inc., 304 pp.

Doswell, C. A., III, and E. N. Rasmussen, 1994: The effect of neglecting the virtual temperature correction on CAPE calculations. *Wea. Forecasting*, **9**, 625-629.

_______, and P. M. Markowski, 2004: Is buoyancy a relative quantity? *Mon. Wea. Rev.*, **132**, 853-863.

Golden, J. H., R. Serafin, V. Lally, and J. Facundo, 1986: Atmospheric Soundings. *Mesoscale Meteorology and Forecasting*. P. S. Ray, Ed., Amer. Meteor. Soc., 50-70.

Holton, J. R., 1979: *An Introduction to Dynamic Meteorology*. 2nd edition, Acad. Press, New York, 300 pp.

Iribarne, J. V., and W. L. Godson 1973. *Atmospheric Thermodynamics*. D. Reidel Publishing Co., Boston, MA, 222 pp.

Rasmussen, E. N., and R. B. Wilhelmson, 1983: Relationships between storm characteristics and 1200 GMT hodographs, low level shear and stability. Preprints, *13th Conf. on Severe Local Storms*, Tulsa, OK, Amer. Meteor. Soc., 55-58.

Rogers R. R., and M. K. Yau, 1996: *A short course in cloud physics*. 3rd edition. Butterworth-Heinemann, Woburn, MA, 290 pp.

Wright, J. M., Jr., Federal meteorological handbook No. 3, cited 1997. Rawinsonde and pibal observations. [Available online at http://www.ofcm.gov/fmh3/text/default.htm]

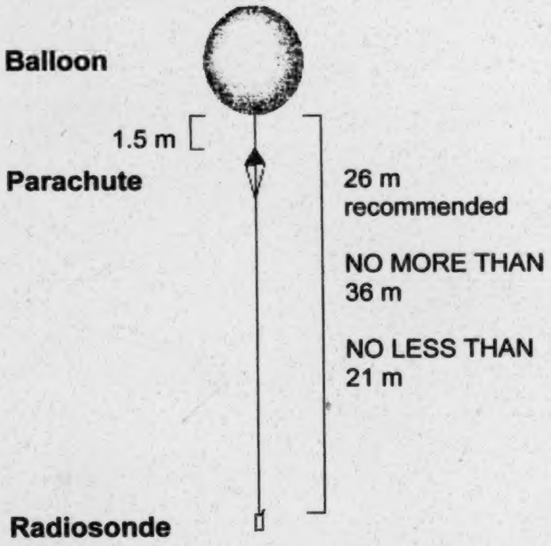
Balloon
1.5 m
Parachute
26 m
recommended
NO MORE THAN
36 m
NO LESS THAN
21 m
Radiosonde

Fig. 1. Schematic of a sonde with balloon, parachute, and train. (From Wright 1997)

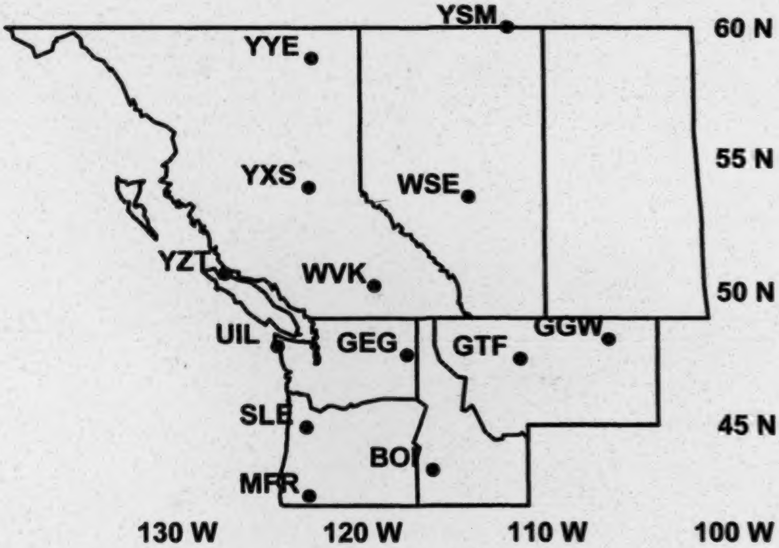
YSM
YYE
YXS
WSE
YZT
WVK
UIL
GEG
GTF
GGW
SLE
BOI
MFR
60 N
55 N
50 N
45 N
130 W
120 W
110 W
100 W

Fig. 2. Map of western Canada and northwest U.S. showing the upper air reporting stations: Fort Nelson (YYE), Prince George (YXS), Vernon (WVK), Port Hardy (YZT), Fort Smith (YSM), Stony Plain (WSE), Quillayute (UIL), Spokane (GEG), Salem (SLE), Medford (MFR), Boise (BOI), Great Falls (GTF), and Glasgow (GGW).

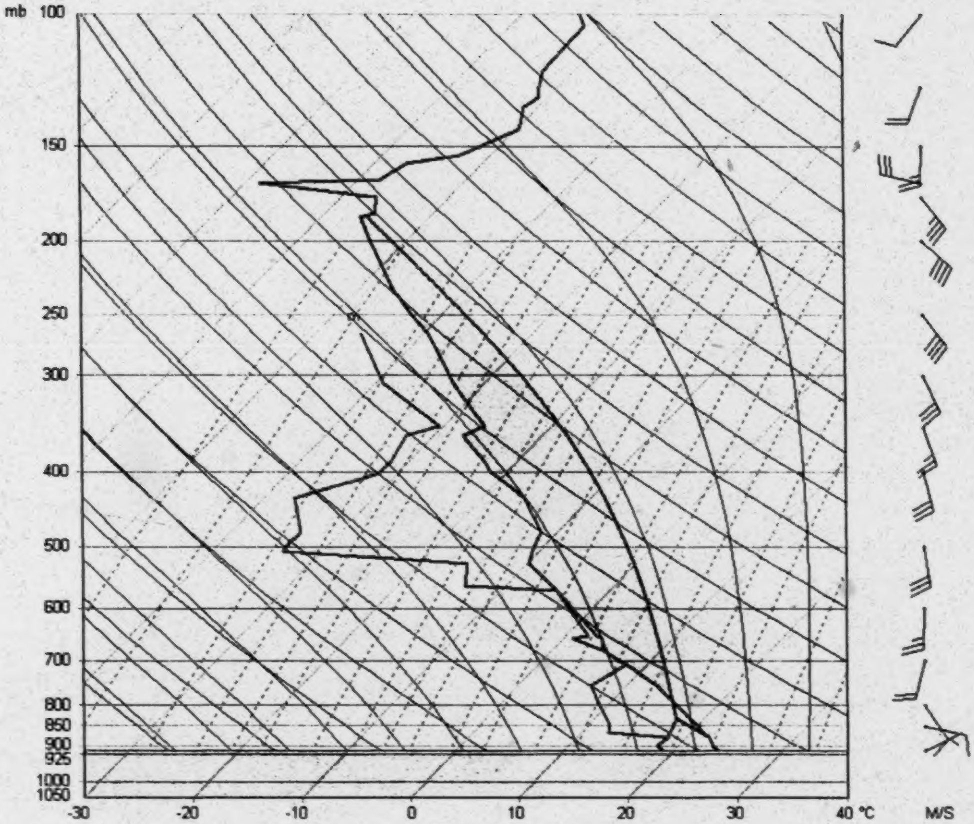

Fig. 3. Skew T-log *p* diagram for the WSE 01 August 1987 0000 UTC sounding. The plot on the right is the temperature (°C) and the plot on the left is the dewpoint (°C). The curved line on the far right is the best level parcel ascent curve. The shaded area indicates the CAPE. Winds are plotted along the right side in m $s^{-1}$. Half barbs denote 5 m $s^{-1}$ and full barbs denote 10 m $s^{-1}$.

# Chapter III

# Forecasting Tornadic Thunderstorms in Alberta using Environmental Sounding Data

## Part I: Wind Shear and Buoyancy

Accepted for publication by: Weather and Forecasting, AMS

## ABSTRACT

This study investigates, for Alberta, whether observed sounding parameters such as wind shear and buoyant energy can be used to help distinguish between thunderstorms with significant (F2 to F5) tornadoes, thunderstorms with weak (F0 and F1) tornadoes, and Non-Tornadic severe thunderstorms. The observational data set contains 87 severe convective storms all of which occurred within 200 km of the upper air site at Stony Plain. Of these storms, 13 spawned significant (F2-F5) tornadoes, 61 spawned weak (F0-F1) tornadoes, and 13 had no reported tornadoes yet produced 3 cm or larger hailstones.

The observations suggest that bulk shear contained information about the probability of tornado formation and the intensity of the tornado. Significant Tornadic storms tended to have stronger shear values than Weak Tornadic or Non-Tornadic severe storms. All Significant Tornado cases had a wind shear magnitude in the 900-500 mb layer exceeding 3 m $s^{-1}$ $km^{-1}$. Combining the 900-500 mb shear with the 900-800 mb shear increased the probabilistic guidance for the likelihood of Significant Tornado occurrence. The data suggest that buoyant energy alone (quantified by the

Most Unstable Convective Available Potential Energy) provided no skill in discriminating between tornadic and Non-Tornadic severe storms, or between Significant and Weak Tornadoes.

## 1. Introduction

During the summer months, severe convective storms with hail and, occasionally, tornadoes are often formed over Alberta, Canada (Smith and Yau 1993a,b; Smith et al. 1998; Hage 2003). Doppler radar observations are often used to provide watches or warnings for tornadic storms. A criterion for issuing a tornado watch is that the Doppler wind measurements indicate meso-cyclone rotation. However, not all tornadoes are preceded by meso-vortices, and not all supercells with meso-vortices spawn tornadoes (Brooks et al. 1994a; Jones et al. 2004). The caveat of current Doppler-derived meso-vortex algorithms is that they only indicate storm rotation once it has commenced. The short lead time for issuing and disseminating tornado watches offers little help for predicting the likelihood of tornado potential with lead times exceeding about 30 minutes.

To forecast the possibility of tornado potential several hours prior to the formation of thunderstorms, one can consider forecasting techniques based on pre-storm sounding data, either from synoptic balloon soundings or from Numerical Weather Prediction soundings at model grid points. Pioneering work in The Thunderstorm Project (Byers and Braham 1949) established the concept of a three stage lifecycle of a thunderstorm from initial cumulus development through storm maturity and eventual dissipation. Byers and Braham discussed the relation between wind shear and convective development. They noted that wind shear tends to retard the growth of non-precipitating cumuli as the sheared flow displaces the centre of maximum buoyancy relative to the core updraft. However, for precipitating storms with sufficiently strong updrafts, shear can enhance the circulation because the shear displaces precipitation out of the updraft, freeing it from the effects of precipitation drag. Fawbush et al. (1951) made early attempts at forecasting tornado potential by relating tornado events with observed soundings of temperature, dewpoint, and wind. Darkow and Fowler (1971) found that tornado environments were characterized by strong wind shear and veering of winds with height. Chisholm and Renick (1972) compared composite hodographs for different types of convective storms observed in Alberta. Weak wind shear was associated with short-lived airmass thunderstorms; while multi-cell storms tended to develop in strong uni-directional shear. Supercells were observed when there was strong directional shear in the lowest 2 km. Rasmussen and Wilhelmson (1983) found that tornadic storms tended to form in environments with high vertical wind shear and high Convective Available Potential Energy (CAPE), while non-rotating storms often formed in environments with low shear and low CAPE. Kerr and Darkow (1996) determined the relationship between environmental instability and tornadic intensity does not always hold. Bluestein and Jain (1985) constructed supercell mean profiles for storms in Oklahoma. McCaul (1991) notes these profiles approximate the findings of other composite tornado proximity studies (e.g. Maddox 1976; Schaefer and Livingston 1988).

Not all supercells produce tornadoes. It still remains uncertain whether tornadic storms develop in a shear environment markedly different from Non-Tornadic severe thunderstorms and whether the intensity of tornadic storms is related to the amount of wind shear. However, there is evidence that the character of vertical wind shear, especially the near-ground layer, does play a significant role in tornado development.

Strong winds in the mid-upper levels are suggested to be associated with Significant Tornadoes (Lemon and Doswell 1979). Colquhoun and Shepherd (1989) examined the relationship between wind shear and tornado intensities. They found the magnitude of surface to 600 mb wind shear was correlated with tornado F-scale intensity. Brooks et al. (1994a) used numerical modeling to show the strength and persistence of low-level meso-cyclones is influenced by the strength of the storm-relative mid-level flow environment. A study of cool season California storms indicated that environmental shear could be used as a discriminating factor between Significant Tornadic thunderstorms and severe thunderstorms which produced only Weak Tornadoes or no tornadoes at all (Monteverdi et al. 2003). Thompson et al. (2003) categorized three groups of severe storms as non-tornadic, weakly tornadic (F0-F1), and significantly tornadic (F2 and greater). They found the 0-1 km vector shear magnitude showed discrimination between the Significant Tornadic and Non-Tornadic events while the 0-6 km vector shear magnitude discriminated between supercells and non-supercells but not between tornadic and non-tornadic events.

The Bulk Richardson Number (BRN) is defined as BRN = CAPE / ($\frac{1}{2}$ $U^2$), (where U represents the difference between the density weighted mean winds in the 0-6 km and 0-500 m layers). As the BRN decreases, multi-cell convection becomes better organized, and at small enough values, quasi-steady supercell convection may occur. A storm environment with a high CAPE value and a BRN value less than about 50 increases the likelihood of a supercell storm, whereas a BRN larger than 50 tends to be associated with multicell storms (Weisman and Klemp 1982, 1986; Thompson et al. 2003). Rasmussen and Wilhelmson (1983) proposed that non-rotating thunderstorms could be found in environments of low shear and low CAPE while tornadic storms occurred with moderate-strong shear ($> 3.5 \times 10^{-3}$ $s^{-1}$ ) and high CAPE ( $> 2500$ J $kg^{-1}$). However, the notion that high threshold values of shear and CAPE can readily discriminate between environments with severe and non-severe thunderstorms may be an overgeneralization. Turcotte and Vigneux (1987) found that combined shear and CAPE criteria could not discriminate between tornadic and non-tornadic severe storms. Brooks et al. (1994b) suggested this lack of discrimination is related to the theory that the occurrence of tornadoes is more closely associated with the development of low-level meso-cyclones (i.e. below 1 km AGL) which are not characterized by CAPE. Brooks et al. (1994b) found that combinations of CAPE and shear did not discriminate between tornadic and non-tornadic severe storms. Rasmussen and Blanchard (1998) showed some shear and CAPE combinations (such as the Energy Helicity Index) seemed useful to identify environments that formed tornadic storms. However, they emphasized that the false alarm rate for these discriminators is still very high. Craven and Brooks (2005) introduced a Strong Tornado Parameter (based on a combination of shear and CAPE) which showed separation between Significant Tornado and significant hail/wind events. Thompson et al. (2003) found marginal differences in CAPE between significant, weak and non-tornadic events. They also found 0-1 km vector shear magnitude provided discrimination between the significant, weak and non-tornadic events, but 0-6 km shear vector magnitude did not. These and other studies (e.g. Kerr and Darkow 1996; Rasmussen and Blanchard 1998; Monteverdi et. al. 2003) emphasize the important point that severe thunderstorm and tornadoes occur within a broad range of shear and CAPE environments. It is extremely important to keep in mind that it is likely the interaction of a number of physical processes that leads to tornadogenesis, and these processes may (or may not) be well represented by particular environmental parameters or variables we choose to examine (e.g. Rasmussen and Blanchard 1998). Even though, for example, the large-scale environment may contain enough deep layer shear there may be insufficient low-level shear or buoyancy to develop a tornado. In addition there may be geographical differences in the storm environment and these differences should also be taken into account when assessing the importance of various sounding derived parameters Rasmussen (2003) showed that climatologically higher lifted condensation levels were associated with combined non-significant supercell plus significant tornadic storms for the Great Plains compared to regions further east. Monteverdi et al. (2003) examined tornadic and non-tornadic severe thunderstorms confined to California. Our research, which examines sounding derived parameters, is also confined to a small region being central Alberta.

This paper deals with forecasting the potential for tornadic development, given the existence of a severe thunderstorm, in the province of Alberta in Canada (Fig.1). Smith et al. (1998) reported that, on average, Alberta has 51 days with hail each summer and 20 days with hailstones greater than 2 cm in diameter. Hage (2003) compiled an extensive tornado climatology covering the period 1879 to 1984. He reported that an average of about 10 tornadoes occur over Alberta each year, slightly less than Newark's (1984) estimate. Tornadic storms in central Alberta are generally associated with hail falling somewhere from the storm complex; yet less than 10% of Alberta hailstorms spawn tornadoes. Similar to other regions, tornadoes in Alberta are classified according to the Fujita damage scale (Fujita 1981) and most are rated at F0 or

F1. However, most of the structural damage, injuries, and fatalities come from the more significant F2, F3, and F4 tornadoes. The motivation for our study is to investigate whether environmental sounding parameters, such as bulk shear, shear ratio, and buoyant energy can be used to distinguish between tornadic and Non-Tornadic severe storms in central Alberta. Furthermore, we want to explore whether sounding parameters can provide guidance to distinguish between Significant (F2-F5) and Weak (F0-F1) Tornadoes. In Part II of this paper we will focus on additional parameters, computed from the sounding data that may be related to tornadogenesis. Specifically, we will examine the role of storm-relative helicity, vortex spin-up by storm convergence, and the amount of vertically integrated atmospheric water vapor (Precipitable Water).

## 2. Observations

The storm climatology data set consists of 87 severe storm events occurring within 200 km of Stony Plain (WSE) between 1967 and 2000 (Fig. 1). The data come from two sources. The storms prior to 1985 were taken from Hage's (2003) dataset, while those from 1985 and later were taken from the Severe Storm Archive of Environment Canada. Hage (2003) documented the date, location, and detailed type of damage of all recorded tornadoes occurring over Alberta based on newspaper reports, municipal records, insurance claims, and other archival data. He distinguished between tornadoes and other wind damage events such as downbursts. In this paper a "tornado event" is defined as a single tornado, not several spatially separate sightings of the same tornado. When accounts of a tornado occurred at separate locations within close proximity, this was assumed to be sightings of the same tornado and was taken to be a single event. When several reports of the same tornado occurred, the location with the greatest damage was used for the F-scale rating. All tornado events in Hage's Alberta Tornado Climatology that occurred prior to 1967 were eliminated because there were no soundings released in Alberta before 1967. Environment Canada's Severe Storms Archive was used to find tornado events for the period 1985 to 1997 plus the F3 Pine Lake tornado of 14 July 2000 (Erfani et al. 2002). In addition, we added 13 Non-Tornadic severe storms from the Environment Canada dataset. All these Non-Tornadic severe storms produced hail with sizes reported as 3 cm or larger. We refrained from using surface reports of damaging winds as an additional selection criterion for Non-Tornadic severe storms because Environment Canada's Severe Storms Archive may not always distinguish between convective and non-convective wind gusts.

Storm events were selected within a 200 km radius from the sounding site. Alberta has only one sounding site located at Stony Plain, WSE (53.5° N, 114.1° W, 766 m MSL). The 200 km threshold radius captured most of the Significant Tornado events (≥ F2) while still maintaining a reasonable spatial proximity. The Hage dataset does not record the exact time of day for tornado occurrence, therefore the 0000 UTC (1800 local daylight time) sounding corresponding to the day of the tornado event was chosen. Most Alberta thunderstorms occur in the late afternoon or evening (Newark 1984). From the Environment Canada dataset the mean time for storms with hail sizes of 1 cm or greater is about 2350 UTC with roughly 93% occurring within ± 6 hrs of 0000 UTC. Therefore we feel the choice of 0000 UTC sounding was reasonably representative of the temporal diagnostic storm environment in question. All storms after 1984 occurred with a time window within ± 6 hrs of 0000 UTC. Smaller spatial and temporal constraints may provide better proximity soundings, but at the expense of a smaller data set. To ensure the soundings were most likely to represent the storm environment we implemented additional quality controls. Each sounding was manually inspected using RAOB for Windows software from Environmental Research Services (Shewchuk 2002). Soundings were rejected if the Most Unstable CAPE (Doswell and Rasmussen 1994) was less than 50 J $kg^{-1}$. This eliminated soundings more indicative of dry micro-bursts, dry dust devils, and saturated profiles which may indicate the sounding ascended through a thunderstorm. Soundings suspected of indicating frontal passages were checked against the previous 1200 UTC sounding and rejected if a frontal passage appeared likely. These restrictions resulted in 74 tornado and 13 non-tornado severe thunderstorm events in our dataset while eliminating 30 tornado cases and 1 non-tornado case. The choices of spatial and temporal soundings emphasize the difficulties associated with obtaining a sufficiently large dataset for rare events.

The frequency of tornado occurrence versus F-scale values for our data set is shown in Fig. 2. The F0 tornado events dominate (49 cases) out of the total 74 cases. There were 12 F1 tornadoes, 6 F2 tornadoes, and 6 F3 tornadoes. The F3 Holden tornado of 29 July 1993 and the F3 Pine Lake tornado of 14 July 2000 were analyzed by Dupilka and Reuter (2004). There was only one F4 tornado, the Edmonton F4 tornado of 31 July 1987 (Dupilka and Reuter 2004). There has not been an F5 tornado reported in Alberta. Shown for comparison (Fig. 2; solid line) is the frequency of F-scale tornadoes in Canada during the period 1958 to 1998 (Brooks and Doswell 2001; Dotzek et al. 2003). Approximately 23% of Canadian tornadoes occur in Alberta. The frequency distribution of the Alberta tornado events is similar to that of the entire Canadian tornado events.

Following the study of Thompson et al. (2003), we categorized the tornadic events into two separate classes: Significant Tornado (ST) events that consisted of F2, F3 and F4 tornadoes, and Weak Tornado (WT) events that consisted of F0 and F1 tornadoes. With these two categories the Alberta data set divided into 18% ST cases and 82% WT cases. The ratios of the entire Canadian data set were identical; 18% ST and 82% WT.

### 3. Calculation of sounding parameters

Environmental Research Services has developed an extensive software package (RAOB) to display and analyze sounding data. RAOB software was used to compute sounding parameters for WSE soundings data. Sounding data were obtained from a CD-ROM, *Rawindsonde Data of North America 1946-1992,* and through an on-line database (post 1992) produced jointly by the National Climate Data Center (NDCD) and the Forecast Systems Laboratory (FSL). The sounding data are available online through http://raob.fsl.noaa.gov. Since the wind measurements were archived at fixed pressure levels, bulk shear was computed using

$$\mathrm{SHR} = \frac{\sqrt{(u_2 - u_1)^2 + (v_2 - v_1)^2}}{|z_2 - z_1|} \tag{1}$$

where ($u_x$, $v_x$) denote the zonal and meridional components of the wind vector and $z_x$ denotes the height at pressure level $p_x$. We computed bulk shear in the layers from 900-800 mb (SHR8), 900-700 mb (SHR7), 900-600 mb (SHR6), and 900-500 mb (SHR5).

The terrain of Alberta varies significantly, ranging from mountainous in the west to flatland in the east with numerous valleys and hills in between. The surface pressure values of the storm environment range from about 940 to 900 mb. The wind measurements sampled from surface observation sites indicate significant temporal and spatial variability, which tends to be affected by the differential heating of the uneven terrain. To reduce surface complexities we computed bulk shear values using the 900 mb wind from the sounding rather than the surface-based wind observation. In previous studies wind shear was often computed for specified altitudes instead of pressure levels (e.g. Brooks et al. 1994b, Thompson et al. 2003). The reason for sticking to pressure levels is because these are commonly used by Alberta forecasters. MUCAPE is computed using the virtual temperature of the most unstable parcel in the lowest 300 mb (Doswell and Rasmussen 1994). MUCAPE values are sensitive to the temperature and humidity sounding. Since spatial and temporal variability in temperature and humidity can dominate in the lower-levels, MUCAPE values derived from proximity soundings may not always be representative of the local storm environment.

## 4. Environmental wind shear

### *a. Bulk shear*

Our focus is on finding the correlation between observed shear with the occurrence of Significant Tornado (ST) events, Weak Tornado (WT) events, and Non-Tornadic severe hail (NT) events. Figure 3 shows box and whisker plots for bulk shear (SHR8, SHR7, SHR6, and SHR5) values. The horizontal bar indicates the median value; the gray boxes denote the 25th to 75th percentiles (the so-called 50% boxes), and the whiskers show the full range of shear values. For the 900-800 mb shear the median for the NT case was 5.0 m $s^{-1}$ $km^{-1}$, for the WT case it was lowest at 4.1 m $s^{-1}$ $km^{-1}$, while the ST case was greatest at 7.4 m $s^{-1}$ $km^{-1}$. For the 900-500 mb shear the median for the NT case was 3.4 m $s^{-1}$ $km^{-1}$, for the WT case it was again lowest at 2.2 m $s^{-1}$ $km^{-1}$, and the ST case was largest at 5.0 m $s^{-1}$ $km^{-1}$. For all four layers shown, the median shear values for ST cases were larger than for WT or NT cases. A similar finding is apparent in the 50% gray boxes. The 50% boxes of shear values for the ST events showed little overlap with the WT cases and generally small overlap with the NT cases. For instance, in the 900-500 mb layer, the 25th percentile for the ST (4.3 m $s^{-1}$ $km^{-1}$) cases is separated from the 75th percentile for WT cases (3.8 m $s^{-1}$ $km^{-1}$) and only slightly overlapping the NT 50% box (75th percentile of 4.8 m $s^{-1}$ $km^{-1}$). For all four layers, the WT 50% boxes were consistently lowest. The NT 50% boxes were slightly higher than the WT cases but, generally with a large overlap between these two events.

To determine whether the shear differences between the storm categories within each layer were statistically significant we performed Mann-Whitney (e.g. Miller et al. 1990) tests for the SHR8, SHR7, SHR6, and SHR5 values for pairings of the ST, WT, and NT events. The Mann-Whitney test is a non-parametric rank-randomization two sample test. Whereas the popular student t-test has the inherent assumption that values have a normal bell-shaped distribution, the Mann-Whitney test has no such constraint. The test ranks all of the values from two groups together from lowest to highest, and compares the mean values of the ranking of the two groups. The result is a confidence probability for the question: "If the means of the two groups are the same, what is the chance that random sampling would result in sample means being as far apart as observed in the test?" The student t-test requires samples sizes of 30 or more while the Mann-Whitney test provides statistically reliable results when both sample sizes are greater than 8 (Miller et al. 1990 pp 198 and 308). The Mann-Whitney test for the SHR8 and SHR5 parameters found statistically significant differences at the 1% level between the ST and WT events. Statistically significant differences at the 3-5% level were found for NT-WT pairs based on SHR5, and also NT-ST pairs based on SHR7. There were no significant differences between NT-WT pairs based on SHR8, SHR7 and SHR6 shears. Overall, SHR5 showed statistically significant differences at the 5% or less level between all three categories. This suggests that the bulk shear for the 900 to 500 mb layer provides the best assistance in discriminating between ST, WT, and NT cases, although there appears to be useful discrimination information contained in all shear layers.

It has been suggested that tornadogenesis is closely connected to the formation of a low-level meso-cyclone (e.g. Thompson et al. 2003). Therefore, the shear in the 900-800 mb layer (SHR8) may be associated with the production of low-level meso-cyclones through tilting of horizontal vorticity into the vertical within the inflow region of the updraft. Since SHR8 showed significant differences between the WT and ST cases, it may also be a useful parameter for distinguishing between Weak and Significant Tornado formations.

### *b. Bulk shear ratio*

Reuter and Jacobsen (1993) drew attention to the fact that convection is not only affected by the amount of the bulk shear, but also to the ratio of low-level shear to the total shear. They reported the following findings based on slab-symmetric modeling. When the wind profile indicates a concave bulge (i.e. low-level shear is larger than the deep-layer shear), the updraft/downdraft circulation becomes stronger and more organized in comparison with the linear wind profile. Conversely, the circulation becomes weaker when the wind profile had a convex shape. For a fixed gross shear magnitude, increasing the concave bulge tends to intensify the circulation. Thus the detail of the wind profile can affect the convective storm intensity. Based on the findings by Reuter and Jacobsen, we were interested to determine whether the ratio of shears $\beta$, defined as

$$\beta \equiv \frac{\mathrm{SHR8}}{\mathrm{SHR5}}$$

(2)

could provide information about the likelihood of tornado potential. The box and whisker plot (Fig. 4) compares the $\beta$ values for NT, WT, and ST events. The data suggest that the $\beta$ value did not help distinguish between the three groups. The 25th to 75th percentile range for all cases was similar. The widest overall range occurred for the WT cases ($0.2 \le \beta \le 6.8$), the smallest range was for ST values ($0.1 \le \beta \le 3.6$). The median values showed a very slight increase from NT (1.3) to WT (1.5) to ST (1.7). The small variation in the 50% boxes of all events suggests that the low-level shears were strongly coupled with the deep layer shears. The frequency distribution of $\beta$ values for the combined set of all NT, WT, and ST events (Fig. 5) indicates the narrow range of distribution for a large percentage of $\beta$ values ($1 \le \beta \le 2.$). The maximum frequency of 0.17 occurs for $\beta = 1.4$.

The Alberta storm data suggest that ST events tended to have strong wind shear in the deep layer from 900 to 500 mb. Mann-Whitney statistics showed the SHR5 values appeared to provide the best discrimination between severe thunderstorms that could potentially produce F2-F4 tornadoes from those that likely produced either F0-F1 tornadoes or no tornadoes at all. The low-level shear (900 – 800 mb) could also distinguish significant from Weak Tornadoes. These findings add support to the hypothesis put forth by Johns and Doswell (1992) that severe storms may form tornadoes when low-level shear in the buoyant inflow layer is coupled with deep-layer shear to generate a meso-cyclone. Johns and Doswell state that, in general, strong to violent supercell tornado events observed in lower buoyancy environments are associated with stronger low-level shear values than those observed with higher buoyancy cases. Later work has shown that tornadoes can develop in environments of both low CAPE and low environmental wind speed. (e.g. Kerr and Darkow 1996). This implies that different combinations of buoyancy and shear values could result in tornado development. For example, in low-buoyancy environments, where the amount of deep layer shear is sufficient for the formation of supercells, the low-level shear may augment the updraft enough to promote tornadic development. Observed and modeling results (e.g. Weisman and Klemp 1982; Thompson 2003) have indicated that thunderstorms growing in environments of 0-6 km shear of 3-5 m $s^{-1}$ $km^{-1}$ show a slight tendency for organization into supercells, whereas those growing in environments of 0-6 km shear > 5 m $s^{-1}$ $km^{-1}$ have a some tendency to become stronger and more persistent supercells. Our results show that NT and ST storms had SHR5 shear values in the 25th to 75th percentile that were generally greater than 3 m $s^{-1}$ $km^{-1}$, similar to values for supercell formation. The weaker F0-F1 storms tended to have lower shear values, possibly suggesting that these tornadoes were not all spawned by supercell thunderstorms.

### c. *Directional shear*

As discussed in the introduction, the development and maintenance of supercells and possible tornado formation can be influenced by veering of the wind in the low-levels. To quantify the wind speed and amount of veering we examined an INIS parameter introduced by Colquhoun and Shepherd (1989), which accounts for both speed and directional shear. INIS is proportional to the length of a hodograph between two pressure levels (see Fig. 2 in Colquhoun and Shepherd 1989):

$$\mathrm{INIS} \equiv \frac{\left|\sum[\mathrm{IN(L)} \cdot \Delta p]\right| + \left|\sum[\mathrm{IS(L)} \cdot \Delta p]\right|}{\sum \Delta p \sum |\Delta \mathrm{z}|} \tag{3}$$

where $\mathrm{IN(L)} = |\mathbf{V}_{\mathrm{p}}| \sin\theta$ and $\mathrm{IS(L)} = |\mathbf{V}_{\mathrm{p}}| \cos\theta - |\mathbf{V}_{\mathrm{p+\Delta p}}|$. Here $\theta$ is the angle between wind vectors $\mathbf{V}_p$ and $\mathbf{V}_{p+\Delta p}$ at pressures $p$ and $p + \Delta p$; IN(L) and IS(L) are, respectively, the components of the wind shear in a given layer L, normal to and in the direction of the wind at the base of the layer; IN(L) relates to the directional shear and IS(L) to the speed shear. The INIS values were calculated between pressure levels $p$ and $p + \Delta p$ where $\Delta p$ = 50 mb increments and $\Delta z$ was the height difference between pressure levels.

Similar to bulk shear, we calculated INIS values in the layers 900-800 mb, 900-700 mb, 900-600 mb, and 900-500 mb. Box and whisker plots for INIS shear values are shown for the three storm categories (Fig. 6). As with the SHR bulk shear values, the middle 50% of the INIS shear values of the four layers for the ST cases generally showed significant separation from the WT and NT cases, while there was a large overlap between WT and NT cases. The ST cases had distinctly greatest medians values: the median values for the 900-500 mb layer range from 0.40 (NT) to 0.35 (WT) to 0.63 (ST); for the 900-800 mb layer the median values are 2.91 (NT), 2.69 (WT), and 4.60 (ST). Mann-Whitney tests for paired cases of INIS values within each layer confirmed that the ST cases had statistically significant differences in values (at the 1% or less level) from the NT and WT cases. However, other paired cases generally did not show differences at the 5% level. Overall, INIS values provided slightly less separation of the three cases than SHR bulk shears. Since bulk shear is conceptually a more direct parameter, while offering better discrimination for our data set, it may be more useful for the operational forecaster than INIS shear for assessing tornadic potential.

## 5. Most Unstable CAPE and Bulk Richardson Number

Studies (e.g. Brooks et al. (1994b); Thompson et al. 2003) have found that the amount of buoyant energy by itself offered no useful assistance in discriminating between tornadic and Non-Tornadic severe storms. We turn our attention to the use of Most Unstable Convective Available Energy (MUCAPE) to determine whether total buoyant energy can distinguish between NT, WT, and ST events occurring in Alberta. Figure 7 compares the box and whisker plots for the three storm groups. The ST and NT events had similar median MUCAPE values of about 1050 J kg$^{-1}$ while the WT events had the lowest median value (~ 900 J kg$^{-1}$). The WT events showed the widest overall range of MUCAPE values, consistent with the fact that this group contained the most storms. There is no trend toward increasing MUCAPE values being associated with NT through ST storms. The Mann-Whitney tests indicated there were no statistically significant differences for the MUCAPE values between the NT, WT, and ST groups. This suggests that MUCAPE alone offers little help in predicting the likelihood of tornado formation or about the likely intensity of the tornado should it form. We also calculated the mean parcel CAPE (MLCAPE) using lowest 100 mb as the mixed layer (Craven et al. 2002). We found MLCAPE gave a similar distribution to the MUCAPE values, there were no significant differences between the NT, WT, and ST groups.

We next examined a modified form of the Bulk Richardson Number (BRN) to determine if it was useful for discriminating between the three storm types (ST, WT, and NT). Values of BRN were calculated using MUCAPE and 900-500 mb shear (rather than the traditional shear between the 0-0.5 km layer and 0-6 km density weighted mean wind). Figure 8 shows BRN values indicated some discrimination of the ST events from the WT and NT groups. The median values for the NT, WT, and ST cases are 9, 14, and 4 respectively. A Mann-Whitney test confirmed the ST cases showed a difference from the WT cases that is statistically significant at the 5% level. There were no statistically significant differences between the other combinations of cases. Therefore, BRN offers less guidance than shear, but more than MUCAPE. Results showed BRN values of all groups up to the 75th percentile fell below ~ 50, suggesting that many events might have been associated with supercell storms.

## 6. Assessing the risk for Significant Tornadoes

The Alberta data suggest that SHR8 and SHR5 values provide information concerning the conditional likelihood of tornado formation given the occurrence of a severe storm. The scatter plot of SHR5 and SHR8 values (Fig. 9) suggests that a pair of SHR5 and SHR8 threshold values might be more useful than either shear parameter threshold alone to distinguish between ST and WT cases. For each threshold pair (SHR5*, SHR8*) we can associate the (quadrant) parameters space (SHR5 ≥ SHR5*, SHR8 ≥ SHR8*). Figure 9 shows two specific cases of threshold pairs. Using the threshold pair (SHR5* = 3 m $s^{-1}$ $km^{-1}$ , SHR8* = 6 m $s^{-1}$ $km^{-1}$) 77 % of all ST events occurred within this parameter space whereas only 18 % of the WT events were contained here (solid box in Fig. 9; see Table 1). Also, only 23% of the NT cases occurred here. This suggest that the threshold pair (SHR5* = 3 m $s^{-1}$ $km^{-1}$, SHR8* = 6 m $s^{-1}$ $km^{-1}$) offers some skill in providing probabilistic guidance about the conditional likelihood of Significant Tornadoes versus non-Significant Tornadoes. Specifically, it was found that only 23% of all ST events had SHR5 and SHR 8 values that lay outside of the quadrant (SHR5 ≥ 3 m $s^{-1}$ $km^{-1}$, SHR8 ≥ 6 m $s^{-1}$ $km^{-1}$). If we lower the threshold values for the shear values, we increase the size of the quadrant; and this is associated with an increased frequency percentage of ST events. So essentially we can increase the "Probability of Detection" of ST events, however, this also results in an associated increase of the "False Alarm Ratio" of ST events. Suppose we keep the threshold SHR5* = 3m $s^{-1}$ $km^{-1}$, but decrease the SHR8* threshold from 6 m $s^{-1}$ $km^{-1}$ to 4 m $s^{-1}$ $km^{-1}$. Table 1 shows that the frequency percentage values for ST events increases from 77% to 85%, yet at the same time the percentage frequencies for WT and NT events are increased to 30% (from 18%) and 38% (from 23%), respectively. In order to capture all ST events, one could relax the SHR8* threshold to zero m $s^{-1}$ $km^{-1}$ (indicated as the dashed line in Fig. 9). This suggests that *all historic* ST cases for Alberta had a 900-500 mb shear exceeding 3 m $s^{-1}$ $km^{-1}$, yet there were many cases of WT events and NT events that had shears also exceeding that threshold. Increasing the SHR8* threshold to 8 m $s^{-1}$ $km^{-1}$, lowers the percentage frequency of ST events to 46% but improves the "False Alarm Rate" as there were only 8% of WT and NT cases included in this parameter space. It may unwise to place too much emphasis on an inferred False Alarm Rate. Rasmussen and Blanchard (1998) point out that even for relatively strong discriminators their False Alarm Rate was very high. This could likely be generalized to our results as well.

Table 1. Percent occurrence of ST, WT, and NT events for 900-800 and 900-500 mb (SHR8*, SHR5*) shear threshold pairs. Shear is in m $s^{-1}$ $km^{-1}$.

| Shear Thresholds | | Percent Occurrence | | |
|---|---|---|---|---|
| SHR5* | SHR8* | ST | WT | NT |
| 3.0 | 8.0 | 46 | 8 | 8 |
| 3.0 | 6.0 | 77 | 18 | 23 |
| 3.0 | 4.0 | 85 | 30 | 38 |
| 3.0 | 0.0 | 100 | 34 | 54 |

From the preceding discussions it is apparent that a forecaster should decide upon an "acceptable" probability of occurrence of ST events, while still maintaining a sufficiently low frequency percentage of WT or NT events. In some cases, the risks of missing a significant event may be so crucial that is better to "over forecast" the likely occurrence of Significant Tornadoes. In other situations it may be more prudent to lower the percentage of "false alarms", while allowing for more tolerance of missing a significant event. This probabilistic nature of the risk assessment has been discussed in more detail by Brooks (2004).

## 7. Conclusion and discussion

We investigated the usefulness of selected sounding parameters for discriminating between Significant Tornado (ST), Weak Tornado (WT) and Non-Tornadic severe thunderstorm (NT) events. Bulk shear within the 900-500 mb layer (SHR5) showed statistically significant differences for values between the NT, WT and ST events. The low-level shear in the 900-800 mb layer (SHR8) also showed skill in discriminating ST events from WT events. These differences suggest that shear threshold pairs (SHR5*, SHR8*) might help to assess the potential for thunderstorms to become tornadic. Also, the thresholds could be useful for separating Significant Tornadoes from Weak Tornadoes. The Alberta data suggest that the threshold pair of (SHR5* = 3 m $s^{-1}$ $km^{-1}$, SHR8* = 6 m $s^{-1}$ $km^{-1}$) would have captured roughly about 75% of the ST cases. To use these thresholds, a forecaster would have to decide if the corresponding percentage of "False Alarms" is acceptable. Lowering the number of "False Alarm" values is, however, associated with a corresponding lowering of the probability of detection of these significant events (Brooks 2004). It is interesting to note the F4 Edmonton tornado of 31 July 1987 (Dupilka and Reuter 2004) had SHR5 and SHR8 values of 6.5 m $s^{-1}$ $km^{-1}$ and 9.3 m $s^{-1}$ $km^{-1}$ and respectively, well within the parameter space defined by the thresholds in Table 1.

A large portion of the 900-500 mb shear values for NT and ST storms were greater than 3 m $s^{-1}$ $km^{-1}$, similar to the 3-5 m $s^{-1}$ $km^{-1}$ values associated with supercell formation found by other authors (e.g. Weisman and Klemp 1982, Thompson et al. 2003). The weaker WT storms tended to have lower shear values, which may suggest that not all of these storms were associated with supercell thunderstorms. The ratio of shears, $\beta$ (= SHR8/SHR5) did not show any statistically significant differences between any of the three storm groups (NT, WT, ST). The greatest frequency of $\beta$ values occurred between about 1-2. The Edmonton tornado, discussed previously, had $\beta = 1.4$ which corresponded to the maximum frequency of $\beta$ for our tornado data set (Fig. 5).

We found that buoyant energy alone could not distinguish between the three categories of events. A modified form of the Bulk Richardson Number (BRN) showed limited skill in distinguishing between WT and ST events, related to the finding that buoyant energy was not well correlated with different storm categories.

It is important to realize the shortcomings and complications inherent to our empirical study. A major issue is to what extent the observed sounding data released from WSE at 0000 UTC are indeed representative for the airmass which feeds the severe storms. Brooks et al.(1994b) and Monteverdi et al. (2003) discussed the complexities associated with observed proximity soundings. Parameters such as MUCAPE can be very sensitive to low-level changes in temperature and dewpoint. Numerical cloud modeling by Brooks et al. (1994a) showed effects of convection can cause changes in these parameters on the space and time scale comparable to the development of thunderstorms. Markowski et al. (1998) concluded that major variations in thermodynamic parameters can occur over time and space scales comparable to the duration of thunderstorm development. In contrast, Markowski et al. (1998) noted that 0.5-6 km wind shear was fairly uniform over large distances. A study of storm motion by Bunkers (2002) also suggests shear parameters derived from proximity soundings could be more robust and less sensitive to local variations compared to other parameters such as MUCAPE. Our study also is also limited by the relatively small number of

Significant Tornado events. These cases are rare and are coupled with the sparseness of upper air stations in Alberta. The problem of sounding scarcity in Alberta is not likely to change in the foreseeable future. Numerical modeled sounding data may help obtain a larger dataset and also allow for smaller proximity ranges. Future work should include expanding the dataset and investigating the use of numerical model soundings to better simulate local storm environments.

In conclusion, we would like to stress that there does not exist a *complete* understanding of the processes of tornadogenesis, and that our findings should be used as *guidelines*. Our results on shear threshold values should be considered in a probabilistic manner. That is, within the parameter space there are regions where, given the development of a severe thunderstorm, the probability of that thunderstorm becoming tornadic is greater than in other areas. Additionally, there are regions in the parameter space where a given thunderstorm has a greater potential to develop a Significant Tornado.

*Acknowledgements.* This research is supported by the Canadian Foundation for Climate and Atmospheric Sciences (CFCAS). This work would not have been possible without the careful and detailed work by Dr. Keith Hage in assembling a climatology of Alberta tornadoes. The authors are appreciative for the comments and constructive criticisms of the anonymous reviewers.

# REFERENCES

Bluestein, H. B., and M. H. Jain, 1985: Formation of mesoscale lines of precipitation: Severe squall lines in Oklahoma during the spring. *J. Atmos. Sci.,* **42,** 1711-1732.

Brooks, H. E., 2004: Tornado-warning performance in the past and future: A perspective from signal detection theory. *Bull. Amer. Meteor. Soc.*, **85**, 837–843.

_______, and C. A. Doswell III, 2001: Some aspects of the international climatology of tornadoes by damage classification. *Atmos. Res.*, **56**, 191– 202.

_______, _______, and R. B. Wilhelmson, 1994a: The role of midtropospheric winds in the evolution and maintenance of low-level mesocyclones. *Mon. Wea. Rev.*, **122**, 126-136.

_______, _______, and J. Cooper, 1994b: On the environment of tornadic and non-tornadic mesocyclones. *Wea. Forecasting*, **9**, 606-618.

Bunkers, M. J., 2002: Vertical wind shear associated with left-moving supercells. *Wea. Forecasting,* **17**, 845–855.

Byers, H. R., and R. R. Braham Jr., 1949: *The Thunderstorm.* U.S. Government Printing Office, 287 pp.

Chisholm, A. J., and J. H. Renick, 1972: The kinematics of multicell and supercell Alberta hailstorms. Research Council of Alberta Hail Studies Report 72-2, 7 pp.

Colquhoun, J. R., and D. J. Shepherd, 1989: An objective basis for forecasting tornado intensity. *Wea. Forecasting*, **4**, 35-50.

Craven, J. P., and H. E. Brooks 2005: Baseline climatology of sounding derived parameters associated with deep, moist convection. *Nat. Wea. Dig.*, in press.

Darkow, G. L., and M. G. Fowler, 1971: Tornado proximity wind sounding analysis. Preprints, *Seventh Conf. on Severe Local Storms*, Kansas City, MO, Amer. Meteor. Soc., 148-151.

Doswell, C. A., III, and E. N. Rasmussen, 1994: The effect of neglecting the virtual temperature correction on CAPE calculations. *Wea. Forecasting*, **9**, 625-629.

Dotzek, N., J. Grieser, and H. E. Brooks, 2003: Statistical modeling of tornado intensity distributions. *Atmos. Res.*, **67-68**, 163-187.

Dupilka, M. L., and G. W. Reuter, 2004: A case study of three severe tornadic storms in Alberta, Canada. Preprints, *22nd Conf. on Severe Local Storms*, Hyannis, MA, Amer. Meteor. Soc., CD-ROM, 3A.6.

Erfani, A., A. Methot, R. Goodson, S. Belair, K. S. Yeh, J. Cote, and R. Moffet, 2002: Synoptic and mesoscale study of a severe convective outbreak with the nonhydrostatic Global Environmental Multiscale (GEM) model. *Meteor. Atmos. Physics*, **82**, 31-53.

Fawbush, E. J., R. C. Miller, and L. G. Starrett, 1951: An empirical method of forecasting tornado development. *Bull. Amer. Meteor. Soc.*, **32**, 1-9.

Fujita, T. T., 1981: Tornadoes and downbursts in the context of generalized planetary scales. *J. Atmos. Sci.*, **38**, 1511-1534.

Hage, K. D., 2003: On destructive Canadian prairie windstorms and severe winters. *Natural Hazards*, **29**, 207-228.

Johns, R. H., and C. A. Doswell III, 1992: Severe local storms forecasting. *Wea. Forecasting*, **7**, 588–612.

Jones, T. A., K. M. McGrath, and J. T. Snow, 2004: Association between NSSL Mesocyclone Detection Algorithm-detected vortices and tornadoes. *Wea. Forecasting*, **19**, 872-890.

Kerr, B. W., and G. L. Darkow, 1996: Storm-relative winds and helicity in the tornadic thunderstorm environment. *Wea. Forecasting*, **11**, 489-505.

Lemon, L. R., and C. A. Doswell III, 1979: Severe thunderstorm evolution and mesocyclone structure as related to tornadogenesis. *Mon. Wea. Rev.*, **107**, 1184-1197.

Maddox, R. A., 1976: An evaluation of tornado proximity wind and stability data. *Mon. Wea. Rev.*, **104**, 133-142.

Markowski, P. M., J. M. Straka, E. N. Rasmussen, and D. O. Blanchard, 1998: Variability of storm-relative helicity during VORTEX. *Mon. Wea. Rev.*, **11**, 2959-2971.

McCaul, E. W., Jr., 1991: Bouyancy and shear characteristics of hurricane-tornado environments. *Mon. Wea. Rev.*, **119**, 1954-1978.

Miller, I., J. E. Freund, and R. A. Johnson, 2000: *Probability and Statistics for Engineers*. 4th ed. Prentice Hall, 612 pp.

Monteverdi, J. P., C. A. Doswell III, and G. S. Lipari, 2003: Shear parameter thresholds for forecasting tornadic thunderstorms in northern and central California. *Wea. Forecasting*, **18**, 357-370.

Newark, M. J., 1984: Canadian tornadoes, 1950-1979. *Atmos. Ocean*, **22**, 343-353.

Rasmussen, E. N., 2003: Refined supercell and tornado forecast parameters. *Wea. Forecasting*, **18**, 530–535.

_______, and R. B. Wilhelmson, 1983: Relationships between storm characteristics and 1200 GMT hodographs, low level shear and stability. Preprints, *13th Conf. on Severe Local Storms*, Tulsa, OK, Amer. Meteor. Soc., 55-58.

_______, and D. O. Blanchard, 1998: A baseline climatology of sounding-derived supercell and tornado forecast parameters. *Wea. Forecasting*, **13**, 1148-1164.

Reuter, G. W., and O. Jacobsen, 1993: Effects of variable wind shear on the mesoscale circulation forced by slab-symmetric diabatic heating. *Atmos. Ocean*, **31**, 451-469.

Shewchuk, J., 2002: RAOB (the Rawinsonde Observation Program) for Windows. Version 5.1, Environmental Research Services. [Available from Environmental Research Services, 1134 Delaware Dr., Matamoras, PA 18336.].

Schaefer, J. T., and R. L. Livingston, 1988: The typical structure of tornado proximity soundings. *J. Geophys. Res.*, **93**, 5351-5364.

Smith, S. B., and M. K. Yau, 1993a: The causes of severe convective outbreaks in Alberta. Part I: A comparison of a severe outbreak with two nonsevere events. *Mon. Wea. Rev.*, **121**, 1099-1125.

_______, and _______, 1993b: The causes of severe convective outbreaks in Alberta. Part II: Conceptual and statistical analysis. *Mon. Wea. Rev.*, **121**, 1126-1133.

_______, G.W. Reuter, and M.K. Yau, 1998: The episodic occurrence of hail in central Alberta and the Highveld of South Africa. *Atmos. Ocean*, **36**, 169-178.

Thompson, R. L., R. Edwards, J. A. Hart, K. L. Elmore, and P. Markowski, 2003: Close proximity soundings within supercell environments obtained from the Rapid Update Cycle. *Wea. Forecasting*, **18**, 1243-1261.

Turcotte, V., and D. Vigneux, 1987: Severe thunderstorms and hail forecasting using derived parameters from standard RAOBS data. Preprints, *Second Workshop on Operational Meteorology*, Halifax, Nova Scotia, Canada, Atmos. Environ. Service/Canadian Meteor. and Oceanogr. Society, 142-153.

Weisman, M. L., and J. B. Klemp, 1982: The dependence of numerically simulated convective storms on vertical wind shear and buoyancy. *Mon. Wea. Rev*., **110**, 504-520.

_______, and _______, 1986: Characteristics of isolated storms. *Mesoscale Meteorology and Forecasting*, P. S. Ray, Ed., Amer. Meteor. Soc., 331-357.

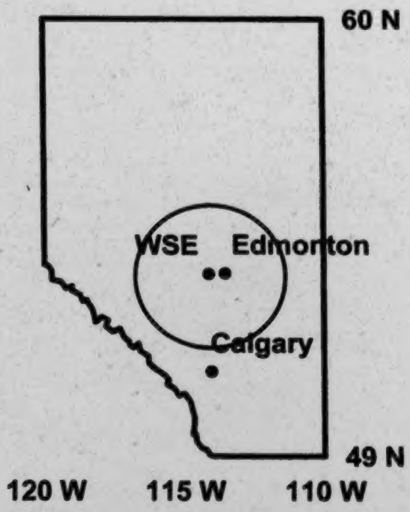
60 N
WSE
Edmonton
Calgary
49 N
120 W
115 W
110 W

Fig. 1. Outline of Alberta showing the locations of the upper air station at Stony Plain (WSE) and the cities of Edmonton and Calgary. The circle marks the 200 km radius from WSE.

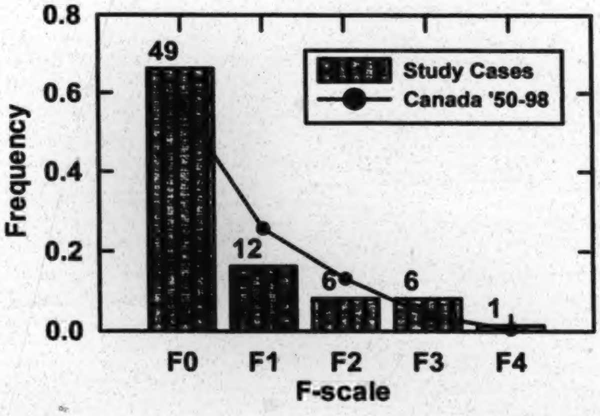

Fig. 2. Frequency of tornadoes in F-scale categories. The bars show the frequency for the study cases in central Alberta during the period from 1967 – 2000. The total number of cases is 74. The value above each bar indicates the number of study cases in that F group. The dots and line shows the frequency of events in Canada during the period from 1950 to 1998.

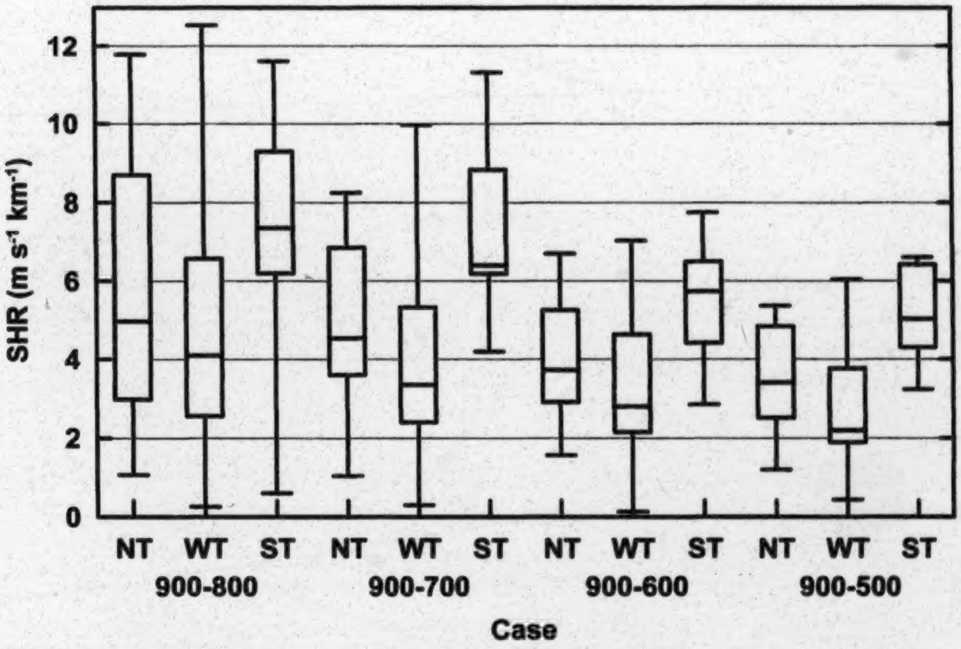

Fig. 3. Box and whiskers plots of bulk shear (SHR) values for Non-Tornado (NT) and tornado (WT, ST) cases in the layers 900-800, 900-700, 900-600, and 900-500 mb. Gray boxes denote 25th to 75th percentiles, with a heavy solid horizontal bar at the median value. The vertical lines (whiskers) extend to the maximum and minimum values.

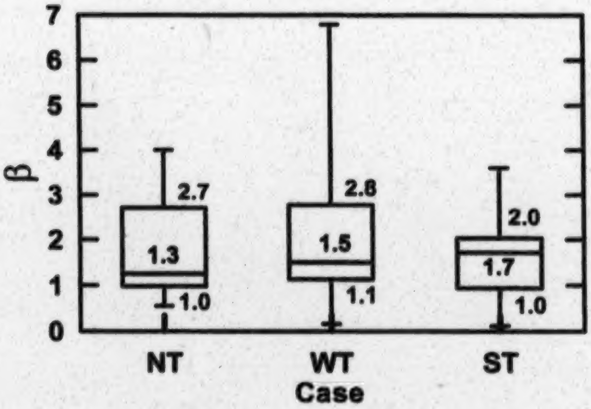

Fig. 4. Box and whisker plots of $\beta$ = SHR8/SHR5 for Non-Tornado (NT) and tornado (WT, ST) cases.

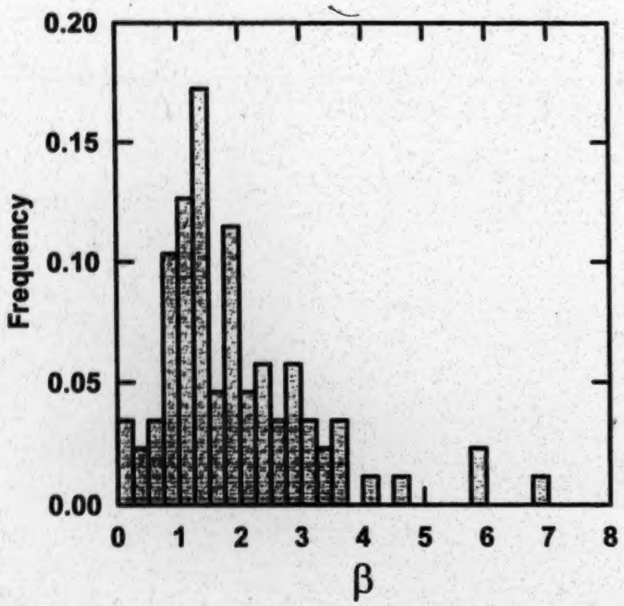

Fig. 5. Frequency of occurrence of $\beta$ for the combined set of cases in the study (NT, WT, and ST).

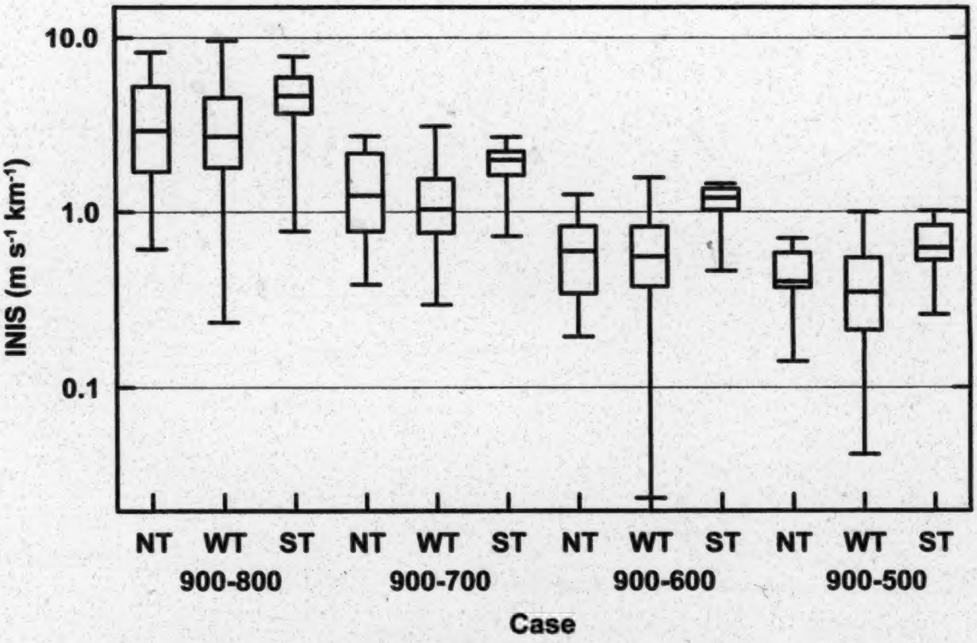

Fig. 6. Box and whiskers plots of INIS values for Non-Tornado (NT) and tornado (WT, ST) cases in the layers 900-800, 900-700, 900-600, and 900-500 mb.

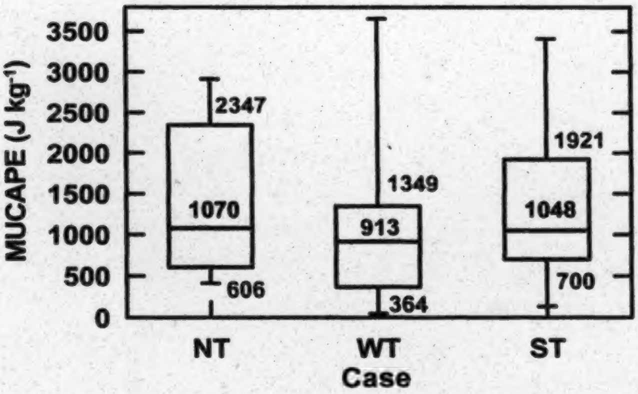

Fig. 7. Box and whiskers plots of MUCAPE for Non-Tornado (NT) and tornado (WT, ST) cases.

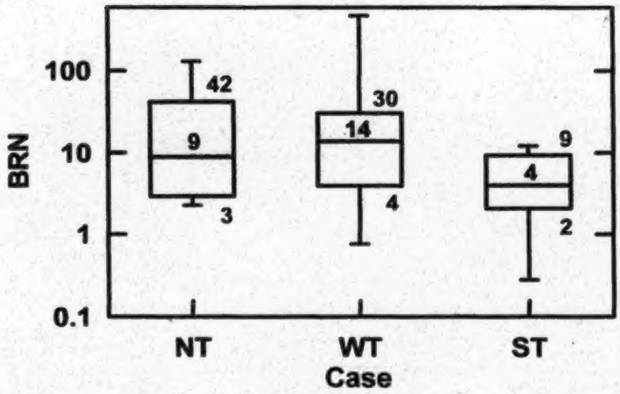

Fig. 8. Box and whiskers plots of Bulk Richardson Number (BRN) for Non-Tornado (NT) and tornado (WT, ST) cases.

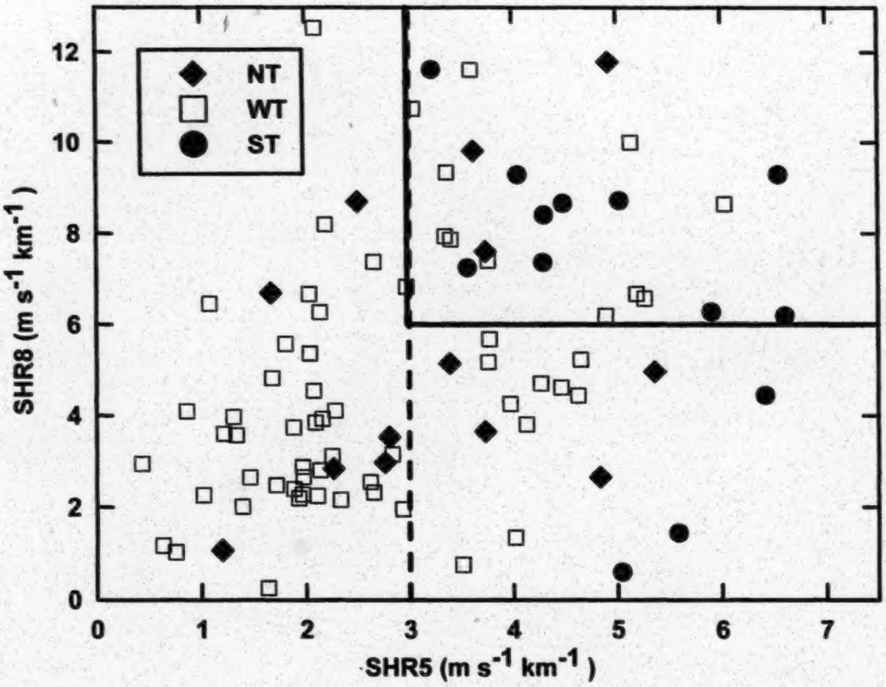

Fig. 9. Scatter plot of SHR8 versus SHR5 for the 87 Alberta storms categorized into NT (diamonds), WT (squares) and ST (dots) cases. The solid (dashed) line marks the 77% (100%) threshold for ST events.

# Chapter IV

## Forecasting Tornadic Thunderstorms in Alberta using Environmental Sounding Data

## Part II: Helicity, Precipitable Water, and Storm Convergence

Accepted for publication by: Weather and Forecasting, AMS

## ABSTRACT

Sounding parameters are examined to determine whether they can help distinguish between Alberta severe thunderstorms that spawn Significant Tornadoes (F2-F4), Weak Tornadoes (F0-F1), or non–tornadic severe storms producing large hail. Parameters investigated included Storm-Relative Helicity (SRH), Precipitable Water (PW), and Storm Convergence (C). The motivation for analyzing these parameters is that, in theory, they might affect the rate of change of vertical vorticity generation through vortex stretching, vortex tilting, and baroclinic effects.

Precipitable Water showed statistically significant differences between Significant Tornadic storms and those severe storms which produced Weak Tornadoes or no tornadoes. All Significant Tornadic cases in our dataset had PW values exceeding 22 mm, with a median value of 24 mm. Values of PW between 19-23 mm were generally associated with Weak Tornadic storms. Computed values of Storm Convergence, height of the Lifted Condensation Level (LCL) and Normalized Most Unstable CAPE (NMUCAPE) did not discriminate between any of the three storm categories. The SRH showed discrimination of Significant Tornadoes from both Weak

Tornadic and Non-Tornadic severe storm groups. The Alberta data suggest that Significant Tornadoes tended to occur with SRH >150 $m^2$ $s^{-2}$ computed for the 0-3 km layer whereas Weak Tornadoes were typically formed for values between 30 and 150 $m^2$ $s^{-2}$. Threshold values of SRH were lower than those suggested in studies based on storm observations throughout much of the United States.

## 1. Introduction

The purpose of this series is to determine to what extent proximity sounding data can be used to distinguish between the potential occurrence of severe storms that spawn no tornadoes, Weak Tornadoes (F0 and F1), and Significant Tornadoes (F2, F3 and F4). The focus is on forecasting severe convective storms in central Alberta, Canada. In Part I of this series (Dupilka and Reuter 2005; hereafter referred to as Part I) the focus was on wind shear, buoyancy (quantified by the Most Unstable Convective Available Energy MUCAPE), and the Bulk Richardson Number. The purpose of this paper is to further explore which characteristic sounding features are supportive for tornadogenesis, and which sounding parameters could help to make a probabilistic distinction between the occurrence of weak and strong tornadoes.

The results presented in Part I indicate that Significant Tornadic storms tended to have larger shear values than both Weak Tornadic and Non-Tornadic severe storms. In contrast, the MUCAPE provided insignificant guidance to predict whether severe storms would spawn tornadoes. A general conclusion of Part I was that most of the Significant Tornadoes in Alberta were formed within supercell storms. However, there were likely many supercell storms which occurred in Alberta that spawned only Weak Tornadoes, and there were storms that produced 3 cm or greater hail but had no recorded tornadoes. This leads to the question: Why do some supercells in Alberta form tornadoes while others fail to do so?

A useful concept to analyze storm rotation is Storm-Relative Helicity (SRH). It is defined for a layer of depth *h* as (Davies-Jones et al. 1990):

$$\mathrm{SRH} = -\int_0^h \mathbf{k} \cdot \left[ (\mathbf{V} - \mathbf{c}) \times \frac{\partial \mathbf{V}}{\partial z} \right] dz \qquad (1)$$

where **V** is the horizontal velocity and **c** is the storm's velocity. The depth *h* is typically chosen as 1 to 3 km. One can visualize SRH as minus twice the area swept out by the hodograph with the origin at the storm motion location. From Eq. (1) it is evident that the magnitude of SRH depends critically on the storm motion **c**. Different methods have been used in an attempt to predict **c** based upon observed sounding data. Maddox (1976) suggested that the speed of the storm motion can be estimated as 75% of the mean wind speed, and that the storm motion vector is directed 30° to the right of the mean wind direction. Other approaches include a balance of mass flux (Colquhoun 1980), and Bunkers internal dynamics technique (Bunkers et al. 2000). However, storm motion algorithms do not include external boundaries (e.g. fronts, drylines, orographic influences) which can radically change their motion resulting in much different SRH values than the general environment. A primary finding from project VORTEX was that SRH was highly variable in both time and space (Markowski et al. 1998b). It may thus be difficult to use SRH based on proximity sounding data for determining whether a specific storm will become tornadic.

The conceptual model of a supercell storm (Lemon and Doswell 1979) includes a Rear-Flank Downdraft (RFD). The strength and persistence of the RFD may be related to downward buoyancy caused by evaporative cooling of rain. Brooks et al. (1994a) postulate that relative humidity in the low levels should affect the amount of evaporative cooling and this, in turn, impacts the dynamics of the RFD. Rasmussen and Blanchard (1998) reported that supercells, with adequate CAPE and shear, often failed to spawn tornadoes and seemed to be correlated with an over abundance of outflow. They suggest relatively low values of boundary layer relative humidity support more evaporative cooling through the evaporation of rain thus leading to stronger outflows. An indicator for the amount of relative humidity in the boundary layer is the Lifted Condensation Level (LCL). Larger LCL heights are generally associated with lower relative humidity. Rasmussen and Blanchard (1998) found the LCL for Significant Tornadic soundings was lower than for Non-Tornadic supercells. Craven and Brooks (2005) determined that mean 100 mb layer LCL heights for Significant Tornadoes were noticeably lower compared to both strong and weak thunderstorms. One might speculate that, since a greater LCL height implies a longer vortex to stretch from cloud base to ground, it may be more difficult to develop a tornado from a higher LCL height than a lower one. However, recently, Rasmussen (2003) suggests that LCL heights of storms may simply be correlated with geographical differences and have little to do with the occurrence or non-occurrence of tornadoes.

Brooks et al. (1994a) suggest that the thermodynamic environment profile affects the formation of low-level meso-cylones. The amount of water vapor available to the storm should affect the amount of precipitation generated and, as a result, the potential for evaporation and generation of vorticity (Brooks et al. 1994a,b). Greater moisture content may mean that the meso-cyclone can move more rain toward the rear flank of the storm, thereby enhancing the development and maintenance of a significant

RFD and resultant vorticity generation. It is speculated that thermodynamic differences may exist between RFDs associated with tornadoes compared to those associated with non-tornadic supercells. Tornadoes are often more likely, and their intensity increases, as the equivalent potential temperature in the RFD increases (Markowski et al. 2002) Markowski et al. tentatively suggested that evaporative cooling and entrainment of mid-level potentially cold air play a smaller role in the formation of RFDs associated with tornadic supercells compared to non-tornadic supercells. Greater water vapor in an airmass may mean there is less potential for evaporative cooling A parameter suitable to quantify the amount of water vapor potentially available is Precipitable Water (PW), which is the total mass of water vapor in a column with unit cross-sectional area:

$$\mathrm{PW} \equiv \int_0^\infty q\rho\, dz \tag{2}$$

where $q$ is the specific humidity and $\rho$ is air density. Precipitable Water has units of kg $m^{-2}$, but it is often expressed in mm of equivalent water depth. Djurić (1994) suggested that minimum PW values supportive for thunderstorms might be regional. He states that in the southern and central United States PW values of 25 mm or more are typically associated with convection; however, over the high plains convection can occur with PW values as small as 10 mm. We were interested to determine whether there are threshold values of PW which characterize environments more conducive to potential tornado development in Alberta. We stress that a high enough "threshold" value for PW may be necessary but certainly not sufficient for the development of significant tornadic storms. Bluestein and Jain (1985) discussed the concept of Tropospheric Humidity (TH) defined as the ratio of precipitable water to saturation precipitable water. This number quantifies an "averaged" relative humidity for the troposphere which may provide additional information about the vertical humidity structure. Clearly, the detailed vertical distribution of water vapor has a significant impact on storm development.

A supercell typically has a meso-cyclone that may be influenced by the interaction of the storm updraft with the vertical shear of the environmental airflow: For a typical supercell the meso-cyclone has a horizontal scale of ~5 km and vertical vorticity of $\zeta \sim 0.01\ s^{-1}$. For the formation of a tornado, the vorticity must be increased one hundred-fold to about $\zeta \sim 1.0\ s^{-1}$, whereas the diameter of the tornado vortex has to be contracted to ~ 100 m. This rapid vortex spin-up may be related to convergence near the storm base which would enhance the vorticity by stretching of the vortex tubes (Lemon and Doswell 1979; Rotunno and Klemp 1985; Ziegler et al. 2001; Dowell and Bluestein 2002b). In Section 4 we will investigate whether there exists a correlation between storm convergence and the potential for tornadogenesis.

In Part II we extend our examination of environmental sounding parameters, using the same data set as in Part I. The focus here is on Storm-Relative Helicity (SRH), Lifting Condensation Level (LCL), Precipitable Water (PW), Tropospheric Humidity (TH), and Storm Convergence (C). The objective is to determine which, if any, of these sounding parameters provide useful information to distinguish between Non-Tornadic, Weak Tornadic, and Significant Tornadic storms in central Alberta. For this study we used a data set containing 87 storms formed over central Alberta. A detailed discussion of the storm data is presented in Part I, and here only a brief summary is given. The storms were categorized into three classes denoted by ST, WT and NT. The 13 ST storms spawned Significant Tornadoes (F2, F3 and F4); the 61 WT storms spawned

Weak Tornadoes (F0 or F1); the 13 NT storms produced hail with reported sizes ≥ 3 cm but they formed no tornadoes. All storms contained in the data set occurred within a radius of 200 km from Stony Plain (WSE) located at 53.5° N, 114.1° W. The unmodified 0000 UTC sounding was used as proximity sounding data for the environmental conditions of the Alberta storms. The RAOB software package from Environmental Research Services was used to calculate selected sounding parameters.

## 2. Storm-Relative Helicity (SRH)

Values of SRH were calculated using Eq. (1) for 0-1 km and 0-3 km AGL layers. The storm motion vector **c** was estimated using Bunker's method (Bunkers et al. 2000). Figure 1a compares box and whisker plots of the 0-1 km SRH results for the ST, WT and NT storms. There was a slight separation of the SRH values between the three cases, with the 50% boxes showing a general increase from NT to WT to ST events. The median values rose from 7 (NT) to 19 (WT) to 60 $m^2 s^{-2}$ (ST). A Mann-Whitney test showed the only statistically significant difference at the 5% level for SRH values occurred between the WT and ST cases. Values of 0-3 km SRH (Fig. 1b) showed a marked difference between the ST events and the other two cases. The median values were 104 (NT), 71 (WT), and 184 $m^2 s^{-2}$ (ST). Mann-Whitney tests confirmed that 0-3 km SRH values for ST events differ from the other two events at the 1% or less level. There was no statistically significant difference between NT and WT values. The 50% box for ST and WT 0-3 km SRH values ranged from about 140 to 230 $m^2 s^{-2}$ for ST storms, compared to 30-130 $m^2 s^{-2}$ for the WT storms. Our results showing 0-3 km SRH provides better discrimination than the 0-1 km SRH is interesting in that other studies

(Thompson et al. 2003, Rasmussen 2003) have found key SRH information was contained in the near ground 0-1 km layer. We tentatively speculate that terrain effects in Alberta may influence the discrimination. The varying terrain in Alberta can cause large spatial and temporal variability in the boundary layer winds. Therefore, 0-3 km layer may be a more robust indicator of SRH for Alberta storm environments.

In Part I we found the 900-500 mb bulk shear (SHR5) provided useful information to distinguish ST cases from WT and NT cases. We emphasize that all of our results are conditional on the existence of a thunderstorm and do not indicate whether or not a thunderstorm will in fact develop. It is desirable to examine the scatter plot of 0-3 km Storm-Relative Helicity versus shear to determine whether a pair of SHR5 and 0-3 km SRH values together is more useful than either parameter alone to distinguish between the three storm categories. The data (Fig. 2) suggest that high bulk shear values were correlated positively with high SRH values. However, there were some data points that indicated high bulk shear environments exhibited low SRH conditions. The 900-500 mb bulk shear value of 3 m $s^{-1}$ $km^{-1}$ presented an effective threshold value, in that all ST cases had shear magnitudes exceeding this threshold. In contrast, ST cases showed a broad range of 0-3 km SRH values ranging from near 0 to 250 $m^2$ $s^{-2}$. Choosing a threshold value of SRH = 140 $m^2$ $s^{-2}$ would include 77% of all ST cases however, 23% of the ST cases occurred with lower SRH values. The scatter plot (Fig. 2) suggests that bulk shear was a more robust indicator for the potential occurrence of ST cases compared to Storm-Relative Helicity. Furthermore, we find that the Storm-Relative Helicity value added little information beyond that available from bulk shear in terms of distinguishing between the potential occurrence of ST, WT and

NT cases. In addition, bulk shear can be computed more directly from a sounding wind profile as it does not depend on methods for estimating the storm motion vector.

An interesting finding is that typical values for Storm-Relative Helicity in Alberta storms are smaller than those found in regions of the continental United States. Thompson et al. (2003) computed SRH values using Bunker's method for a large data set of severe storms in the U.S. Thompson et al. reported a range for 0-3 km SRH values, within the 25th to 75th percentiles, from 172-317 $m^2 s^{-2}$ for storms spawning Significant Tornadoes, while the Weak Tornadic storms had a range from 116-280 $m^2 s^{-2}$. It is not clear why the storm environments in Alberta exhibited less Storm-Relative Helicity conditions in comparison to storms occurring south of 49° N latitude. Even though values of SRH appear to differentiate well between Significant and Weak Tornadoes in both Alberta and the U.S., we find it disconcerting that the magnitude of the values seems to be dependent upon geographical location. This poses a dilemma for the operational forecaster in deciding where to switch from one set of thresholds to another. More research is needed in order to clarify to what extent appropriate threshold values for SRH may depend on geographical regions.

### 3. Humidity parameters

We wished to determine whether the LCL values were correlated with the tendency for thunderstorms to become tornadic and whether they could provide information about the likely intensity of tornadoes. We calculated the height of the lifted condensation level for each case using both the most unstable parcel method (MULCL) and the mean layer parcel method (MLLCL) with the lowest 100 mb mixed layer (Craven et al. 2002). Figure 3 shows the box and whisker plots of MULCL for the NT, WT and ST storms. The WT and ST cases had roughly 50% of the MULCL values between about 500 and 1500 m. The 50% box for the NT events was confined to a narrow range from about 1000 to 1250 m. The median values for all groups were similar at ~ 1000 m. Mann-Whitney tests confirmed there were no statistically significant differences between the groups. This suggests that MULCL was a poor discriminator in central Alberta for the three storm categories. The MLLCL values also indicated no significant distinctions between the groups. The median values for the three MLLCL groups were similar at about 1400 m. It is important to emphasize that with the lifted condensation level, as with most of the other parameters examined in this study, major variations can occur on time and space scales comparable to the development of convective storms (e.g., Brooks et al.1994a; Markowski et al. 1998a) that may not be well represented by proximity soundings. Actual lifted condensation heights of thunderstorms may vary from those presented in this study.

The values of Precipitable Water (PW) for each of the cases in our study are shown in Fig. 4. The median values were 23 (NT), 22 (WT) and 25 (ST) mm. For all cases the 50% box of the PW values encompassed a rather limited range from about 20 to 30 mm with the NT and WT events on the lower end of the range (20-25 mm) and the ST events at the upper end (23-30 mm). This might tentatively suggest that, for our sample, there may have been a greater risk for developing severe thunderstorms (which may then spawn tornadoes) when the environment of the developing storm had values of PW ≥ 20 mm. Precipitable Water values above 20 mm are rare in Alberta where average PW for the summer months (i.e. May through September) is about 15 mm

(Taylor 1999). Therefore PW ≥ 20 mm would put a forecaster for Alberta on alert to further investigate severe thunderstorm potential. The PW box and whiskers plots indicate no clear distinction between values for the NT and WT events. To examine whether PW could be used to separate ST storms the Mann-Whitney test was applied. The results show the difference in values of PW between ST and WT cases are statistically significant at the 1% confidence level. Differences in PW values between ST and NT cases are statistically significant at the 5% level. There was no statistically significant difference in values between the NT and ST cases.

Clearly, the amount of PW is only a single integrated value for the amount of water vapor in the atmosphere, while the details in the humidity profile likely affect storm evolution. It is impractical to analyze and compare the vertical humidity distribution for all the cases. However, we considered it useful to examine the Tropospheric Humidity (TH) values of each event of the dataset. The TH is defined as the ratio of precipitable water to saturation precipitable water (Bluestein and Jain 1985). The saturation precipitable water depends on the temperature profile, rather than the dewpoint profile used for PW. Figure 5 shows the scatter plot of TH versus PW for all storm cases. There is a tendency for larger PW values to be associated with higher TH values, especially for the ST cases. Figure 6 compares the box and whisker plots of TH for the three storm classes. The median values for all three cases were close to 0.6. The Significant Tornado (ST) cases tended to have a large fraction of high TH values.

Based on our findings of typical PW and TH values for Alberta tornadic storms we might speculate that the TH may possibly be associated with the amount of evaporative cooling in RFD formed in Alberta supercells. A higher TH value might be indicative for weaker evaporative cooling, and thus a relatively warm RFD. Since PW and TH are also related, a higher PW value might tend to support warmer RFDs, whereas a lower PW value may suggest cooler RFDs. More research is needed to clarify whether PW values are indeed correlated with the temperature of the descending airflow associated with RFDs in supercells.

## 4. Storm Convergence and Normalized MUCAPE

The evolution of vorticity on the convective scale is given by (e.g. Holton 1979):

$$\frac{d}{dt}(\zeta+f)=-(\zeta+f)\left(\frac{\partial u}{\partial x}+\frac{\partial v}{\partial y}\right)-\left(\frac{\partial w}{\partial x}\frac{\partial v}{\partial z}-\frac{\partial w}{\partial y}\frac{\partial u}{\partial z}\right)+\frac{1}{\rho^2}\left(\frac{\partial \rho}{\partial x}\frac{\partial p}{\partial y}-\frac{\partial \rho}{\partial y}\frac{\partial p}{\partial x}\right) \quad (3)$$

where $(u, v, w)$ denote the wind components in $(x, y, z)$ coordinates, $\zeta = \partial v/\partial x - \partial u/\partial y$, $f$ is the Coriolis factor, $p$ is the perturbation pressure, and $\rho$ is the air density. On the convective time scale appropriate for tornadogenesis, $f$ is small compared to $\zeta$ and can be neglected (Lemon and Doswell 1979). Equation (3) states that the rate of change of vorticity following the motion is given by the sum of the convergence term, the tilting term, and the baroclinic term. Alternatively, the three terms are called the vortex stretching term, the twisting term, and the solenoidal term. Dutton (1986) argued that for the high concentration of vorticity present in tornadoes formed within supercells there is likely a two-step process: first the horizontal vorticity is tilted into the vertical and then the vertical vorticity is amplified through vortex stretching. The importance of tilting the vortex tube by the interaction of storm updraft with vertical shear has long been recognized. Lemon and Doswell (1979) estimated the magnitudes of the vortex tilting and the vortex stretching terms in supercells. They concluded that the tilting term is likely the dominant factor, but that the convergence term is a close rival, especially in the low levels. Dowell and Bluestein (2002a,b) investigated Eq. (3) for a Texas tornadic storm and concluded that tilting of low-level horizontal vorticity into the vertical followed by stretching of the vertical vorticity could be a significant contribution to vorticity production. They further postulated that long-lived tornadoes persist in a region where air near the surface has large vertical vorticity and is convergent. Ziegler et al. (2001) confirmed that tornadogenesis in a low-level mesocyclone was preceded by a period of intense stretching growth of vertical vorticity.

In this study we investigate the possible role of the convergence (or vortex stretching) term in enhancing low-level meso-cyclones. Initially the vorticity is small, but as the mesocyclone develops, $\zeta$ increases in magnitude. Consider the case where the vortex stretching effect is so dominant that the tilting and baroclinic effects can be neglected:

$$\frac{d\zeta}{dt} = \zeta \frac{\partial w}{\partial z} = \zeta \, \mathrm{C} \tag{4}$$

where $\mathrm{C} = \partial w/\partial z = -(\partial u/\partial x + \partial v/\partial y)$ is the convergence. Doppler radar observations indicate that many supercell storms have a meso-cyclone in the layer just above cloud base. Furthermore, the updraft velocity tends to increase above cloud base due to thermal buoyancy causing vortex stretching. It seems feasible there might be a positive correlation between the intensification of the low-level meso-cyclone and storm convergence near the cloud base. Our focus is to compare environmental storm convergence values C with the observed occurrence of ST, WT and NT storms.

In convective storms, observed updrafts are often short-lived and intermittent. Core updrafts can vary significantly from their adiabatic values obtained from a sounding analysis. Nevertheless, we found it worthwhile to use the proximity sounding to obtain a rough estimate of an average value of the Storm Convergence (C). Specifically we estimate

$$\mathrm{C} = \frac{\partial w}{\partial z} \approx \frac{w(z_0 + \delta z) - w(z_0)}{\delta z} \tag{5}$$

where $w(z)$ was assumed to be the adiabatic storm updraft as a function of height $z$. The Level of Free Convection (LFC) is given by $z_0$, while $\delta z$ denotes the vertical extent. The adiabatic storm updraft can be approximated by integrating the thermal buoyancy and assuming $w(z_0) \approx 0$. For each proximity sounding we computed the convergence profile C = C(z) at 5 mb pressure level intervals. We then averaged the C values for the layer from the LFC to 50 mb above the LFC (C50). Figure 7a compares the box and whiskers plots of C50 values for storms categorized into the NT, WT and ST cases. The median C50 values for the three classes is similar at about C50 = 10 x $10^{-3}$ $s^{-1}$. As well, the 50% boxes do not offer a discernable separation between the C50 values for the three cases. The 50% box for the three cases ranges from about 7-12 x $10^{-3}$ $s^{-1}$. It is not obvious that 50 mb is the optimal pressure interval to best quantify the storm convergence. Thus, we also calculated Storm Convergence for the layer from the LFC to 100 mb above the LFC (C100). The box and whisker plots for C100 (Fig 7b) provide similar information to those of C50. The median C100 values for the WT and ST cases were about ~ 9 x $10^{-3}$ $s^{-1}$ while the median for the NT group was only marginally greater at ~ 10 x $10^{-3}$ $s^{-1}$. The Mann-Whitney tests confirmed that no statistically significant differences at the 5% level existed between values of any of the three groups for both C50 and C100. The Alberta data suggest that Storm Convergence above the LFC is not a promising discriminator to assess the potential for development of tornadic thunderstorms. Calculations were made for different layers, but in all cases our findings were that the Storm Convergence had little predictive skill to distinguish between the three storm categories.

The Storm Convergence profile is the derivative of the storm updraft velocity profile, which is related to the vertical profile of thermal buoyancy. The basic idea of scrutinizing the vertical distribution of storm updraft essentially becomes an analysis of scrutinizing the vertical distribution of thermal buoyancy. The total thermal buoyant energy or CAPE depends on the depth of the Free Convection Layer (FCL; Blanchard 1998) and the average magnitude of the buoyancy. Thermal buoyancy can be quantified by the average virtual temperature excess ($\Delta T$) between the lifted parcel and the ambient air temperature. The depth of the FCL is the layer extending from the Level of Free Convection (LFC) to the Equilibrium Level (EL). The same CAPE value could be generated from various combinations of FCL and $\Delta T$. For example, a deep narrow positive area could have the same CAPE value as a shallow wide positive area on a Skew T – log $p$ diagram. The convergence term and also the tilting term in the vorticity equations suggest that, not only is the maximum storm updraft velocity at the Equilibrium Level important, but the vertical distribution of storm updraft velocity may be critical. It follows that the distribution of CAPE, rather than the total CAPE, may have a larger impact upon the enhancement of vertical vorticity (McCaul and Weisman 1996). Blanchard (1998) suggests that parcels will experience faster upward accelerations when large values of CAPE are the result of large buoyancy (i.e. large $\Delta T$) rather than a great depth between the LFC and EL. Greater accelerations may lead to greater stretching of the low-level vortex resulting in intensification of a meso-cyclone which may support and enhance tornadogenesis. Rasmussen and Blanchard (1998) investigated the distribution of CAPE for the 3 km layer above the LFC and found very little difference between significant tornadic storms and supercell storms without significant tornadoes. To examine the distribution of CAPE we have followed the study of Blanchard (1998). We first calculated the Most Unstable CAPE using the virtual temperature of the most unstable parcel in the lowest 300 mb (Doswell and Rasmussen 1994). Then we computed the Normalized Most Unstable CAPE (NMUCAPE) using:

$$\mathrm{NMUCAPE} \equiv \frac{\mathrm{MUCAPE}}{\mathrm{FCL}} \tag{6}$$

We calculated the NMUCAPE value for each sounding to determine whether these values may help distinguish between the potential for ST, WT or NT storms. Figure 8 compares NMUCAPE values for the three storm categories. The box and whisker plots do not suggest any useful skill in discriminating between the three groups. A Mann-Whitney test confirmed that there were no statistically significant differences between the NMUCAPE values for the three categories. As with the Storm Convergence, this suggests that NMUCAPE alone is a poor parameter to use when assessing the risk for a thunderstorm to become tornadic. While there were no significant differences between the groups, the results may suggest that, for our dataset, severe thunderstorms and storms capable of spawning tornadoes had a greatly reduced risk of developing in environments where the NMUCAPE values were less than about 0.06 (i.e. below the

25th percentile of all cases). However, since we did not examine non-severe thunderstorms (e.g., storm producing only small hail) our results do not indicate if NMUCAPE values greater than this threshold are actually common to most thunderstorms. The most strongly correlated values were between the NT and ST groups. This may suggest that the NT supercell events developed in a similar thermal buoyancy environment as ST tornadic storms and supports the notion that CAPE by itself cannot be used to discriminate between events types.

The computed values for Storm Convergence and NMUCAPE are very sensitive to the low-level temperature and dew-point profiles. In Part I we discussed the complexities and uncertainties inherent in using proximity soundings, particularly for near surface conditions. Large variations in thermodynamic quantities can occur on temporal and spatial scales of thunderstorms. The results presented here for the Alberta cases might be affected by the inaccuracies of extending proximity sounding data to the local storm environment. We hasten to point out that these results are based upon analyses of a seemingly small sample of events. However, considering the good reliability of the statistical significance of the results (as pointed out in Part I), it is uncertain whether a larger data set would provide significantly different results.

## 5. Identifying the likelihood of Significant Tornado events

The Alberta data suggest that the following parameters might assist in identifying risk situations of ST cases (we stress that these findings are conditional on the prior existence of a severe thunderstorm and should not be used as a means to predict thunderstorm development): Bulk Shear from 900 to 500 mb (SHR5), low-level shear from 900 to 800 mb (SHR8), 0-3 km Storm-Relative Helicity (0-3 km SRH), and Precipitable Water (PW). SHR5 was found to be more discriminatory than either SHR8 or 0-3 km SRH, and was often correlated with them.

It is instructive to consider the scatter plot of PW versus SHR5 values (Fig. 9). The Significant Tornado events (dots) occur mostly in the upper right quadrant. For each threshold pair (SHR5*, PW*) we can associate a quadrant (SHR5 $\geq$ SHR5*, PW $\geq$ PW*). Table 1 lists the percentage frequency occurrence of ST, WT and NT events for some selected threshold pairs (SHR5*, PW*). For all ST cases, 77% occurred within the quadrant (SHR5 $\geq 3$ m $s^{-1}$ $km^{-1}$, PW $\geq$ 23 mm). However these threshold values allowed the inclusion of 20% of all WT cases and 15% of all NT cases. Increasing the moisture threshold to PW* = 25 mm reduces the historic WT cases to 11% and eliminates all NT cases. However, a 25 mm PW threshold would also lower the frequency of ST cases from 77% to 46%. On the other hand, reducing the moisture threshold to PW* = 21 mm, would identify all ST cases, but with many WT and NT cases as well. Depending on the objectives of a probabilistic forecast of ST events, one might select an "optimal" threshold pair value for (SHR5*, PW*). If it essential to have a high "Probability of Detection" one should use relatively low values for SHR5* and PW* thresholds. In contrast, if it is essential to have a low "False Alarms Ratio" then this implies higher values for SHR5* and PW.

Table 1. Percent occurrence of ST, WT, and NT events for 900-500 mb shear (SHR5*) and Precipitable Water (PW*) threshold pairs. SHR5* is in m $s^{-1}$ $km^{-1}$ and PW* is in mm.

| Thresholds | | Percent Occurrence | | |
|---|---|---|---|---|
| SHR5* | PW* | ST | WT | NT |
| 3.0 | 25 | 46 | 11 | 0 |
| 3.0 | 23 | 77 | 20 | 15 |
| 3.0 | 21 | 100 | 25 | 23 |

## 6. Conclusions

The goal of this study is to explore whether environmental parameters from a proximity sounding can be used to help discriminate between environments of Non-Tornadic severe storms, storms with Weak Tornadoes, and storms with Significant Tornadoes. This study is built on the premise that the formation of a tornado is conditional on the prior formation of a severe thunderstorm and is not intended as a means to predict development of thunderstorms.. The dataset consisted of 74 tornadic storms and 13 Non-Tornadic severe thunderstorms in central Alberta. In Part I we examined bulk shear for different layers and the Most Unstable Convective Available Energy (MUCAPE). In Part II the investigation was extended to examine Storm-Relative Helicity, Precipitable Water, Lifted Condensation Level, Storm Convergence, and Normalized MUCAPE. The major findings were:

1) Of all the tested sounding parameters (listed above), only the 900-500 mb shear (SHR5) provided limited skill to distinguish between WT and NT storms, i.e. the NT and WT categories of storms had very similar distributions of

atmospheric stability, moisture profiles, wind shear and helicity conditions. The Alberta observations suggest that sounding data alone do not provide significant clues about which severe thunderstorms may spawn weak tornadoes.

2) Some sounding parameters such as MUCAPE, NMUCAPE, MULCL, and C did not offer any help in distinguishing between ST, WT and NT cases.
3) Sounding parameters related to the wind regime, such as bulk shear from 900-500 mb, low-level shear from 900-800 mb, and 0-3 km Storm-Relative Helicity provided help to distinguish ST events from both NT and WT events.
4) Precipitable Water provided discrimination of ST events from both NT and WT events.

The general conclusion is that, for Alberta at least, proximity soundings provide limited information to assess the potential intensity of tornadoes should they occur. The historic data suggest that Significant Tornado events occurred in specific parts of parameter space. *All* past Significant Tornado events had 900-500 mb bulk shear values exceeding 3 m $s^{-1}$ $km^{-1}$ and Precipitable Water exceeding 21 mm. Thus, it seems reasonable to conclude that conditional development of a Significant Tornado has a low potential in environments that show lower shear and PW values. The bulk shear threshold of about 3 m $s^{-1}$ $km^{-1}$ for Alberta Significant Tornadoes was similar to the findings reported for a much larger set of storms observed over the continental United States (Rasmussen and Blanchard, 1998; Thompson et al., 2003). Also the Alberta PW threshold for Significant Tornadoes was consistent with Djurić's (1994). The Alberta 0-3 km Storm-Relative Helicity values were generally less than those reported by Thompson et al. (2003).

In Part II we examined the usefulness of a sounding parameter which we termed Storm Convergence (C). This parameter quantifies the vertical derivative of the adiabatic storm updraft, which is related to the vertical gradient of the buoyant energy. Rather than examining the *total* buoyant energy (e. g. Convective Available Energy) the Storm Convergence estimates the local *increase* of buoyancy in a layer selected just above cloud base. Our data analysis using Storm Convergence did not infer any significant skill in distinguishing between different storm categories. However, based on the concept of vortex stretching, there seems to be some theoretical justification for further exploring this parameter. Numerical cloud models might offer a useful tool to clarify whether the magnitudes of Storm Convergence affect the formation and enhancement of storm rotation.

The Alberta dataset of severe storms indicated that deep layer bulk shear (i.e. 900-500 mb shear) values distinguished Significant Tornadic storms from severe storms which produced Weak Tornadoes or no tornadoes. This finding differs from results found in other studies where deep layer shear did not provide discrimination for Significant Tornadoes (Rasmussen and Blanchard 1998; Thompson et al. 2003). As a final comment we would like to offer a tentative speculation of how deep layer shear values may distinguish Significant Tornadoes from Weak Tornadoes and severe Non-Tornadic storms in Alberta. Firstly, we emphasize it is likely the interplay of several environmental variables in sufficient amounts that leads to tornadogenesis (Rasmussen and Blanchard 1998) and isolating any one variable as a type of "magic parameter" is strongly discouraged. For Alberta adequate amounts of water vapor may often not be available for the development of Significant Tornadoes. The limited supply of atmospheric water vapor often curtails the formation of severe thunderstorms. The synoptic conditions necessary to introduce large quantities of water vapor are often associated with the strongest deep layer shear (Smith and Yau 1993). Therefore, stronger deep layer shear may not be, in itself, a deciding factor for the production of Significant Tornadoes. Rather, shear may be associated with a fairly specific synoptic pattern able to provide enough water vapor, among other parameters, to develop Significant Tornadic storms. In contrast, for other regions water vapor may be present in sufficient quantities throughout a much broader range of synoptic conditions and shear regimes. An avenue for further research could include examining various sounding parameters in regions with a similar climatology to Alberta.

In conclusion we suggest that, given the uncertainties in how well proximity soundings represent the actual near-storm environment, one may actually be better off not delving too far into the complexities of proximity sounding details such as the wind profile and gradient of CAPE. This feeling is born out in the nil or weak signals derived from our tested parameters of INIS wind shear, wind shear ratio, NMUCAPE, and storm convergence which depended upon a rather detailed examination of the sounding profile. In contrast, fairly simple approaches such as using bulk shear or precipitable water may, in fact, serve us well when using proximity sounding data to assess the potential for tornadogenesis.

*Acknowledgements*. This research is supported by the Canadian Foundation for Climate and Atmospheric Sciences (CFCAS) through a Research Network Grant and a Project Grant. The authors are appreciative for the comments and constructive criticisms of the anonymous reviewers.

# REFERENCES

Blanchard, D. O., 1998: Assessing the vertical distribution of convective available energy. *Wea. Forecasting*, **13**, 870-877.

Bluestein, H. B., and M. H. Jain, 1985: Formation of mesoscale lines of precipitation: Severe squall lines in Oklahoma during the spring. *J. Atmos. Sci.,* **42,** 1711-1732.

Brooks, H. E., C. A. Doswell III, and J. Cooper, 1994a: On the environment of tornadic and non-tornadic mesocyclones. *Wea. Forecasting*, **9**, 606-618.

_______, _______, and R. B. Wilhelmson, 1994b: The role of midtropospheric winds in the evolution and maintenance of low-level mesocyclones. *Mon. Wea. Rev*., **122**, 126-136.

Bunkers, M. J., B. A. Klimowski, J. W. Zeitler, R. L. Thompson, and M. L. Weisman, 2000: Predicting supercell motion using a new hodograph technique. *Wea. Forecasting* , **15**, 61-79.

Colquhoun, J. R., 1980: A method of estimating the velocity of a severe thunderstorm using the vertical wind profile in the storm's environment. Preprints, *Eighth Conf. on Weather Forecasting and Analysis*, Denver, CO, Amer. Meteor. Soc., 316-323.

Craven, J. P., and H. E. Brooks, 2005: Baseline climatology of sounding derived parameters associated with deep, moist convection. *Nat. Wea. Dig*., in press.

_______, R. E. Jewell, and H. E. Brooks, 2002: Comparison between observed convective cloud-base heights and lifting condensation level for two different lifted parcels. *Wea. Forecasting,* **4**, 885–890.

Davies-Jones, R. P., D. Burgess, and M. Foster, 1990: Test of helicity as a tornado forecast parameter. Preprints, *16th Conf. on Severe Local Storms*, Kananaskis Park, AB, Canada, Amer. Meteor. Soc., 588-592.

Djurić, D. 1994: *Weather Analysis.* Prentice Hall Inc., 304 pp.

Doswell, C. A., III, and E. N. Rasmussen, 1994: The effect of neglecting the virtual temperature correction on CAPE calculations. *Wea. Forecasting*, **9**, 625-629.

Dowell, D. C., and H. B. Bluestein, 2002a: The 8 June 1995 McLean, Texas storm. Part I: Observation of cyclic tornadogenesis. *Mon. Wea. Rev.*, **130**, 2626-2648.

_______, and _______, 2002b: The 8 June 1995 McLean, Texas storm. Part II: Cyclic tornado formation, maintenance, and dissipation. *Mon. Wea. Rev.*, **130**, 2649-2670.

Dupilka, M. L., and G. W. Reuter, 2005: Forecasting tornadic thunderstorm potential in Alberta using environmental sounding data. Part I: Wind shear and buoyancy. Submitted to *Wea. Forecasting*

Dutton, J. A., 1986: *The Ceaseless Wind*. McGraw-Hill, New York, 579 pp.

Holton, J. R., 1979: *An Introduction to Dynamic Meteorology.* 2nd ed. Academic. Press, New York, 300 pp.

Lemon, L. R., and C. A. Doswell III, 1979: Severe thunderstorm evolution and mesocyclone structure as related to tornadogenisis. *Mon. Wea. Rev.*, **107**, 1184-1197.

Maddox, R. A., 1976: An evaluation of tornado proximity wind and stability data. *Mon. Wea. Rev.*, **104**, 133-142.

Markowski, P. M., E. N. Rasmussen, and J. M. Straka, 1998a: The occurrence of tornadoes in supercells interacting with boundaries during VORTEX-95. *Wea. Forecasting*, **13**, 852-859.

_______, J. M. Straka, E. N. Rasmussen, and D. O. Blanchard, 1998b: Variability of storm-relative helicity during VORTEX. *Mon. Wea. Rev.*, **126**, 2959-2971.

_______, _______, and _______, 2002: Direct surface thermodynamic observations within the rear-flank downdrafts of nontornadic and tornadic supercells. *Mon. Wea. Rev.*, **130**, 1692-1721.

McCaul, E. W., and M. L. Weisman, 1996: The dependence of simulated storm structure on variations in the shapes of environment buoyancy and shear profiles. Preprints, *18th Conf. on Severe Local Storms*, San Francisco, CA, Amer. Meteor. Soc., 718-722.

Rasmussen, E. N., 2003: Refined supercell and tornado forecast parameters. *Wea. Forecasting,* **18**, 530–535.

_______, and D. O. Blanchard, 1998: A baseline climatology of sounding-derived supercell and tornado forecast parameters. *Wea. Forecasting*, **13**, 1148-1164.

Rotunno, R., and J. B. Klemp, 1985: On the rotation and propagation of simulated supercell thunderstorms. *J. Atmos. Sci.*, **42**, 271-292.

Smith, S. B., and M. K. Yau, 1993: The causes of severe convective outbreaks in Alberta. Part II: Conceptual and statistical analysis. *Mon. Wea. Rev.*, **121**, 1126-1133.

Taylor, N. M., 1999: Climatology of sounding parameters identifying the potential for convective storm development over Central Alberta. M. S. thesis, Dept. of Earth and Atmospheric Sciences, University of Alberta, 121 pp. [Available from the University of Alberta, 114 St. – 89 Ave., Edmonton, AB, Canada, T6G 2E2.]

Thompson, R. L., R. Edwards, J. A. Hart, K. L. Elmore, and P. Markowski, 2003: Close proximity soundings within supercell environments obtained from the Rapid Update Cycle. *Wea. Forecasting*, **18**, 1243-1261.

Ziegler, C. L., E. N. Rasmussen, T. R. Shepherd, A. I. Watson, and J. M. Straka, 2001: The evolution of low-level rotation in the 29 May 1994 Newcastle–Graham, Texas, storm complex during VORTEX. *Mon. Wea. Rev.*, **129**, 1339-1368.

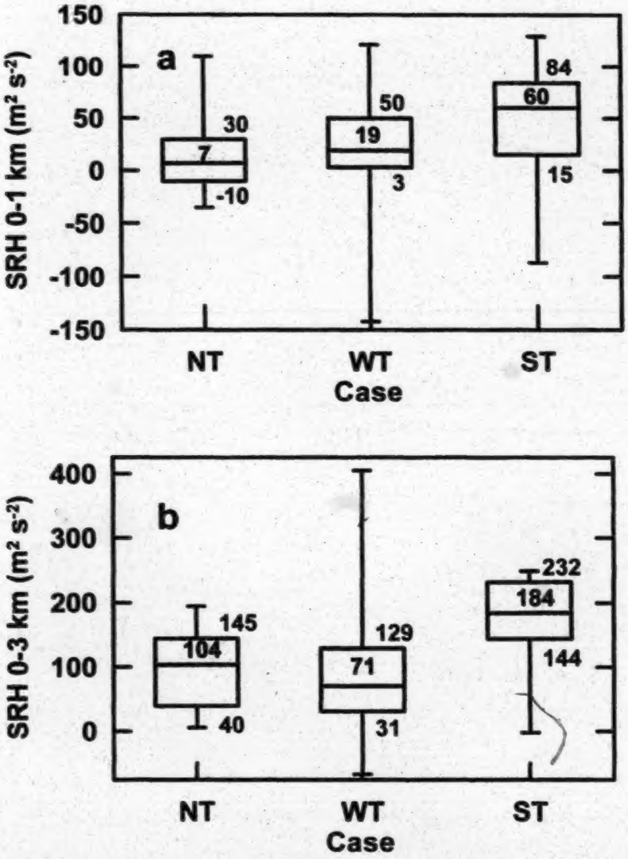

Fig. 1. Box and whiskers plots of SRH estimated via the Bunkers et al. (2000) storm motion algorithm for NT, and WT and ST tornado cases. a) shows SRH in the 0-1 km AGL layer; b) shows SRH in the 0-3 km AGL layer. Gray boxes denote 25th to 75th percentiles, with a heavy solid horizontal bar at the median value. The vertical lines (whiskers) extend to the maximum and minimum values.

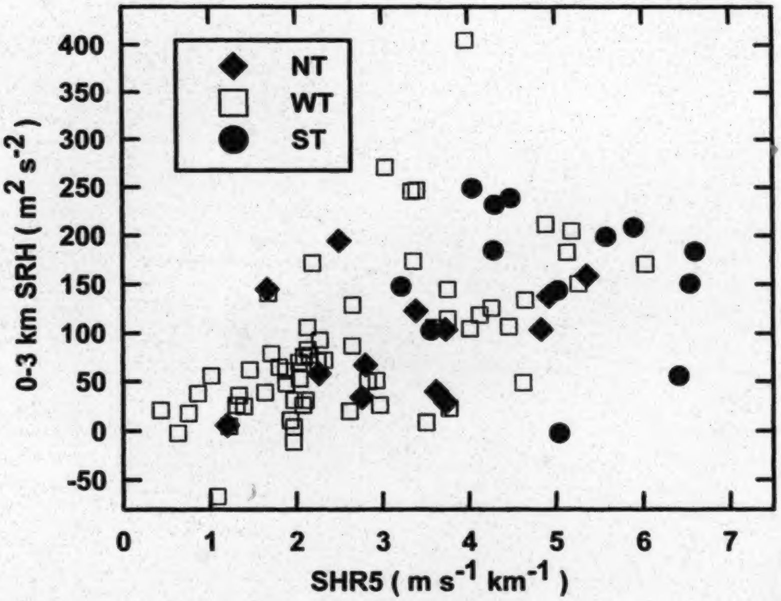

Fig. 2. Scatter plot of 0-3 km SRH versus SHR5 for the 87 Alberta storms categorized into NT (diamonds), WT (squares) and ST (dots) cases.

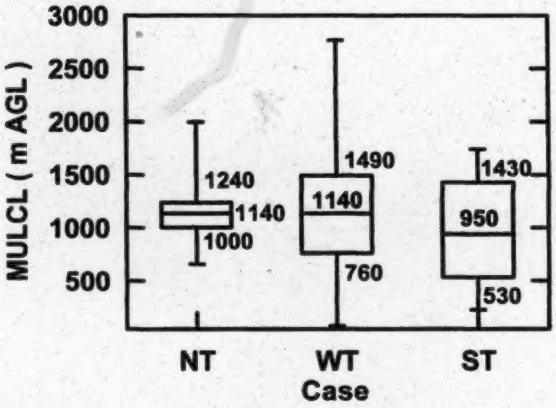

Fig. 3. Box and whiskers plot of the Most Unstable Lifting Condensation Level (MULCL) for Non-Tornado (NT) and tornado (WT, ST) cases.

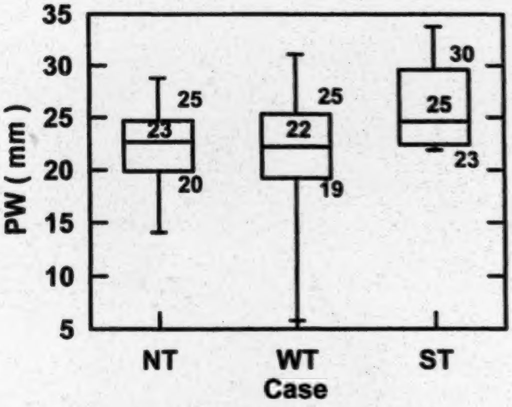

Fig. 4. Box and whiskers plot of Precipitable Water (PW) for Non-Tornado (NT) and tornado (WT, ST) cases

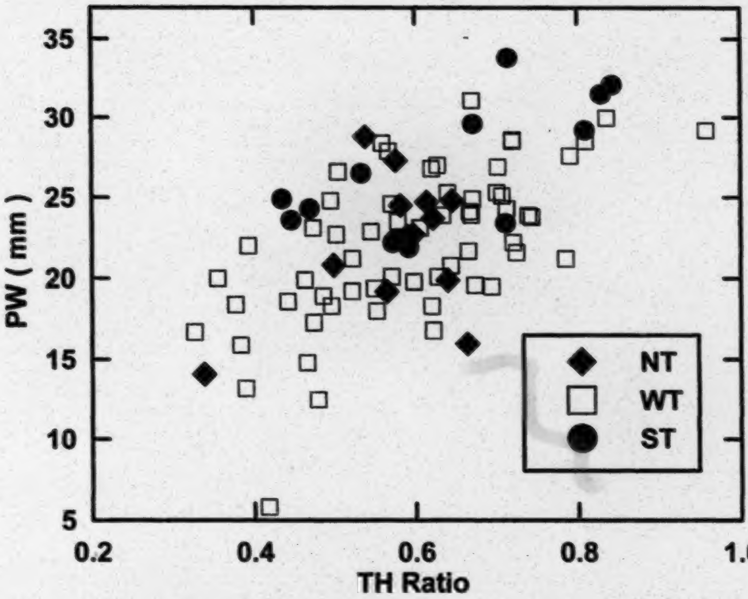

Fig. 5. Scatter plot of Precipitable Water (PW) versus Tropospheric Humidity (TH) for the 87 Alberta storms categorized into NT (diamonds), WT (squares) and ST (dots) cases.

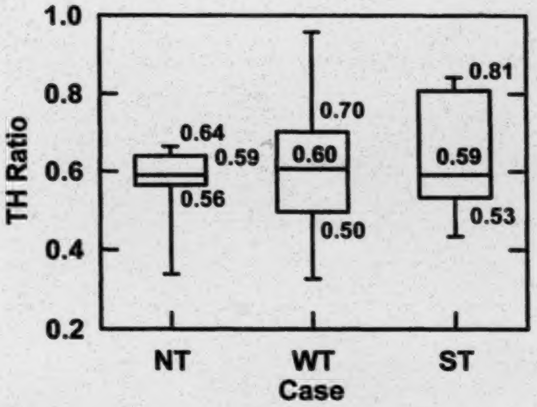

Fig. 6. Box and whiskers plot of Tropospheric Humidity (TH) ratio for Non-Tornado (NT) and tornado (WT, ST) cases

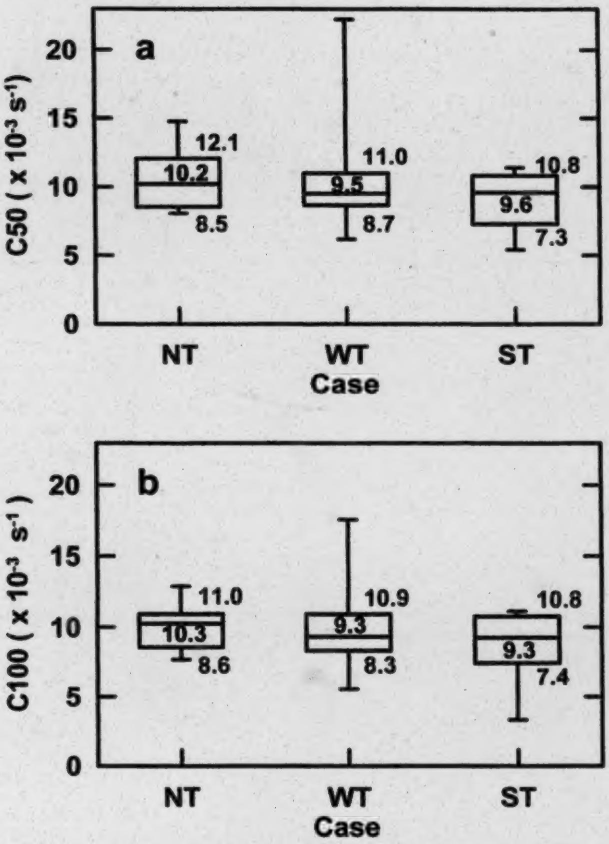

Fig. 7. Box and whiskers plots of average Storm Convergence (C) for Non-Tornado (NT) and tornado (WT, ST) cases: a) C50 in the layer LFC to 50 mb above the LFC; b) C100 in the layer LFC to 100 mb above the LFC.

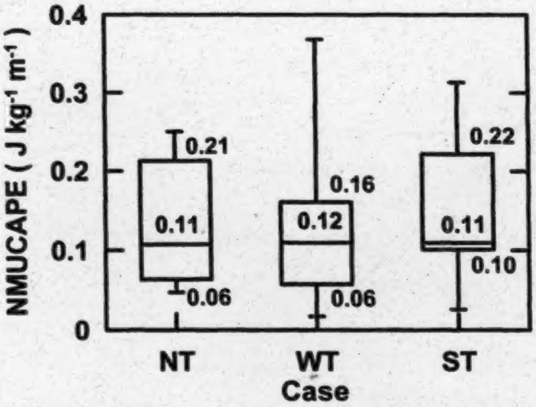

Fig. 8. Box and whiskers plot of Normalized Most Unstable CAPE (NMUCAPE) for Non-Tornado (NT) and tornado (WT, ST) cases

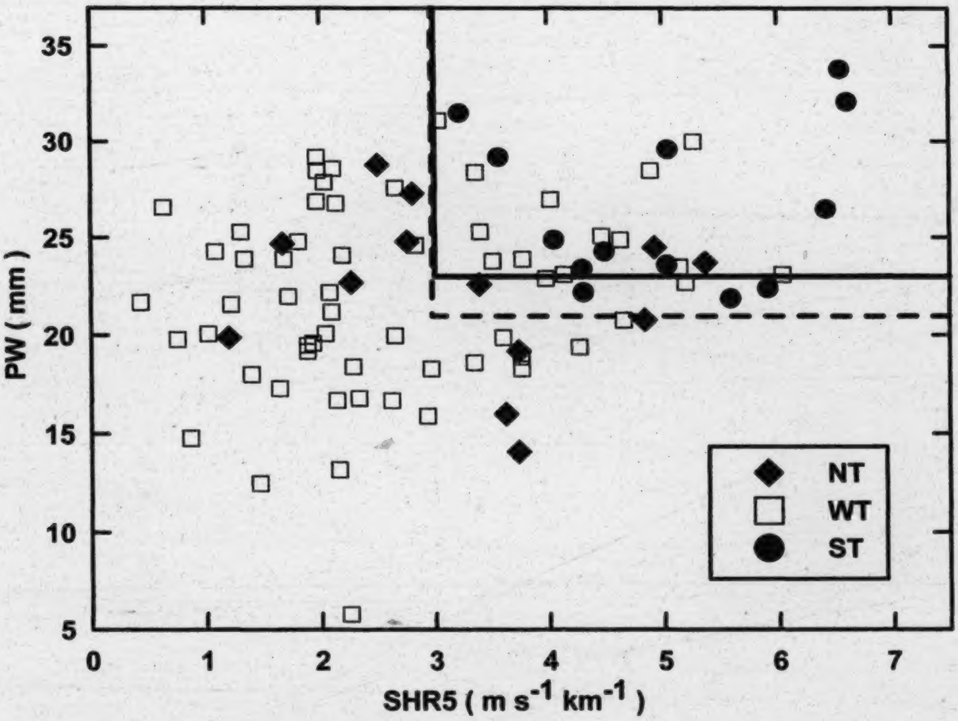

Fig. 9. Scatter plot of PW versus SHR5 for the 87 Alberta storms categorized into NT (diamonds), WT (squares) and ST (dots) cases. The solid (dashed) line marks the 77% (100%) threshold for ST events.

# Chapter V

# An Examination of Three Severe Convective Storms that Produced Significant Tornadoes in Central Alberta

In press: National Weather Digest, National Weather Association

Dupilka, M. L., and G. W. Reuter, 2004: A case study of three severe tornadic storms in Alberta, Canada. Preprints, *22nd Conf. on Severe Local Storms*, Hyannis, MA, Amer. Meteor. Soc., CD-ROM, 3A.6.

## ABSTRACT

Three tornadic thunderstorms with F-scale damage ratings of F3 and F4 occurred in Alberta during the past 20 years. These events were: the Edmonton storm of 31 July 1987, the Holden storm of 29 July 1993, and the Pine Lake storm of 14 July 2000. A synoptic examination of these cases was made with an emphasis on the surface humidity fields. Proximity sounding profiles associated with each event were analyzed. The tracks of the three storms were examined and compared. The intent of this study is to document and compare synoptic and mesoscale patterns and parameters to a previously developed conceptual model of Alberta thunderstorm outbreaks and to deduce meteorological parameters that can be applied operationally to aid forecasters in recognizing the possibility of such outbreaks.

It was found that all three storms developed within a baroclinic zone having bulk vertical wind shear values in excess of 4 m $s^{-1}$ $km^{-1}$. The Holden and Pine Lake

storms were initiated and developed along well-defined surface drylines or moisture fronts. In contrast, the Edmonton storm environment showed no surface dryline as the atmospheric boundary layer was uniformly moist. The three cases showed differences in the vertical profiles of 12 hour temperature change: mainly mid-level cooling affected the Pine Lake storm, mid-level cooling combined with low-level warming below ~850 mb occurred with the Holden storm, while the Edmonton storm was affected by low-level warming below 750 mb, with mid-level temperature change being small. In each case the thermodynamic vertical profile revealed a capping inversion and Convective Available Potential Energy (CAPE) exceeding 2200 J $kg^{-1}$. A comparison of the tracks of the thunderstorms showed that the Pine Lake and Holden storms moved with constant direction and speed. The Edmonton storm, however, made an abrupt change in direction and speed. Thus, extrapolation of thunderstorm movement would not be a viable nowcasting technique in this case.

## 1. Introduction

The Rocky Mountains are an impressive north-south mountain barrier extending 2400 km from Yukon to New Mexico. A significant influence of the mountains is to cause a subsidence inversion that acts as a capping inversion for the build-up of Convective Available Potential Energy (CAPE) in the Alberta region. The capping inversion is a common feature of Alberta whose boundaries extend from 49° to 60° N and 120° to 110° W, with the southwestern border following the Continental Divide (Fig.1). Central Alberta is highly susceptible to severe convection, having on average 52 days with hail fall each summer (Smith et al. 1998). Alberta thunderstorms that spawn tornadoes occur far less frequently (Newark 1984; Bullas and Wallace 1988). Hage (1994, 2003) compiled an extensive tornado climatology starting from 1879 and found that, on average, 10 reported tornadoes occur over Alberta each summer. A major mandate of the Meteorological Service of Canada forecast offices is to issue timely warnings of severe storms so that appropriate safety measures can be taken. The forecasting of severe convective storms will become increasingly important as the populated areas of Alberta continue to expand.

This study focuses on the evolution of three severe convective storms that spawned tornadoes in Alberta. Three convective storm cases were chosen which had the most intense tornadoes recorded during 1983-2003. The cases were: the Edmonton storm of 31 July 1987 that resulted in 27 fatalities and 250 million dollars (Canadian) of property damage (Bullas and Wallace 1988; Charlton et al.1998), the Holden storm of 29 July 1993 which destroyed several well constructed brick and mortar farm buildings

(Knott and Taylor 2000), and the Pine Lake storm of 14 July 2000 that resulted in 12 fatalities and 13 million dollars property damage (Joe and Dudley 2000; Erfani et al. 2002). The Edmonton tornado was classified as F4 on the Fujita F-scale (Fujita 1981). The detailed climatology of Alberta tornados compiled by Hage (1994, 2003) showed that the Edmonton tornado was the only F4 tornado observed in Alberta during recorded history. The Holden and the Pine Lake tornados were both rated F3. There were no other observed F3 tornadoes in Alberta during the period 1983-2003.

A synoptic examination of the three severe storms with an emphasis on the surface atmospheric moisture patterns was conducted. The development of these storms was compared to the conceptual model for severe convection suggested by Smith and Yau (1993a, b). They identified two stages leading to the formation of severe convective storms. Stage 1 is characterized by clear skies and subsiding air ahead of an approaching upper-level ridge, setting up the low-level capping inversion along the foothills. Upper-level warming and associated weak lapse rates contribute to a minimal amount of CAPE. Isolated shallow convection along the foothills may occur as the cap is eroded locally by daytime heating (Reuter and Nguyen 1993). Low-level synoptic pressure gradients cause a light westerly flow which transports moisture away from the foothills. Weak to moderate upper-level winds are associated with relatively weak vertical wind shear. Convective activity is limited to cumulus clouds and isolated thunderstorms along the foothills.

Stage 2 of the conceptual model begins when the upper-level ridge axis moves eastward and an upper-level trough approaches the area. Convection again begins along the foothills during the day. However, strong cooling aloft and surface heating combine with the low-level moisture influx to steepen the lapse rate and buildup a large amount of CAPE. The synoptic pressure gradient over the plains now favors an easterly or southeasterly flow which advects moist air into the low-levels below the capping inversion. There is a continued buildup of latent energy through differential temperature change forming a "loaded gun" sounding (Miller 1972). Low-level heating combined with localized convergence overcome the capping inversion and more vigorous convective storms form along the foothills. These storms move eastward with the mid-tropospheric westerlies. The strong mid-level westerly flow ahead of the advancing trough combines with the intensifying low-level southeasterly flow to create strong vertical wind shear. The convection becomes organized into long-lasting multicell or supercell storms due to the strong vertical wind shear (Chisholm and Renick 1972). The focus of this research is on stage two of development which results in severe thunderstorm outbreaks. Smith and Yau (1993a, b) outline four conditions which are associated with the occurrence of severe storms: a large amount of CAPE, a capping inversion allowing the build up of latent energy, large wind shear, and a trigger to break the cap to release the latent energy. These ingredients are similar to those identified by other researchers (e.g. Fawbush et al 1951; Miller 1972; Johns and Doswell, 1992). Synoptic features for the three thunderstorm events will be compared to determine the validity of Smith and Yau's conceptual model.

A focus of this storm analysis is the evolution of the surface moisture field. Schaefer (1986) suggested that a moisture front can at times trigger thunderstorm development. A moisture front, referred to as a dryline (Fujita 1958), often initiates and organizes spring and summer convection (e.g. Rhea 1966; Ziegler and Hane 1993). The typical criterion for a dryline is a surface dewpoint gradient of 10 °C/100 km or more (Schaefer 1974). In addition, the strong dewpoint gradient must last for at least 6 hours. The 12 °C isodrosotherm (corresponding to vapor mixing ratio of 9 g $kg^{-1}$) was found useful as a "first guess" to locate the dryline position (Schaefer 1973). In the dry air, temperature soundings typically display dry adiabatic lapse rates through the lower troposphere (Schaefer, 1986), whereas the moist air tends to show a low-level capping inversion. Above the capping inversion the air can be well-mixed forming steep mid-level lapse rates. The capping lid allows for the buildup of large CAPE. Thunderstorms that break through the cap can result in supercells. Although the moisture gradient across the dryline is large, the virtual potential temperature contrast is generally small (Ziegler and Hane 1993). A diurnal variation of the moisture gradient often exists (Rhea, 1966) with the afternoon gradient stronger than in the early morning.

This study also serves as a subject of a larger research project in which a database of tornadic and non-tornadic thunderstorm cases in central Alberta is being examined for such parameters as wind shear, helicity, and atmospheric moisture content. The aim of this project is the continuation of a long range goal (Brooks et al. 1994a) to explore whether synoptic scale parameters (e.g. vertical wind shear, precipitable water, buoyancy) can be used to distinguish between the environments of tornadic thunderstorms and non-tornadic severe thunderstorms. A further goal is to determine if these parameters can be useful in discriminating between the F-scale values of tornadic events. Since numerical model prediction of individual thunderstorms and tornadoes is likely to remain problematic (e.g. Brooks et al. 1992), identifying synoptic-scale features that may cause the outbreak of severe convection can be useful for forecasting severe thunderstorms. Here, we examine synoptic features associated with three severe thunderstorms which spawned tornadoes.

This study is organized in the following manner:

- First we describe the synoptic environment associated with the three severe thunderstorm cases. Comparisons between the Smith and Yau conceptual model and the observed synoptic patterns are discussed.
- Next we describe and analyse proximity soundings for each event. Similarities and differences between the Smith and Yau conceptual model and the observed soundings are presented.
- Then we analyse and describe the surface dewpoint fields (dryline) for each event.
- Following this we analyse the storm tracks for the three cases.
- Finally we present a discussion of the results and suggest implementations for operational forecasting.

## 2. Synoptic-scale storm environment

Table 1 compares selected quantities of the three thunderstorms which spawned each of the tornadoes. The times for the tornadoes were: 2100-2200 UTC 31 July 1987 for the Edmonton Tornado, 0345–0405 UTC 30 July 1993 for the Holden Tornado, and 0045-0115 UTC 15 July 2000 for the Pine Lake Tornado. The 0000 UTC (corresponding to 1800 MDT) synoptic charts were chosen for the diagnostic analyses of the three storms. The Pine Lake thunderstorm was well developed at 0000 UTC.

Table 1. A comparison between the Edmonton, Holden, and Pine Lake Tornadoes. The parameters are taken from the 0000 UTC proximity soundings and are described in the text.

| | Edmonton | Holden | Pine Lake |
|---|---|---|---|
| Tornado F-scale value | F4 | F3 | F3 |
| Maximum hail size (cm) | 10 | 8 | 4 |
| Number of fatalities | 27 | 0 | 12 |
| Insured property damage ($Can million) | 250 | 3 | 13 |
| Start time of tornado track | 2100 UTC<br>31 July 1987 | 0345 UTC<br>30 July 1993 | 0045 UTC<br>15 July 2000 |
| End time of tornado track | 2200 UTC<br>31 July 1987 | 0405 UTC<br>30 July 1993 | 0115 UTC<br>15 July 2000 |
| 500 mb wind speed (m $s^{-1}$) | 29 | 24 | 23 |
| 500 mb wind direction | 170° | 180° | 220° |
| 850 mb wind speed (m $s^{-1}$) | 9 | 1 | 7 |
| 850 mb wind direction | 100° | 150° | 350° |
| 12-h $\Delta T$ (°C) at 500 mb | +0.4 | +0.6 | -2.8 |
| 12-h $\Delta T$ (°C) at 850 mb | +4.0 | +3.0 | -4.4 |
| Surface temperature (°C) | 25 | 26 | 23 |
| Surface dewpoint (°C) | 19 | 17 | 14 |
| Cloud base MSL (km) | 2.0 | 2.0 | 1.8 |
| Cloud base temp (°C) | 15 | 14 | 13 |
| Precipitable Water (mm) | 34 | 30 | 23 |
| $\Delta T / \Delta x$ (°C/100 km) at 850 mb | 3.3 | 4.3 | 2.7 |
| CAPE (J $kg^{-1}$) | 2420 | 3190 | 2250 |
| Lifted Stability Index | -8.6 | -8.8 | -8.2 |
| 0-6 km bulk shear (m $s^{-1}$ $km^{-1}$) | 5.2 | 5.0 | 4.3 |
| 0-3 km Storm Relative Helicity ($m^2$ $s^{-2}$) | 153 | -2 | 199 |
| Bulk Richardson Number | 13 | 42 | 18 |

The Edmonton thunderstorm was still active at 0000 UTC with the tornado dissipating. The Holden thunderstorm was developing at 0000 UTC (Knott and Taylor 2000) with the tornado occurring later.

The 500 mb charts valid for 0000 UTC for the Edmonton, Pine Lake and Holden cases are depicted in Fig. 2. Both the Holden and Pine Lake cases (Figs. 2c, e respectively) had a long-wave trough over British Columbia. In the Holden case the trough was oriented south-north through Vancouver Island. The Pine Lake case showed the trough along a more southwest-northeast line, with the southern portion over Vancouver Island and the northern portion advanced into northeast British Columbia. In both cases, the long-wave ridge had advanced over Saskatchewan. Meanwhile the Edmonton case (Fig. 2a) had a low center form over southern British Columbia and a high center located to the northwest. The Holden and Pine Lake patterns were consistent with the Smith and Yau model, which describes an approaching upper-level trough and a ridge moving east of Alberta. The wind speeds at this level over central Alberta were similar in all three cases, ranging from 23 to 29 m $s^{-1}$. The 500 mb wind direction during the Edmonton and Holden storms was southerly while the Pine Lake case had a southwest direction.

At 850 mb a trough was over central Alberta for both the Edmonton (Fig. 2b) and Holden storms (Fig. 2d). This feature would promote a low-level (below ~850 mb) easterly flow into the storm areas throughout the events. Meanwhile the Pine Lake case showed a trough over extreme eastern Alberta, well to the east of the storm location (Fig. 2f). The location of this trough resulted in a north flow across central Alberta. All three cases showed a baroclinic zone over central Alberta. The 850 mb temperature gradient over the baroclinic zone was about 3-4 °C /100 km (Table 1). Similar to 850 mb pattern, the surface pattern for the Edmonton and Holden (Knott and Taylor 2000) storms both showed a low pressure center just east of Edmonton. Meanwhile, the Pine Lake storm had a surface low pressure center in western Saskatchewan.

The 12-h temperature change ($\Delta T$ ) profile is shown in Fig. 3. The $\Delta T$ is the change from the 1200 UTC (morning) sounding to the 0000 UTC (evening) sounding on the day of each tornado event. The values of $\Delta T$ are calculated from actual (where possible) and interpolated sounding temperatures at the surface and then at intervals of 50 mb beginning at 900 mb. Fig. 3 indicates that the Edmonton storm profile showed warming ($\Delta T > 0$) throughout most of the column. Only a narrow region from about 750 to 650 mb showed minimal cooling (< 1 °C). The warming is most pronounced below 850 mb suggesting that diabatic heating played a large role in the destabilization process. The Smith and Yau conceptual model suggests that mid-upper-level cooling is a significant contributor to destabilization, implying that the Edmonton storm differed somewhat from their model. The Holden storm showed significant warming below about 800 mb (the surface warmed by about 11 °C) coupled with cooling of the low to mid-levels from about 800 to 550 mb. The strongest cooling occurred near 800 mb (-2 °C) with steadily decreasing cooling above to 450 mb. The Pine Lake profile showed warming only in a shallow near surface layer (from the surface to about 900 mb) and cooling at all levels above. Similar to the Holden case, the largest cooling occurred near 800 mb (-6 °C). Except for a near ground layer, the whole column cooled with height. The Holden and Pine Lake cases are more consistent with the conceptual model of

Smith and Yau which has mid-level cooling initiated by an advancing trough, while the low-levels are warmed through daytime heating.

### 3. Sounding analysis

Sounding data from the upper air station at Stony Plain (WSE) Alberta (53.55° N, 114.10° W; Fig. 1) were used for this study (Stony Plain is the only upper air station in Alberta). The sounding data are available on a CD-ROM archive of *Rawindsonde Data of North America 1946-1992,* and on-line (1992 to present) produced by the National Climate Data Center (NDCD) and the Forecast Systems Laboratory (FSL). RAOB software from Environmental Research Services was used to calculate various convective parameters.

When examining the convective stability properties of the storm environment it is crucial to use a proximity sounding that indeed contains the thermodynamic profiles of the airmass that the convection forms within (Brooks et al. 1994a). It is recognized that there are important concerns with respect to what constitutes a representative sounding. There cannot be complete confidence that the WSE sounding actually represents the environmental conditions in which the storms developed. Buoyancy, especially, is sensitive to the low-level temperature and dewpoint. For environmental parameters such as CAPE, numerical cloud modeling by Brooks et al. (1994b) shows that the effects of convection can cause changes in these parameters on the space and time scale comparable to the development of thunderstorms. Markowski et al. (1998) concluded that major variations in environmental sounding parameters can occur over time and space scales comparable to the duration of thunderstorm development.

Markowski et al. (1998) also found that shear values from about 500 m to 6 km were fairly uniform over large distances suggesting that shear parameters derived from proximity soundings could be very robust and not as subject to local variations as other parameters such as CAPE.

The following approach was used to synthesize the WSE sounding for the three tornadic storm cases. Low-level adjustments to the temperature and dewpoint were performed on both the 1200 UTC and 0000 UTC. Surface winds were not adjusted. The local surface temperatures and dewpoints for each storm were obtained from the nearest neighbouring weather reporting sites: for the Edmonton and Holden cases the Edmonton city site (YXD) was used and for the Pine Lake Red Deer (YQF; see Fig. 1) was used. The temperature profile was adjusted (if necessary) below 850 mb to ensure that a dry adiabatic lapse rate was not exceeded. The dewpoint values above the surface were not modified for the Edmonton and Holden storms. For the Pine Lake event, however, the 900 mb dewpoint temperature was increased by 2 °C to smooth a large decrease between the adjusted surface and the non-adjusted dewpoints below 850 mb.

The 1200 UTC sounding from WSE for the Edmonton tornado (Fig. 4a) represented conditions prior to thunderstorm development. Very moist conditions prevailed from the surface to about 770 mb. Capping inversions were evident at 850 mb and 730 mb. The lower capping inversion was consistent with the conceptual model of a pre-thunderstorm environment, however, the second cap could add even more to the buildup of CAPE. Over-coming both caps by surface heating alone would require the surface temperature to reach 30 °C (86 °F). Above the two capping inversions there was a drier layer. The wind data sampled by the balloon sounding were not recorded at 1200 UTC.

The 1200 UTC sounding for the Holden storm is shown in Fig. 4c. In this case there is only one capping inversion located at about 800 mb. This single cap is more typical of the conceptual model. Overcoming this cap by surface heating alone would require a temperature of about 30 °C, similar to the Edmonton case. The Holden pre-storm environment was noticeably drier compared to the Edmonton tornado storm case. For the Holden case, the air was close to saturation only near the surface. The observed wind profile showed a weak southerly flow in the low-levels below the capping inversion. The flow became stronger above the cap and veered slightly to the southwest at mid-levels (above ~650 mb). The wind profile had similarities to the conceptual thunderstorm model of Smith and Yau, however the amount of veering in the low-levels was very minimal. The 1200 UTC sounding for the Pine Lake storm environment is depicted in Fig. 4e. A capping inversion was evident at about 850 mb but the inversion was weaker than the Holden case. The surface temperature would have to reach 27 °C to break the capping inversion by surface heating alone. The Pine Lake sounding was the driest of the three cases, showing no layers with saturated air. Winds were light northwest near the surface backing to southwest in the mid-levels. This wind profile is not consistent with the Smith and Yau model of low-level veering winds at 1200 UTC.

The 0000 UTC sounding for the Edmonton storm (Fig. 4b) depicts environmental conditions about 2 hours after the tornado had dissipated, but with the thunderstorm still active. The low-level temperatures and dewpoints were adjusted to the nearest observed values of surface temperature (25 °C) and dewpoint (19 °C). There was several degrees of warming from the surface to about 730 mb. This low-level warming has contributed to eliminating the caps. There was also drying from 870 to about 790 mb. There was very little temperature change above 700 mb. The winds in the low-levels were light easterly which may have continued to advect moist air near the surface. However, there was drying from 850 to 800 mb even though winds in that layer were easterly. Above 800 mb winds veered to southerly. A near saturated layer developed from 700 mb to about 550 mb. Since the thunderstorm developed several hours prior to the 0000 UTC sounding and tracked to the south of WSE there may have been some contamination of the sounding from the thunderstorm itself due to the mid-level southerly flow. Additionally, synoptic scale advection may have contributed to the increased moisture in the mid-levels, however winds above 550 mb were southerly with little change in the moisture profile. This wind profile appeared slightly different than the conceptual model which would suggest a drying southwest flow throughout the mid-levels.

The 0000 UTC sounding for the Holden storm (Fig. 4d.) showed increased moisture throughout most of the column (below 450 mb). Similar to the Edmonton storm a nearly saturated layer developed from 600 to 500 mb. The sounding remained moist well above 500 mb. In this case there were thunderstorms in the vicinity of WSE prior to the Holden storm which may have modified the sounding. Winds in the low-levels became quite light and generally southerly while winds in the 600 to 500 mb layer increased by an average of about 18 m $s^{-1}$ and backed from southwest to south.

The 0000 UTC sounding for the Pine Lake storm is shown in Fig. 4f. Significant cooling occurred from just above the surface to about 400 mb, consistent with the approaching upper trough. The 12-h surface temperature change was only a few degrees indicating that low-level heating alone may not have been the main factor in breaking the capping inversion. Moisture increased significantly below 500 mb. This was especially evident in the low-level layer from ~875 to 790 mb where dewpoints increased by 8-10 °C. Winds in the mid-levels remained quite strong from the southwest throughout the day, consistent with the Smith and Yau model. However, even though the southwest flow in mid-levels persisted, the moisture through that level actually increased.

Profiles of 0000 UTC wet-bulb potential temperature ($\theta_w$) and mixing ratio ($q$) are shown in Fig. 5. The values of $\theta_w$ and $q$ are determined from actual (where possible) and interpolated sounding values of temperature and dewpoint at intervals of 50 mb beginning at 900 mb. Fig. 5a compares the $\theta_w$ profiles for the three cases. All three storms indicated the presence of convective instability below 850 mb (as indicated by a decrease in $\theta_w$ with increasing height). The Edmonton and Holden storms had roughly similar $\theta_w$ profiles below 850 mb while the Pine Lake case had smaller $\theta_w$ values. The Holden storm showed a trend toward a neutral profile from 800 to 650 mb becoming stable above 650 mb. The Pine Lake profile had a stable layer from 850 to 800 mb, then unstable to 750 mb. There was a rather deep neutral layer from 750 to 600 mb. The Edmonton case showed a significant stable layer between 750 and 700 mb, becoming unstable above to 500 mb. The Edmonton storm had much larger $\theta_w$ values in the lower and mid-levels (800-600 mb) than the other two, with the Pine Lake $\theta_w$ values being consistently smallest. The $q$ profiles (Fig. 5b) show the Edmonton storm consistently having the greatest moisture from the 900 to 600 mb than the other two soundings.

Table 1 compares values from the 0000 UTC adjusted proximity soundings for the three events. The Edmonton tornado was the highest rated (F4) on the Fujita damage scale. The 500 mb 12-h temperature changes showed a slight warming in the Edmonton and Holden storm cases, while the Pine Lake storm environment cooled by about 3 °C. At 850 mb the 12-h temperature changes showed warming of 3-4 °C during the Edmonton and Holden storms, unlike the Pine Lake event which cooled by about 4 °C. The 850 mb wind was from the southeast for the Edmonton and Holden storms, whereas the Pine Lake storm had a northerly wind of 7 m $s^{-1}$. The Edmonton storm sounding had the highest Precipitable Water (PW) of 34 mm, similar to the Holden storm (30 mm), while the Pine Lake storm was the driest at 23 mm. The amount of Precipitable Water can act as a threshold for convective precipitation in Alberta (Reuter and Aktary 1995). Djurić (1994, pp. 86) notes that values of PW ≥ 25 mm are conducive to the development of thunderstorms in the southwestern United States.

Convective Available Potential Energy (CAPE) was calculated using the virtual temperature for the ascent curve of the surface-based parcel. The 0000 UTC soundings all had very high values for CAPE, exceeding 2200 J $kg^{-1}$. The Holden storm showed a CAPE that was about 25% greater than the other two. Supercell storms are often associated with CAPE values exceeding ~2500 J $kg^{-1}$ (Rasmussen and Wilhelmson 1983; Rasmussen and Blanchard 1998; Rasmussen 2003). The 0000 UTC sounding 0-6 km bulk wind shear (SHEAR) for the Edmonton and Holden storms was high ( ≥ 5 m $s^{-1}$ $km^{-1}$) while the Pine Lake storm had a slightly lower SHEAR (4.3 m $s^{-1}$ $km^{-1}$) Observational and modeling studies of SHEAR show that environments with values of roughly 2.5-4.0 m $s^{-1}$ $km^{-1}$ are necessary to support supercells (Weisman and Klemp 1982; Bunkers 2002; Thompson et al. 2003).

Storm-Relative Helicity (SRH) is defined for a layer of depth *h* as (Davies-Jones et al. 1990):

$$\mathrm{SRH} = -\int_0^h \mathbf{k} \cdot \left[ (\mathbf{V} - \mathbf{c}) \times \frac{\partial \mathbf{V}}{\partial z} \right] dz \tag{1}$$

where **V** is the horizontal velocity and **c** is the storm's velocity. The depth *h* is typically chosen as 1 to 3 km. One can visualize SRH as minus twice the area swept out by the hodograph with the origin at the storm motion location. The 0000 UTC sounding 0-3 km SRH was calculated using Bunkers' method (Bunkers et al. 2000) to estimate storm velocity. As shown in Table 1 values of SRH were 153 $m^2$ $s^{-2}$ for the Edmonton storm, near zero (-2 $m^2$ $s^{-2}$) for the Holden storm, and 199 $m^2$ $s^{-2}$ for the Pine Lake storm. The low SRH value for the Holden case is indicative of the light winds in the low-levels (Fig. 4d). The 0-3 km SRH values of the three storms are all lower than the median value of 223 $m^2$ $s^{-2}$ for F2-F4 tornadoes in the U.S. found by Thompson et al. (2003).

The Bulk Richardson Number (BRN), defined as BRN = CAPE / (½ $U^2$), (where U represents the difference between the density weighted mean winds in the 0-6 km and 0-500 m layers) quantifies the ratio of the vertical component relative to the horizontal component of the kinetic energy. As the BRN decreases, multicell convection becomes better organized and at small enough values quasi-steady supercell convection may occur. According to Weisman and Klemp (1982, 1986), a storm environment with a high CAPE value and a BRN value less than about 50, increases the likelihood of a supercell storm, whereas a BRN larger than 50 tends to be associated with multicell storms. The BRN of all three storm environments was less than 50: Edmonton, Holden and Pine Lake storms had BRN values of 13, 42, and 18 respectively. Consistent with the Weisman and Klemp's criterion (later verified by Thompson et al. 2003), all three soundings produced organized supercells. However, the degree to which CAPE and BRN can distinguish between supercell and non-supercell environments is still not clear. Rasmussen and Blanchard (1998) found that their BRN values did not discriminate well between supercell and non-supercell environments. Turcotte and Vigneux (1987) found that a combination of CAPE and shear could discriminate well between environments with severe and non-severe thunderstorms. CAPE alone does not appear to distinguish between environments associated with tornadic and non-tornadic storms (e.g. Trucotte and Vigneux 1987; Brooks et al. 1994a; Monteverdi et al. 2003). The Lifted Index (LI) values of the three events were very similar (about -8). Blanchard (1998) suggests that the LI may be better than CAPE alone as a measure of the buoyancy characteristics of the environment. In this sense, it is interesting that the buoyancy environments of the three storms were perhaps more similar than suggested by CAPE alone The maximum reported hail size diameters for the Edmonton and Holden storms were near 8-10 cm while the Pine Lake storm produced about 4 cm hail. This is likely a reflection of the higher CAPE and PW values in the Edmonton and Holden storms.

## 4. Dryline analysis

In Central Alberta, the dryline tends to develop when the moist air originating in a southeast flow from the central United States meets the dry air flowing across the

Rocky Mountains from the west (Knott and Taylor 2000). As an upper-level trough crosses the mountains, a strong low-level westerly downslope flow develops along the foothills of the Rocky Mountains. The westerly flow is significantly drier than the moist southeast flow across the plains. This flow pattern causes a strengthening gradient in low-level moisture along the foothills that often develops into a dryline. The dryline can exist in both quasi-stationary (quiescent) and synoptically active environments (Schaefer 1986). In the quiescent case the dryline lies nearly parallel to the mountains and its motion is largely determined by vertical mixing processes related to the diurnal cycle of heating of the moist and dry air masses. Under these conditions the dryline generally advances eastward during the day time as the dry air mixes with the moist boundary layer and then retreats westward during the evening (Schaefer 1974). Within synoptically active environments, the dryline often extends southward from a surface low pressure system located along a synoptic-scale frontal zone, and therefore can be found much further to the east that in the quiescent case (Hane et al. 2001, 2002). Motion of the dryline in this case is augmented by the motion of the low pressure system and the associated upper-level trough's effect on horizontal and vertical wind motions. Very often, the dryline will develop an eastward bulge during synoptically active situations due to turbulent mixing of subsiding west winds in the dry air (Schaefer 1986).

Some surface atmospheric moisture fields (e.g. mixing ratio) are not standard data available to the forecaster at a weather office. However, hourly dewpoint measurements are routinely available for the Environment Canada weather stations

(Fig. 1). We have used these measurements to plot dewpoint temperature contours for the Edmonton, Holden, and Pine Lake storms.

Surface dewpoint analyses for the Pine Lake case are shown in Fig. 6. At 1300 UTC (Fig. 6a; the morning of the storm) there was evidence of a dewpoint gradient and dryline forming along the foothills in central Alberta. At this time leading edge of the gradient (12 °C isodrosotherm) was near Pine Lake. A bulge in the dryline developed over southern Alberta as the drier westerly air flowed across the mountains and reached the surface east of the foothills in response to the eastward motion of the upper trough. Meanwhile an easterly flow in the low-levels was advecting moist air into central Alberta. As the day progressed the dewpoint gradient intensified and the bulge continued to push eastward. By 1800 UTC (Fig. 6b) a stronger dewpoint gradient had formed along the foothills of central Alberta curving northeastward as a dryline bulge continued to develop. The dryline was slightly south of Pine Lake at this time. The orientation of the Pine Lake storm dryline differed from typical pattern observed over the U.S. (Rhea 1966, Schaefer 1986) where the dryline aligns parallel to the mountains. By 2000 UTC (Fig. 6c) the dryline was well defined along the foothills into south-central Alberta and then curved sharply northeast. From 2100 UTC through 0000 UTC (Fig. 6d, e, f, g) the dryline remained quasi-stationary. The thunderstorm (indicated by a "cross") which later spawned the F3 tornado developed and moved eastward. Due to the orientation of the dryline, the thunderstorm moved into the area of higher dewpoints which enhanced the CAPE. At 0100 UTC the thunderstorm was over Pine Lake and spawned the tornado. The dryline had remained quasi-stationary in terms of intensity and location (Fig. 6h). At 0200 UTC, an hour after the tornado occurred at Pine Lake, the dryline (Fig. 6i) dipped southward and the storm continued its track along the dryline.

Knott and Taylor (2000) made a detailed analysis of the dryline for the Holden storm. The dry line pattern was similar to the Pine Lake case. In both cases the dewpoint gradient was strong along the foothills to near Red Deer (see Fig. 1 for locations) and then bulged eastward across central Alberta. Also, in both cases a supercell which spawned the tornado formed near the dryline.

The surface dewpoint analyses for the Edmonton storm are shown in Fig. 7. The "star" marks the location of the city of Edmonton. At 1800 UTC 31 July 1987 the dewpoint field showed very moist conditions prevailing over nearly all of central Alberta. Dewpoints varied from 14 °C in the west to 18 °C and greater in the east (Fig. 7a). There was no evidence of a dewpoint gradient and corresponding dry line. The 1900 UTC and 2000 UTC surface dewpoint patterns (Fig. 7b, c) show little change in the field. Only some weak drying is evident along the foothills. At 2100 UTC, the time of the tornado touchdown, (Fig. 7d) the dewpoints in the Edmonton area were quite uniform near 18°C. By 2200 UTC, the time of the tornado dissipation, (Fig. 7e) a dewpoint gradient had developed over southern Alberta, still well to the south of Edmonton. The gradient was increasing slightly in the Edmonton area, but not enough to suggest the formation of a surface dryline as defined by Schaefer (1973). The 12 °C isodrosotherm was well south of Edmonton. At 2300 UTC (Fig. 7f) the drier air continued to push across southern Alberta where the dewpoint gradient was continuing to strengthen. Meanwhile, only a slight increase in the gradient occurred across central Alberta.

Figure 8 compares the evolution of the dewpoints at the cities of Edmonton, Red Deer and Calgary for the three storm cases. Edmonton, Red Deer and Calgary are aligned north-south (see Fig. 1) roughly perpendicular to the dryline position. The shaded zone indicates the time interval when the tornado formed. The Edmonton storm (Fig. 8a) shows fairly uniform dewpoints at all locations until near the time of the tornado. The three locations were in the moist air away from the dryline (roughly marked by the 12 °C dewpoint). The dry air advected into Calgary (about 300 km south of Edmonton) during the tornado, while dewpoints remained high at the other two locations. Only well after the tornado did dewpoints decrease at Edmonton and Red Deer. The Holden case dryline (Fig 8b) advanced northward through Calgary at about 1900 UTC, then Red Deer at about 0000 UTC and finally Edmonton near 0300 UTC, which was about an hour before the tornado touchdown. The Pine Lake event (Fig. 8c) showed a quasi-stationary dewpoint regime for most of the duration. Dewpoints at Calgary remained the lowest in the dry air south of the dryline. The dryline remained south of Red Deer until after the tornado. Meanwhile, at Edmonton, the drier air actually began edging into the area from the north (see Fig. 6) as the moist tongue of air across east-central Alberta decreased in extent.

Erfani et al (2002) used a fine scale version of the Global Environmental Multiscale (GEM) model to simulate the Pine Lake storm. The simulated evolution of the surface dewpoint field closely resembled the synoptic observation. The model output at 2100 UTC 14 July 2000 (Fig 15a in Erfani at al. 2002.) created a strong gradient across central Alberta with a bulge to the east similar to Fig 6a. The strongest gradient on both the model and observations occurred to the south of Pine Lake. The model simulations suggest that there was surface wind convergence close to the dryline and this convergence supported the storm development. The observational data set of surface wind measurements is too sparse to identify surface convergence zones for the Pine Lake storm environment. However, the build-up and maintenance of the strong surface dewpoint temperature gradient was clearly recognizable from the surface station network.

## 5. Storm tracks

Storm track positions were obtained using both ground observations and radar data for the Holden (Knott and Taylor 2000) and Pine Lake (Joe and Dudley 2000) thunderstorms. Observations and archived reports (Charlton, et al. 1998) were used to track the Edmonton storm. A plot of the hourly positions of the thunderstorm cells which spawned the three tornadoes is shown in Fig. 9.

The thunderstorm which produced the Edmonton tornado developed along the foothills in the early afternoon (1900 UTC) and then moved eastward at about 40 km $h^{-1}$ (Wallace 1987; Charlton et. al. 1998). Once the cell neared the southern edge of the city of Edmonton it made a sharp turn to the north. The reason for the abrupt change in direction is not clear. It may be due, in part, to the southerly mid-level wind. This does not, however, explain why the storm was moving eastward before the directional shift. There were no archived radar observations sampled prior 1992 and we cannot be certain that the storm did not split. The first reporting of a tornado occurred just south of the city of Edmonton at about 2100 UTC (Wallace 1987; Bullas and Wallace 1988). The storm then continued to intensify with the tornado reaching category F4 as it crossed the eastern outskirts of Edmonton between about 2100 and 2200 UTC. The tornado occurred for slightly over an hour, from its formation south of Edmonton to its dissipation just northeast of Edmonton, producing a damage path of nearly 40 km. The tornado had an average speed of 35 km $h^{-1}$ (Wallace 1987).

The Holden storm also began near the foothills in the early evening (0100 UTC). This storm moved fairly consistently northeast with a speed of about 50 to 60 km $h^{-1}$ (Knott and Taylor 2000). In this case the 0000 UTC 500 mb wind was south at 29 m $s^{-1}$ which indicated the thunderstorm was moving well to the right of the 0-6 km mean wind shear vector. The estimated path length of the tornado was 17 km.

The Pine Lake supercell storm also had a straight track similar to the Holden storm. case. Both storms were generated along the foothills and then tracked eastward with a speed of about 50 km $h^{-1}$ (Joe and Dudley 2000). The 0000 UTC 500 mb wind for this case was southwest 23 m $s^{-1}$. As with the Holden storm, the track of the Pine Lake storm was to the right of the upper wind.

## 6. Conclusions and implications for forecasting

During the last 20 years only three tornadoes have been recorded with F-scale ratings of F3 and F4 in Alberta. The synoptic conditions, the proximity sounding, the surface moisture fields, and storm tracks were examined to determine similarities and differences of contributing factors. The emphasis was on those observations available at the local forecast office that must issue storm warnings. Our analysis revealed the following points:

1) All three cases had a pronounced low-level capping inversion that allowed for the build-up of large amounts of Convective Available Potential Energy (CAPE) exceeding 2200 J $kg^{-1}$. This is in agreement with the Smith-Yau model.

2) All three storms developed in a thermal baroclinic zone with significant 0-6 km bulk wind shear exceeding 4 m $s^{-1}$ $km^{-1}$. The Bulk Richardson Number (BRN) of the three storms were 42 (Holden), 18 (Pine Lake) and 13 (Edmonton). These low BRN values agree with the Weisman and Klemp (1982), Rasmussen and Wilhelmson (1983) and Thompson et al. (2003) criterion for the formation of long-lasting supercells.

3) The build-up of CAPE was caused, in large part, by differential temperature changes at various altitudes. In two cases (Edmonton and Holden), the temperature lapse rate increased by strong low-level warming likely due to diabatic heating. In contrast, for the Pine Lake storm strong cooling at low and mid-levels intensified the latent instability with only a shallow layer near the surface experiencing warming. The Holden and Pine Lake storms showed cooling aloft, compatible with the Smith-Yau model, while the Edmonton storm showed warming throughout most all of the column, which appears contrary to the model. It is interesting to note the Holden and Pine Lake cases showed the greatest cooling near the 800 mb level. From discussions with operational forecasters at the Alberta weather office we have been informed that cooling at the lower levels (~850-700 mb) is often a strong indicator that anticipated significant convection is immanent. We speculate that, while upper-level

cooling is important to increase the buoyancy potential, low-level cooling (850-700 mb) is a major component for breaking the cap and releasing the latent instability.

4) In all three cases the storms developed in very high humidity conditions for Alberta with surface dewpoint temperatures exceeding 13 °C. The Pine Lake and the Holden storms developed at a dryline (moisture front).

5) The Edmonton storm environment did not depict a surface dryline; instead the boundary layer air was extremely humid with spatial uniformity. Thus, Alberta forecasters should keep in mind that the presence of a surface dryline may not be a necessary feature for the formation of thunderstorms.

6) For the Pine Lake and the Holden storms, simple extrapolation of the current storm motion would have been useful for nowcasting their storm tracks. These storms continued to move on a straight track with nearly uniform speed. In contrast, the Edmonton storm moved steadily eastwards for some time, then suddenly made an abrupt turn towards the north and passed over the city of Edmonton. For this case, nowcasting the storm motion would have been impossible with the available data.

Finally, we want to discuss some implications of these findings as they relate to forecasting in Alberta. Conceptual models are an important tool for forecasters to gain a relatively quick overview for the likelihood of severe convection. However, prototypes of atmospheric processes must be combined with an ingredients based approach in order to properly assess the full potential for thunderstorm development. In our study there were some features of the storms which agreed with the Smith-Yau (1993a, b) conceptual model of Alberta thunderstorm development while other aspects appeared contrary to the model. Operational forecasters should receive ongoing training of the current theories and research about thunderstorm and tornado development in order to properly apply the ingredients approach. Forecasters should also have access to hourly contoured surface moisture fields to follow the development and movement of drylines. Drylines provide valuable clues about the location of low-level convergence zones that could trigger and maintain convective outbreaks. However, while surface dewpoint gradients can, at times, provide information about the magnitude of the surface convergence or presence of a cap, they do not quantify the depth of the convergence layer. Xin and Reuter (1996) found that the intensity of the convective triggering depended markedly on both the magnitude and depth of the convergence. A vertical profile of convergence estimated from Doppler radar wind measurements would be needed to determine the depth of the convergence layer (e.g. Xin and Reuter 1998). In addition to real-time moisture fields it would be useful to have three-hourly soundings of thermodynamic and wind observations. Remote sensing of fields such as wind and moisture may be a viable option for a cost effective data profile collection. Lastly, simple extrapolation of storm tracks is not always viable and other nowcasting techniques should be explored for Alberta storms.

## Acknowledgements

The research was supported by grants from the Canadian Foundation for Climate and Atmospheric Sciences.

**Authors**

Max Dupilka is a PhD candidate at the University of Alberta, Canada. His research is focused on Alberta tornadoes; case studies of selected severe events, and statistical studies of parameters contributing to the intensity of tornadoes. He received a B.Sc. in Physics and an M.Sc. in meteorology from the University of Alberta. Max worked for many years as a forecast meteorologist with the Meteorological Service of Canada stationed at the previous Alberta Weather Centre, the Arctic Weather Centre, and the Beaufort Sea Weather Office.

Gerhard Reuter is a professor in Atmospheric Sciences at the University of Alberta, Canada. His research interest spans severe storms, cloud modeling, radar meteorology, precipitation physics, and mesoscale dynamics. He received his PhD in Meteorology from McGill University.

**References**

Blanchard, D. O., 1998: Assessing the vertical distribution of convective available potential energy. *Wea. Forecasting*, **13**, 870-877.

Brooks, H. E., C. A. Doswell III, and R. A. Maddox, 1992: On the use of mesoscale and cloud-scale models in operational forecasting. *Wea. Forecasting,* **7**, 120–132.

_______, _______, and J. Cooper, 1994a: On the environments of tornadic and nontornadic mesocyclones. *Wea. Forecasting*, **9**, 606-618.

_______, _______, and R. B. Wilhelmson, 1994b: On the role of midtroposheric winds in the evolution and maintenance of low-level mesocyclones. *Mon. Wea. Rev.*, **122**, 126-136.

Bullas, J. M., and A. F. Wallace, 1988: The Edmonton tornado, July 31 1987. Preprints, *15th Conf. on Severe Local Storms*, Baltimore MD, Amer. Meteor. Soc., 437-443.

Bunkers, M. J., B. A. Klimowski, J. W. Zeitler, R. L. Thompson, and M. L. Weisman, 2000: Predicting supercell motion using a new hodograph technique. *Wea. Forecasting*, **15**, 61-79.

_______, 2002: Vertical wind shear associated with left-moving supercells. *Wea. Forecasting*, **17**, 845–855.

Charlton, R. B., B. M. Kachman, and L. Wojtiw, 1998: The Edmonton tornado and hailstorm: A decade of research. *CMOS Bulletin*, **26**, 1-56.

Chisholm, A. J., and J. H. Renick, 1972: The kinematics of multicell and supercell Alberta hailstorms. Research Council of Alberta Hail Studies Report 72-2, 7 pp.

Davies-Jones, R. P., D. Burgess, and M. Foster, 1990: Test of helicity as a tornado forecast parameter. Preprints, *16th Conf. on Severe Local Storms*, Kananaskis Park, AB, Canada, Amer. Meteor. Soc., 588-592.

Djurić, D. 1994: *Weather Analysis*. Prentice Hall Inc., Englewood Cliffs, New Jersey.

Erfani A., A. Methot, R. Goodson, S Belair, K. S. Yeh, J. Cote, and R. Moffet, 2002: Synoptic and mesoscale study of a severe convective outbreak with the nonhydrostatic Global Environmental Multiscale (GEM) model. *Met. Atmos. Physics*, **82**, 31-53.

Fawbush, E. J., R. C. Miller, and L. G. Starrett, 1951: An empirical method of forecasting tornado development. *Bull. Amer. Meteor. Soc.*, **32**, 1-9.

Fujita, T. T., 1958: Structure and movement of a dry front. *Bull. Amer. Meteor. Soc.*, **39**, 574-582.

_______, 1981: Tornadoes and downbursts in the context of generalized planetary scales. *J. Atmos. Sci.*, **38**, 1511-1534.

Hage, K. D., 1994: Alberta tornados, other destructive windstorms and lightning fatalities: 1879-1984. University of Alberta Tech. Rep., ISBN 0-9696300-2-6, 67 pp.

_______, 2003: On destructive Canadian prairie windstorms and severe winters. *Natural Hazards*, **29**, 207-228.

Hane, Carl E., M. E. Baldwin, H. B. Bluestein, T. M. Crawford, and R. M. Rabin, 2001: A case study of severe storm development along a dryline within a synoptically active environment. Part I: Dryline motion and an Eta Model forecast. *Mon. Wea. Rev.*, **129**, 2183–2204.

_______, 2002: A case study of severe storm development along a dryline within a synoptically active environment. Part II: Multiple boundaries and convective initiation. *Mon. Wea. Rev.*, **130**, 900–920.

Joe, P. and D. Dudley, 2000: A quick look at the Pine Lake storm. *CMOS Bulletin*, **28**, 172-180.

Johns, Robert H., and C. A. Doswell III, 1992: Severe local storms forecasting. *Wea. Forecasting,* **7**, 588–612.

Knott, S. J., and N. M. Taylor, 2000: Operational aspects of the Alberta weather outbreak of 29 July 1993. *Natl. Wea. Dig.*, **24**, 11-23.

Markowski, P. M., J. M. Straka, E. N. Rasmussen, and D. O. Blanchard, 1998: Variability of storm-relative helicity during VORTEX. *Mon. Wea. Rev*, **11**, 2959-2971.

Miller, R. C., 1972: Notes on analysis and severe-storm forecasting procedures of the Air Force Global Weather Central. Tech. Rep. 200 (Rev.), Air Weather Service (MAC), Offutt Air Force Base, Nebraska.

Monteverdi, J. P., C. A. Doswell III, and G. S. Lipari, 2003: Shear parameter thresholds for forecasting tornadic thunderstorms in Northern and Central California. *Wea. Forecasting*, **18**, 357-370.

Newark, M. J., 1984: Canadian tornadoes, 1950-1979. *Atmos. Ocean*, **22**, 343-353.

Rasmussen, E. N., and R. B. Wilhelmson, 1983: Relationships between storm characteristics and 1200 GMT hodographs, low-level shear and stability.

Preprints, *13th Conference on Severe Local Storms*, Tulsa, OK, Amer. Meteor. Soc., 55-58.

_______, and D. O. Blanchard, 1998: A baseline climatology of sounding-derived supercell and tornado forecast parameters. *Wea. Forecasting*, **13**, 1148-1164.

_______, 2003: Refined supercell and tornado forecast parameters. *Wea. Forecasting*, **18**, 530–535.

Reuter , G.W., and C.D. Nguyen, 1993: Organization of cloud and precipitation in a severe Alberta storm. *Atmos. Research*, **30**, 127-141.

_______, and N. Aktary, 1995: Convective and symmetric instabilities and their effect on precipitation: Seasonal variations in Central Alberta during 1990 and 1991. *Mon. Wea. Rev.*, **123**, 153-162.

Rhea, J. O., 1966: A study of thunderstorm formation along drylines. *J. Appl. Meteor.*, **5**, 59-63.

Schaefer, J. T., 1973: The life cycle of the dryline. *J. Appl. Meteor.* **13**, 444-449.

_______, 1974: A simulative model of dryline motion. *J. Atmos. Sci.*, **31**, 956-964.

_______, 1986: The dryline. *Mesoscale Meteorology and Forecasting.* P. S. Ray, Ed., Amer. Meteor. Soc., Boston, 549-572.

Smith, S. B., and M. K. Yau, 1993a: The causes or severe convective outbreaks in Alberta,. Part I: A comparison of a severe outbreak with two non-severe events. *Mon. Wea. Rev.*, **121**, 1099-1125.

_______, and _______, 1993b: The causes of severe convective outbreaks in Alberta. Part II: Conceptual and statistical analysis. *Mon. Wea. Rev.*, **121**, 1126-1133.

_______, G. W. Reuter, and M. K. Yau, 1998: The episodic occurrence of hail in central Alberta and the Highveld of South Africa. *Atmos. Ocean,* **36**, 169-178.

Thompson, R. L., R. Edwards, J. A. Hart, K. L. Elmore, and P. Markowski, 2003: Close proximity soundings within supercell environments obtained from the Rapid Update Cycle. *Wea. Forecasting,* **18**, 1243–1261.

Turcotte, V., and D. Vigneux, 1987: Severe thunderstorms and hail forecasting using derived parameters from standard RAOBS data. Preprints, *Second Workshop on Operational Meteorology*, Halifax, Nova Scotia, Canada, Atmos. Environ. Service/Canadian Meteor. and Oceanogr. Society, 142-153.

Wallace, A. F., 1987: Track of the Edmonton tornado, July 31, 1987. Tech Note, Environment Canada, 22 pp. [Available from Meteorological Service of Canada, Environment Canada, 4999-98th Ave., Edmonton, AB T6B 2X3.].

Weisman, M. L., and J. B. Klemp, 1982: The dependence of numerically simulated convective storms on vertical wind shear and buoyancy. *Mon. Wea. Rev*., **110**, 504-520.

_______, and _______, 1986: Characteristics of isolated storms. *Mesoscale Meteorology and Forecasting*. P. S. Ray, Ed., Amer. Meteor. Soc., 331-357.

Xin, L., and G.W. Reuter, 1996: Numerical simulation of the effects of mesoscale convergence on convective rain showers. *Mon. Wea. Rev*., **1242**, 2828-2842.

_______, and _______, 1998: VVP technique applied to an Alberta storm. *J. Atmos. Oceanic Technol.*, **15**, 587-592.

Ziegler, C. L., and C. E. Hane, 1993: An observational study of the dryline. *Mon. Wea. Rev*., **121**, 1134-1151.

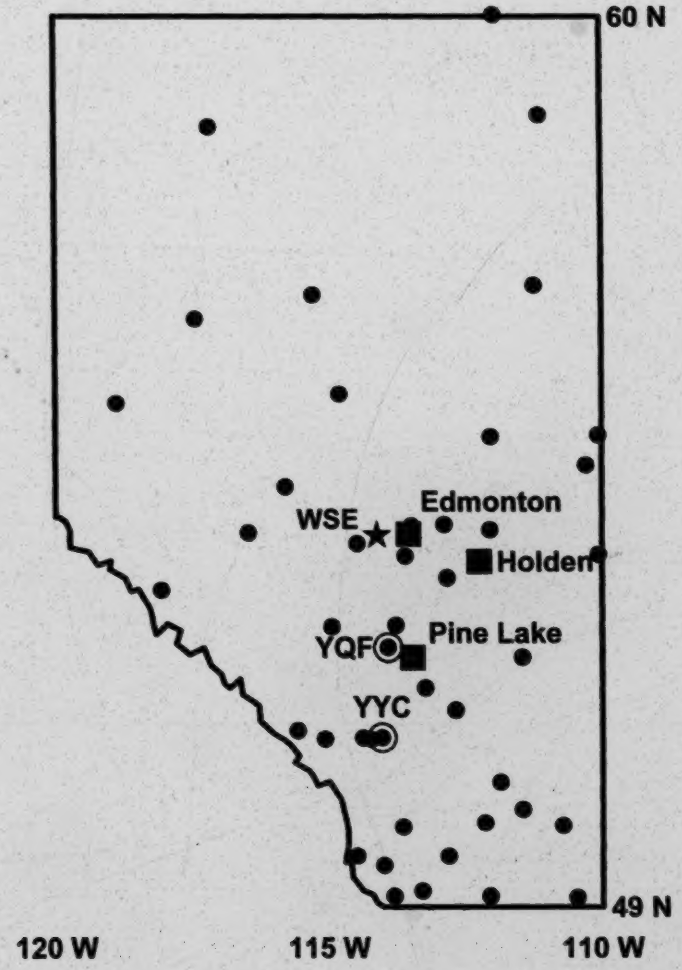
60 N
WSE
Edmonton
Holden
YQF
Pine Lake
YYC
49 N
120 W
115 W
110 W

Fig. 1. Location of surface weather observing stations (dots) within the province of Alberta. The squares show the sites of the Edmonton, Holden, and Pine Lake storms. The circles show the cities of Red Deer (YQF) and Calgary (YYC). The location Stony Plain (WSE) upper air station is marked by the star.

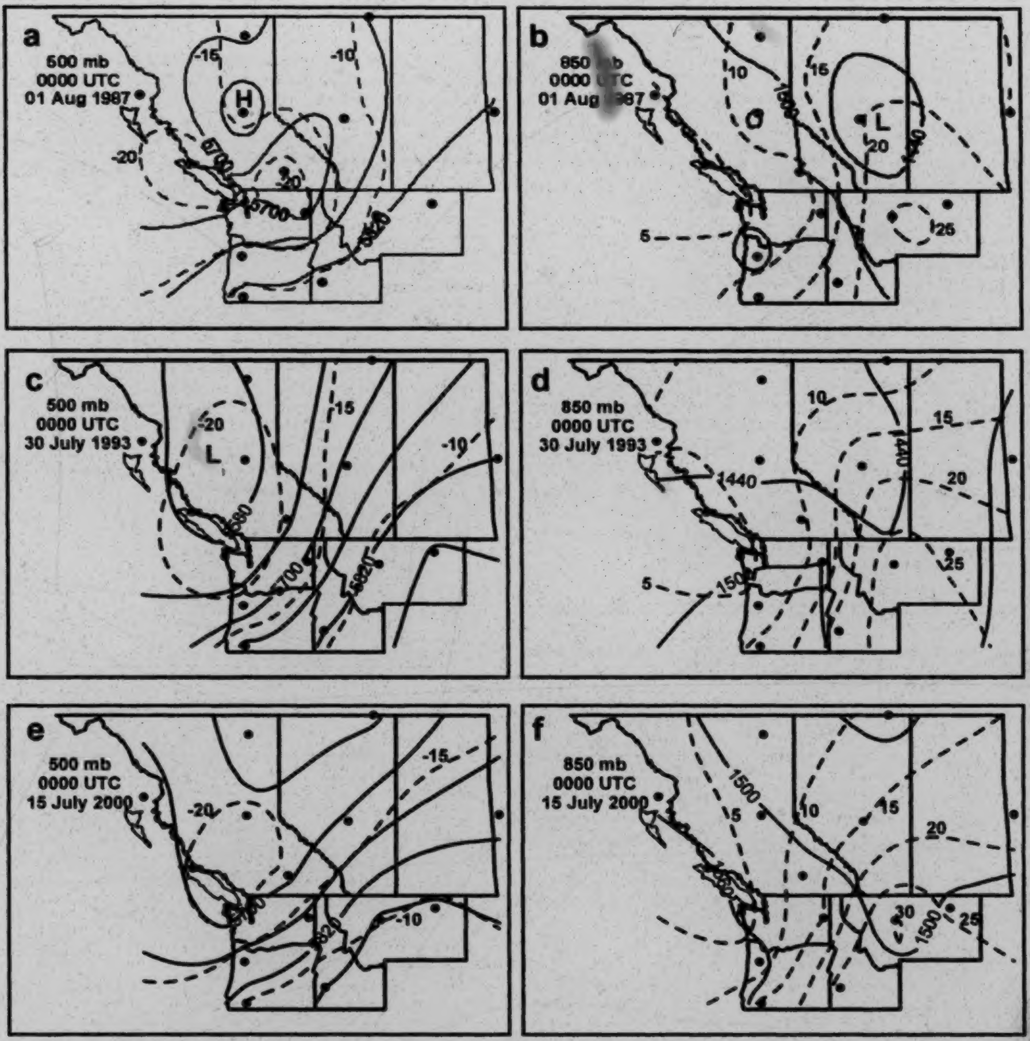
a
500 mb
0000 UTC
01 Aug 1987
-15
-10
H
-20
5700
5820
b
850 mb
0000 UTC
01 Aug 1987
10
15
1500
L
20
1440
5
25
c
500 mb
0000 UTC
30 July 1993
-20
L
-15
-10
5580
5700
5820
d
850 mb
0000 UTC
30 July 1993
10
15
1440
20
25
5
1500
e
500 mb
0000 UTC
15 July 2000
-15
-20
-10
5820
f
850 mb
0000 UTC
15 July 2000
1500
5
10
15
20
30
25

Fig. 2. 500 mb and 850 mb height contour maps at 0000 UTC for the Edmonton tornado (top panel), Holden tornado (middle panel) and Pine Lake tornado (bottom). Geopotential heights (solid) are contoured every 60 m, isotherms (dashed) are contoured every 5°C.

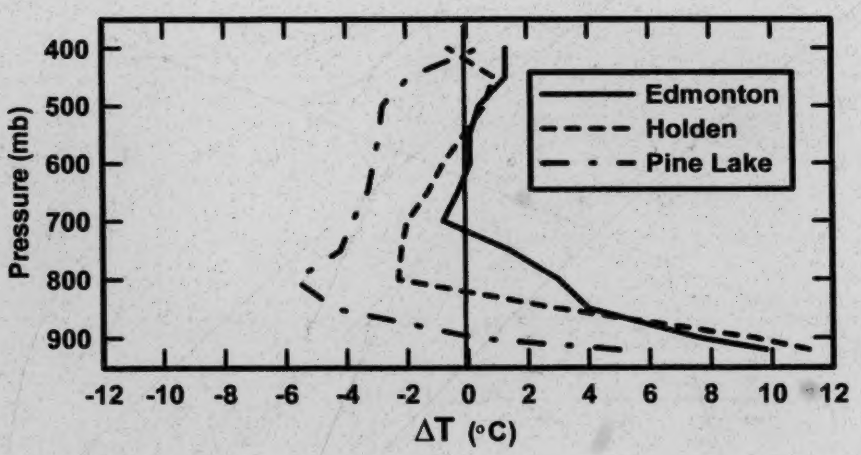

Fig. 3. Vertical profile of the 12-h temperature change (ΔT ) from 1200 UTC to 0000 UTC for the three tornado cases.

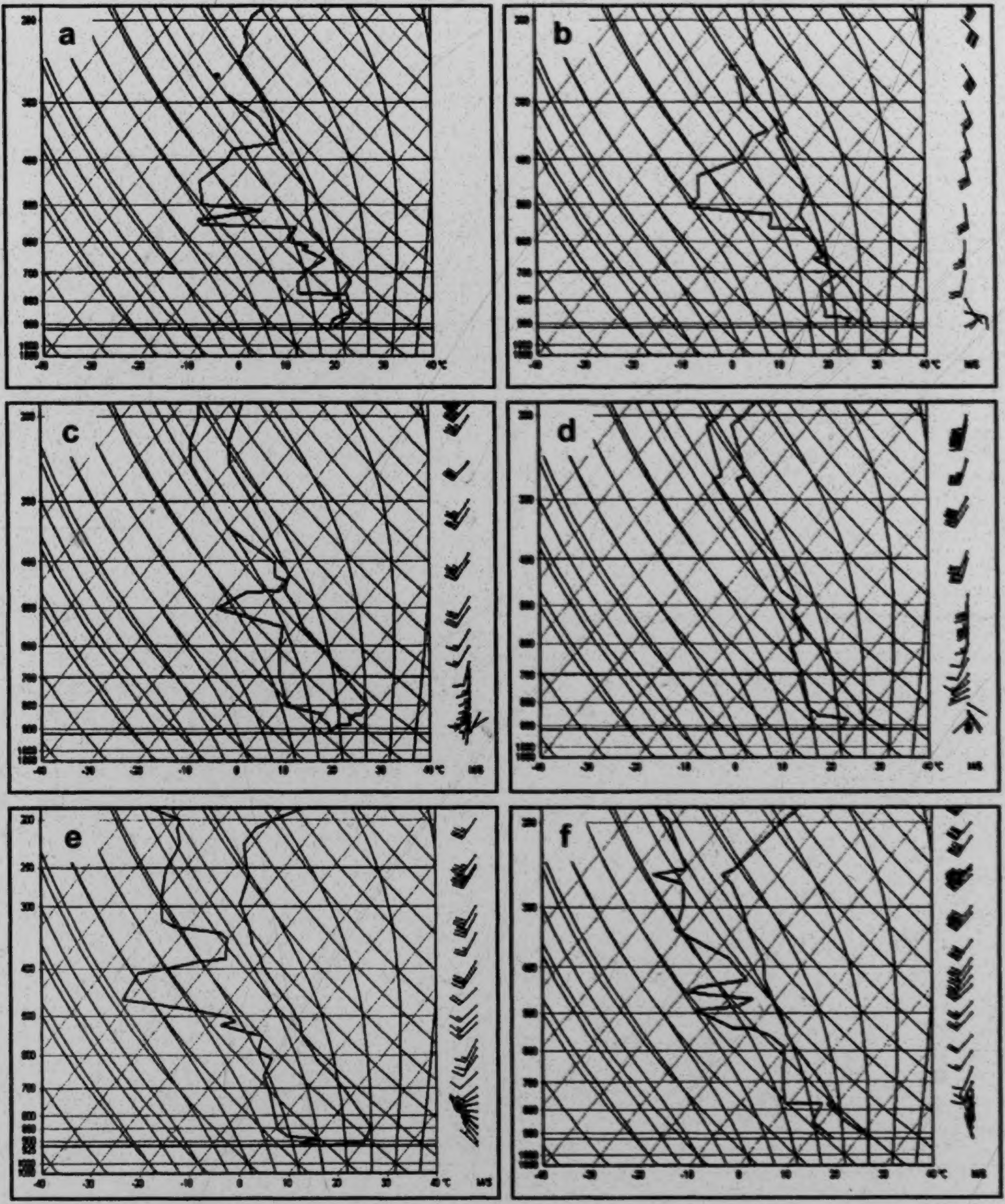

Fig. 4. Adjusted Skew T-log *p* diagrams for the Edmonton tornado (top panel), the Holden tornado (middle panel), and the Pine Lake tornado (bottom panel) for a), c), and e) 1200 UTC (morning of the events); b), d), and f) 0000 UTC (evening of the events). Wind vectors (in m $s^{-1}$) are shown at selected pressure levels at the right of each sounding.

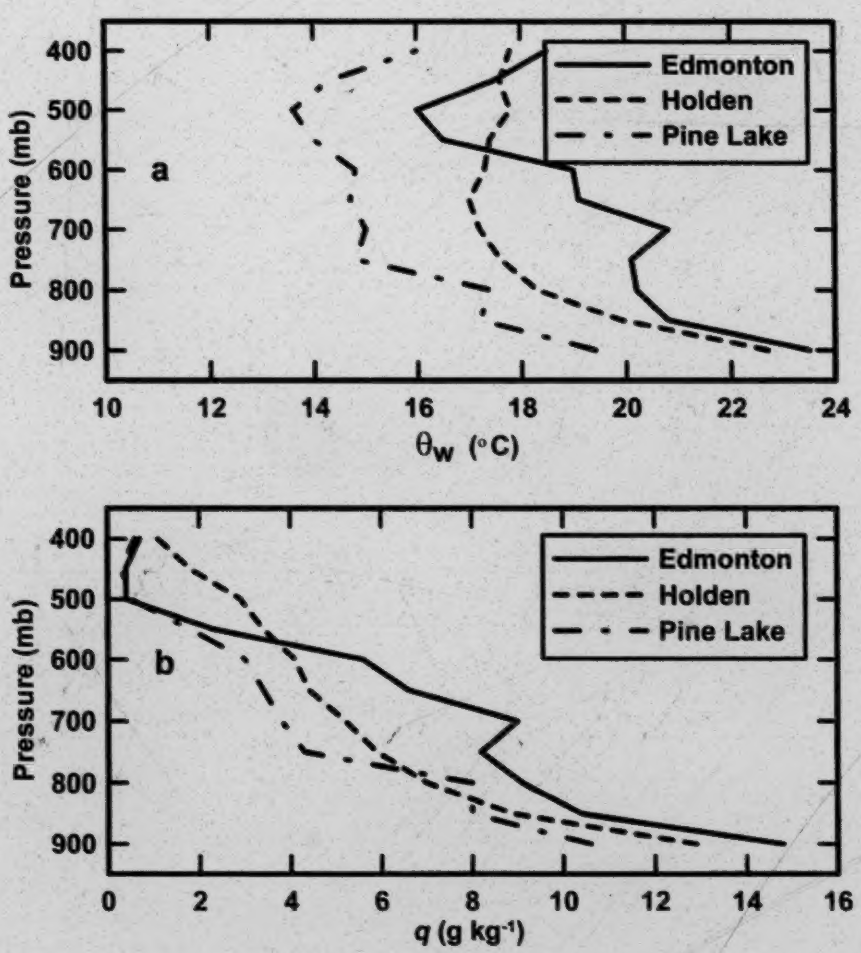

Fig. 5 Vertical soundings at 0000 UTC of a) wet-bulb potential temperature ($\theta_w$ in °C), b) vapor mixing ratio ($q$ in g kg$^{-1}$) for the Edmonton, Holden, and Pine Lake storms.

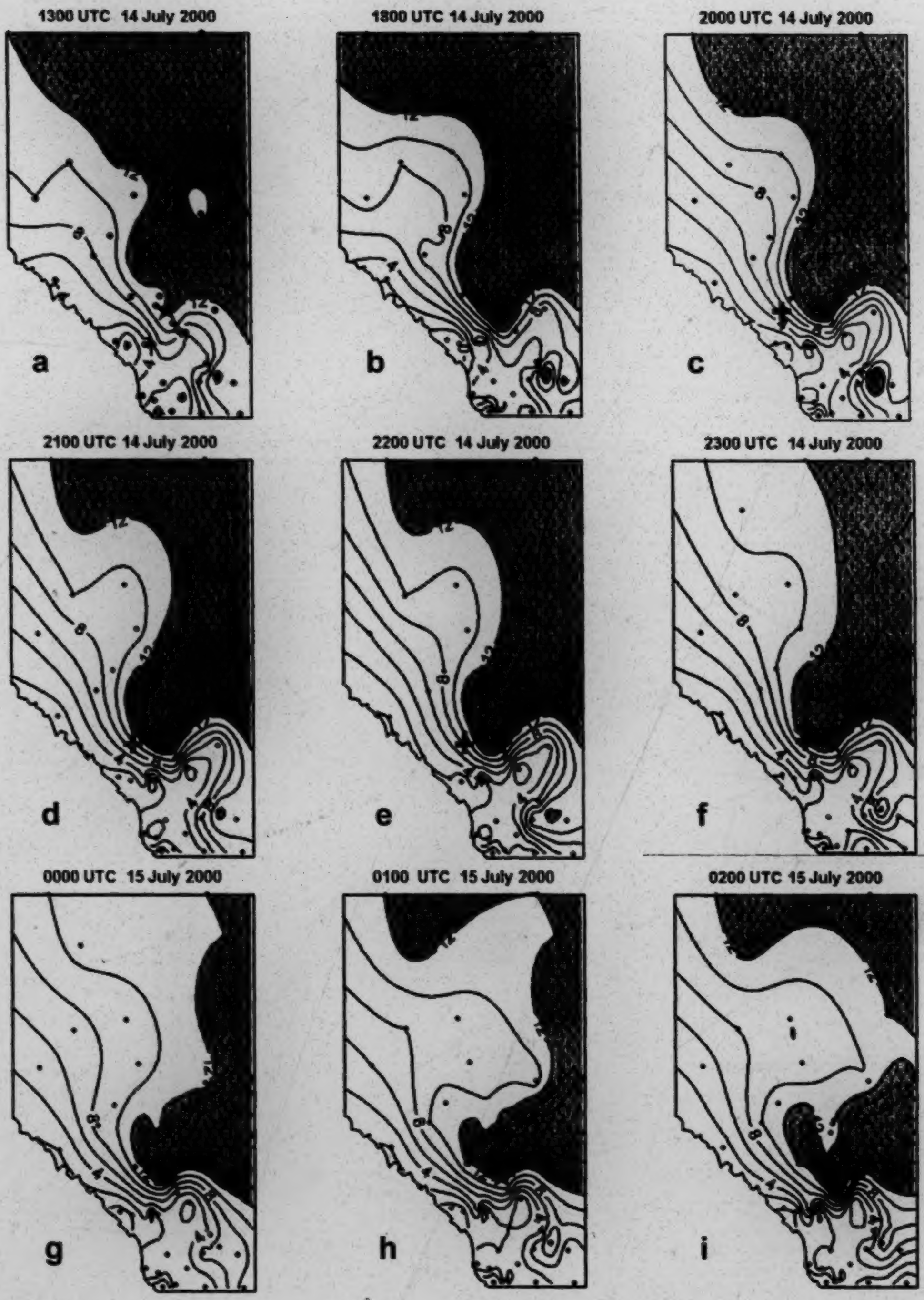
1300 UTC 14 July 2000
1800 UTC 14 July 2000
2000 UTC 14 July 2000
a
b
c
2100 UTC 14 July 2000
2200 UTC 14 July 2000
2300 UTC 14 July 2000
d
e
f
0000 UTC 15 July 2000
0100 UTC 15 July 2000
0200 UTC 15 July 2000
g
h
i
12
8
4

Fig. 6. Contour analysis of surface dewpoint temperatures for the Pine Lake storm from 1300 UTC 14 July 2000 to 0200 UTC 15 July 2000. Contours are drawn every 2 °C, with shading for $T_d > 12$ °C. Dots show dewpoint observations, the star shows the Pine Lake storm site, and the cross marks the storm.

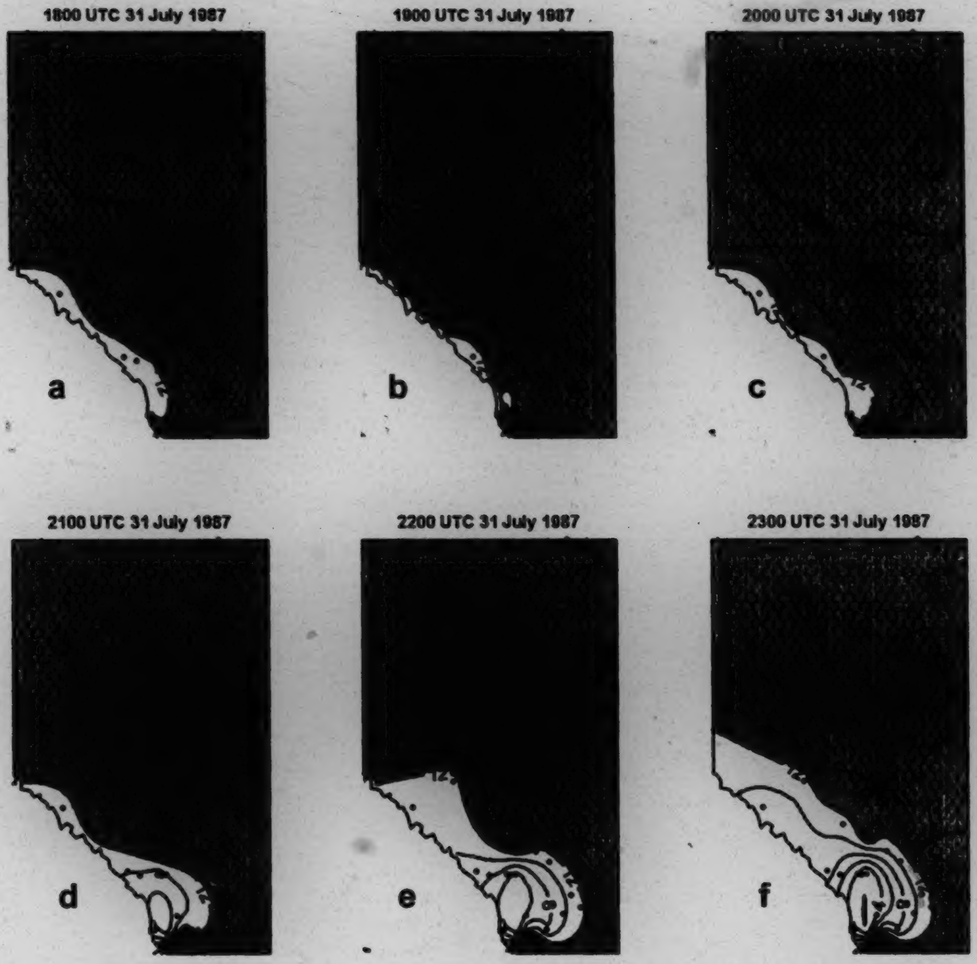
1800 UTC 31 July 1987
1900 UTC 31 July 1987
2000 UTC 31 July 1987
a
b
c
2100 UTC 31 July 1987
2200 UTC 31 July 1987
2300 UTC 31 July 1987
d
e
f

Fig. 7. Hourly evolution of the surface dewpoint field for the Edmonton storm from 18 UTC to 23 UTC 31 July 1987. Contours are drawn every 2 °C, with shading for $T_d > 12$ °C. The star marks the city of Edmonton.

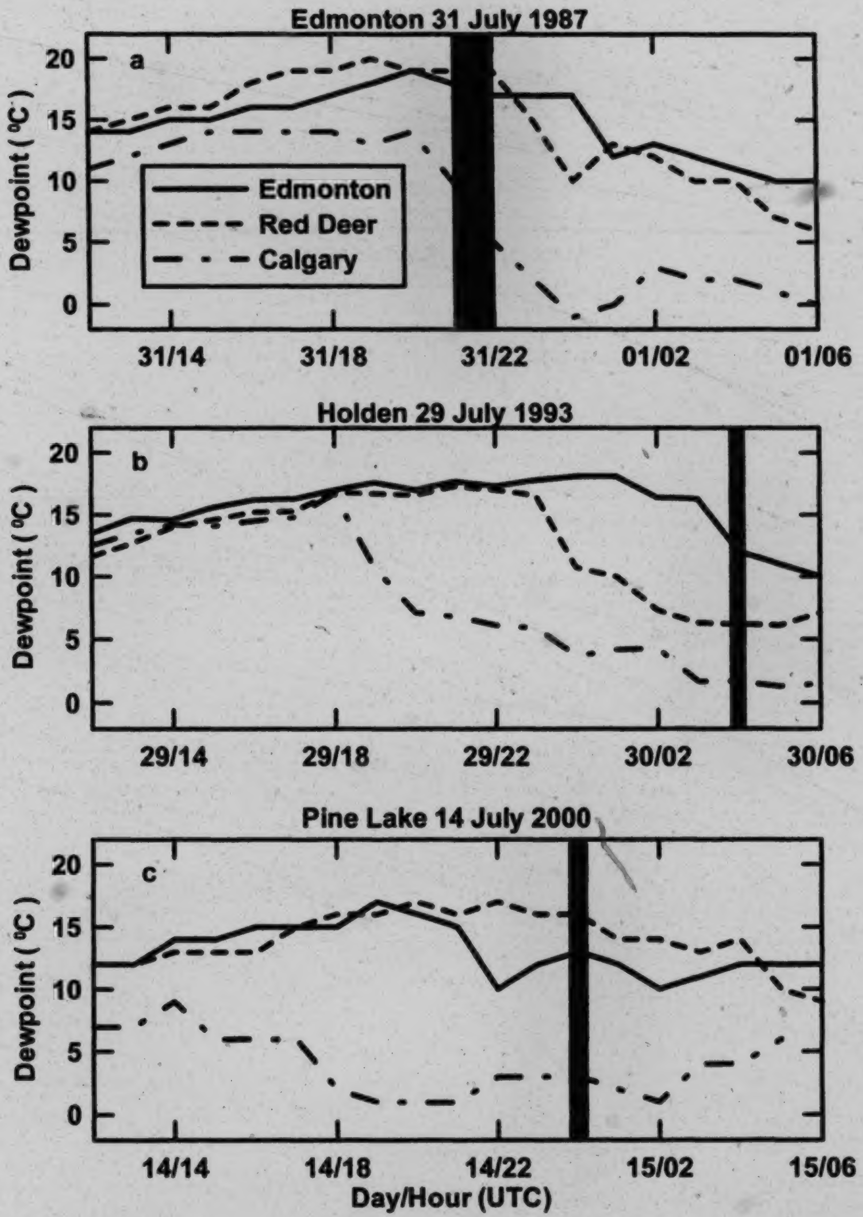

Fig. 8. Evolution of surface dewpoint temperatures (in °C) recorded at Edmonton (solid), Red Deer (short dashed), and Calgary (long dashed) airports for the a) Edmonton, b) Holden, and c) Pine Lake storm events. The shaded zones indicate the approximate duration of each tornado.

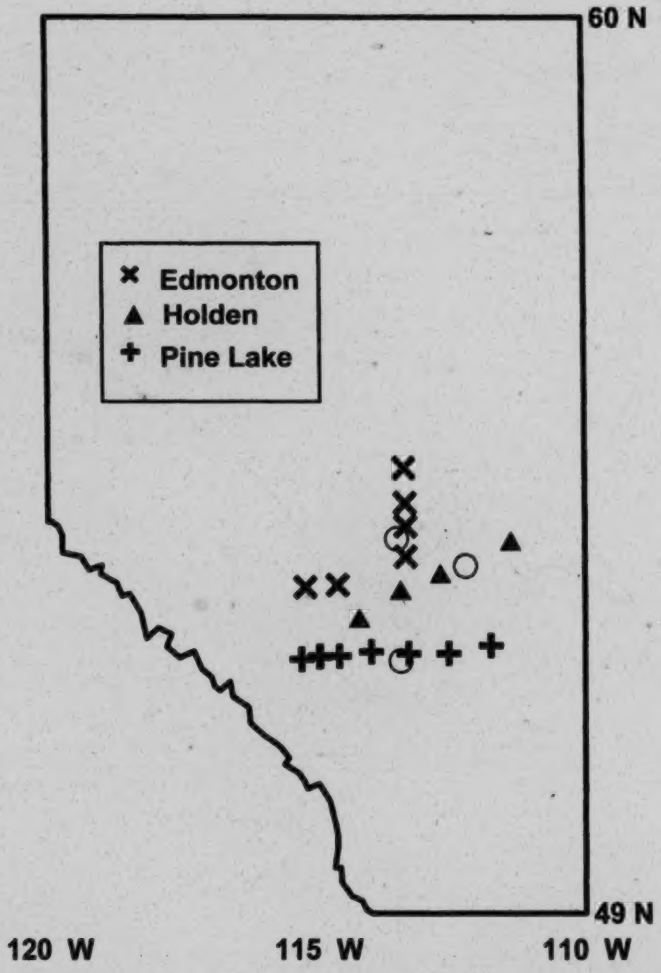
60 N
× Edmonton
▲ Holden
+ Pine Lake
49 N
120 W
115 W
110 W

Fig. 9. Thunderstorm tracks plotted every hour for the Edmonton storm (1900 UTC 31 July 1987 to 0000 UTC 01 August 1987), the Holden storm (0100 UTC 30 July 1993 to 0400 UTC 30 July 1993), and the Pine Lake storm (2000 UTC 14 July 3000 to 0200 UTC 15 July 2000). The three circles mark the locations of the tornado sites (see Fig. 1).

# Chapter VI

## On Predicting Maximum Snowfall Amounts in Alberta

Published:

Dupilka, M. L., and G. W. Reuter 2004: On predicting maximum snowfall amounts in Alberta. *Atmos. Ocean*, **42**, 281-292.

## ABSTRACT

Snowfall in excess of 10 cm per day in Alberta is usually associated with large-scale ascent within a wave cyclone and the maximum amount of snowfall depends on the maximum amount of vapor available for deposition. Using the principle of conserving water substance, the maximum snowfall amount is related to the saturated vapor mixing ratio at cloud base and cloud top levels. The inherent uncertainties of the input data allow for numerical approximations that lead to a linear relationship between maximum snowfall and cloud base temperature. To test the validity of the linear snowfall-temperature relationship, an analysis was made of the correlation of 24 hour snowfall measurements with temperature observations from upwind soundings. The data set covered all of Alberta (with the exception of the mountainous west) for the period October 1990 to April 1993. The data suggest that the snow amounts depend roughly linearly on the 850 mb temperature with a correlation coefficient of 0.62. We further investigated whether the snowfall-temperature relationship can be used to compliment the Quantitative Precipitation Forecast (QPF) available for a NWP model. Specifically, the snowfall-temperature

relationship offered value above what was available from the output of the European Centre for Medium-Range Weather Forecasts (ECMWF) model. The implications of this finding on predicting heavy snowfall for Alberta are discussed.

## 1. Introduction

About one half of the annual precipitation in Alberta occurs in the form of snow (about 150 cm) (Reuter and Beaubien, 1996). A major task of the Prairie and Northern Region Weather Office is to predict snowfall amounts and provide timely warnings of heavy snowfall. For Alberta, heavy snowfall warnings are issued for an event when the snow accumulations are expected to be 10 cm or greater within a 24 hour period. Major snowfall events in Alberta are usually associated with lee cyclogenesis that is forced when a baroclinic wave disturbance moves over the Rocky Mountains (Chung et al., 1976). Numerical Weather Prediction (NWP) models are skilful to resolve and track these large-scale baroclinic disturbances and the resulting lee cyclogenesis. During the last two decades improvements in model grid resolution, physical parameterization and initialization, have led to useful guidance concerning the occurrence of snow storms. However, model predictions of snowfall accumulations are often inaccurate, particularly for heavy snowfall (Kocin and Uccellini, 1990; Aktary and Reuter, 1993). The operational forecaster could benefit from techniques, complementary to NWP guidance, to assist in deciding whether the 24 hour accumulation of snow will exceed 10 cm or not.

The amount of snow falling from synoptic-scale weather systems depends largely on the amount of vapor available for condensation or deposition. Local sources of atmospheric moisture within Alberta are limited during the cold months (with most lakes frozen), suggesting that heavy snowfall depends on transport of vapor from elsewhere. Major Alberta snowstorms fit well with the classical cyclone model with its warm and cold conveyer belt circulation. This conceptual model postulates that much of the precipitation comes from conversion of moisture transported within the warm conveyor belt (e.g. Carlson, 1980). The flow in the warm sector south of the surface low pressure centre, ascends turning northwards, as it enters the cyclone. During the ascent deposition occurs resulting in a broad shield of cloud and precipitation. From satellite and radar observations it is known that, in Alberta cyclones, the instantaneous rate of precipitation field tends to be organized in banded formations parallel to the warm surface front (Aktary and Reuter, 1993; Reuter and Aktary, 1995; Reuter and Beaubien, 1996). Specifically, Constant-Altitude Plan Position Indicator (CAPPI) radar reflectivity maps indicate long bands of high rates of precipitation that sweep across the province. However, the snowfall amounts accumulated during the entire event show a much smoother field as it integrates the accumulation over time.

The usefulness of issuing a heavy snowfall warning to the transportation industry and public at large depends greatly on the lead time, i.e. the time between issuing the warning and the actual event. For many decisions a lead time of 6 to12 hours is needed. Thus, while radar observations are useful for providing nowcasts with lead times of 1 to 3 hours (e.g. Reuter and Beaubien, 1996), they offer little guidance for forecasts with lead times of 6 hours and more. Auer (1987) suggested an aid to forecasting heavy snowfall episodes based partly on thermodynamic and moisture variables evident from soundings.

Here we advocate a two-step approach when deciding whether to issue a heavy snowfall warning for a particular region within Alberta. The first step is to decide if, indeed, there will be snowfall for the location in question. This decision of whether it will snow or not is generally based on numerical guidance from NWP models (such as the

Canadian GEM model). Once it has been established that there will be snow, the second step consists of estimating the amount of snowfall accumulation for the event. It is here that, we believe, this paper offers some guidance in providing an estimate for the maximum snowfall amount based on available moisture from upwind sources. The emphasis is on establishing what temperature value at cloud base is needed to yield snowfall amounts equal to or larger than 10 cm.

It should be mentioned that our study forms part of a larger research project, namely the Mackenzie GEWEX Study (MAGS). The northern regions of Alberta are located within the vast basin of the Mackenzie River. The mean annual discharge of the Mackenzie into the Arctic Ocean is approximately 9000 $m^3 s^{-1}$ with large inter-annual variability (Rouse et al., 2002). The primary goals of MAGS, within the Global Energy and Water Cycle Experiment (GEWEX) are to understand and model the high-latitude water and energy cycles (Stewart et al., 1998). Snowfall is an important source of water substance throughout much of the year, and heavy snowfall can impact the local water budgets (Szeto, 2002). The precipitation efficiency of high-latitude baroclinic cloud systems was found to exhibit strong sensitivity to low-level humidity conditions (Szeto et al., 1997). Specifically, higher humidity values resulted in higher precipitation efficiency. This is consistent with the idea that the amount of available atmospheric moisture is correlated with the accumulated precipitation amounts.

The purpose of this paper is to offer a tool to assist in predicting the amount of snowfall accumulation based on thermodynamic estimates. Specifically, the snowfall amount is related to the temperature at the 850 mb level observed at an upwind sounding.

This paper is organized in six sections. The theory of relating maximum snowfall amounts to cloud base temperature and cloud depth is developed in section 2. In section 3 we describe the observational data set for testing the linear relationship for snowfall amounts. This section also contains the motivation for the choice of snow and sounding observations, and scatter diagrams of snowfalls plotted versus 850 mb temperatures. Finally, the results are summarized and interpreted in section 4. The forecasting skill of the snowfall-temperature relationship is compared to the skill of a numerical weather prediction model in section 5. In section 6 we speculate why NWP models have difficulty in quantitative predictions of snowfall cases in Alberta, and why the temperature near cloud base is so relevant. In the last section, some limitations and suggestions for further work are outlined.

## 2. Theory of maximum snow accumulation

During ascent, vapor will condense into water, or deposit on ice. By assuming that all of the condensed water precipitates as rain (or snow), we may estimate the mass of precipitation per unit area (i.e. time-integrated precipitation flux) using

$$P = \int_{z_0}^{z_1} \left( \rho q_s(z_0, T_0) - \rho q_s(z) \right) dz \tag{1}$$

Here $P$ denotes the snow mass per unit area (kg m$^{-2}$), $z_0$ and $z_1$ denote the heights of cloud base and cloud top, $T_0$ denotes cloud base temperature, $\rho$ denotes air density, and $q_s$ denotes saturated water vapor mixing ratio. A basic assumption of Eq. (1) is that height-integrated horizontal moisture flux convergence is very small and can thus be neglected. This assumption is invalid for convective precipitation produced in cumulus clouds that have significant horizontal convergence near cloud base. In fact, the convective precipitation is roughly proportional to the magnitude times the depth of the meso-scale convergence (Xin and Reuter, 1996). Water budgets of frontal cloud systems can also be affected by low-level convergence zones associated with baroclinic fronts. Usually the synoptic cloud systems producing heavy snowfall over Alberta are transitory and moving eastwards. Thus when using Eq. (1) for predicting daily snowfall amounts it is reasonable to assume that the horizontal moisture fluxes into a particular vertical column are small when integrated over 24 hours. Essentially, we make the assumption that the maximum accumulated snowfall over 24 hours is not controlled by horizontal moisture convergence, which differs from the assumption that the instantaneous snowfall rate depends on the short-lived moisture convergence. Using the hydrostatic balance and approximating the integral by triangulation gives

$$P = \frac{1}{g}\int_{p_1}^{p_0}\left(q_s(p_0,T_0)-q_s(p)\right)dp = \frac{1}{2}\frac{1}{g}\left[q_s(p_0,T_0)-q_s(p_1,T_1)\right]100\left(p_0-p_1\right) \qquad (2)$$

where $g$ denotes the acceleration due to gravity, $p$ denotes pressure, and $p_0$ and $p_1$ denote pressure (in mb) at $z_0$ and $z_1$, respectively. The saturated mixing ratio at the cloud base level is given by

$$q_s(p_0,T_0) = 0.622\left(p_0\right)^{-1} e_s(T_0) \qquad (3)$$

where $e_s(T)$ is the saturation vapor pressure which is a function of temperature only. $e_s$ can be approximated as (Djuric, 1994, pp. 70), $e_s(T) = 6.1\,exp(0.073\,T)$, where $T$ is in °C and $e_s$ in mb. For supercooled clouds, one might substitute $e_s$ by $e_{si}$ the saturated water vapour pressure with respect to ice. The two are related by $e_{si}(T)$ = $e_s(T)\,(273/T)^{-1}$ = $(273/T)^{-1}$

6.1 *exp*(0.073 *T*) (Rogers and Yau, 1989, pp. 20). We continue with Eq. (3) to derive

$$q_s(p_0,T_0)=3.79\,(p_0)^{-1}\,exp(0.073\,T_0) \qquad (4)$$

A further simplification is possible by expanding the exponential into a series and neglecting all second order and higher terms (which are small for -10 °C < $T_0$ < 10 °C):

$$q_s(p_0,T_0)=3.79\,(p_0)^{-1}\,(1+0.073\,T_0)=0.28\,(p_0)^{-1}\,T_0+3.79\,(p_0)^{-1} \qquad (5)$$

Upon substitution in Eq. (2), we have

$$P=50\frac{1}{g}\left[0.28(p_0)^{-1}\,T_0+3.79\,(p_0)^{-1}-q_{s1}\right](p_0-p_1) \qquad (6)$$

where $q_{s1} = q_s(p_1, T_1)$. For given values of $q_{s1}$, $p_0$, $p_1$ and $g = 10$ m s$^{-2}$, we can express *P* as a linear function of the cloud base temperature

$$P = a\ T_0 + b \qquad (7)$$

where $a=1.4\,(1-p_1/p_0)$ and $b=18.9\,(1-p_1/p_0)-5\,q_{s1}(p_0-p_1)$. What are the typical range of values for *a* and *b* for Alberta winter conditions? Typical pressure observations at ground level range from about 900 to 920 mb depending on the topography and synoptic conditions. For winter months the pressure level for nimbus cloud bases is usually close to 850 mb with tops ranging from about 600 mb to 300 mb. Typical cloud top saturation mixing ratios range from $10^{-4}$ to$10^{-5}$ kg kg$^{-1}$. Table 1 shows that for these conditions, *a* ranges from 0.41 to 0.90. Thus for every increase of 1 °C the total snowfall *P* increases by about 0.4 to 0.9 kg m$^{-2}$.

In Alberta snowfall measurements are recorded in depth rather than mass per unit area. To convert the *P* into snow depth (*S*, in cm) we have

$$S = (\rho_{snow})^{-1} P = (\rho_{snow})^{-1} (aT_0 + b) \quad (8)$$

where $\rho_{snow}$ denotes the density of accumulated snow at the ground. It depends on the crystal habitat and surface temperature, with a typical values ranging from 80 kg m$^{-3}$ for dry powdery snow to 200 kg m$^{-3}$ for wet snow (Roebber et al., 2003).

Table 1. Values of $a$ and $b$ for the prediction for different values of cloud top pressure $p_1$ (mb) for $p_0$ = 850 mb and $q_{s1}$ = 0.2 g kg$^{-1}$.

| $p_1$ (mb) | $a$ (kg m$^{-2}$ $^0$C$^{-1}$) | $b$ (kg m$^{-2}$) |
|---|---|---|
| 600 | 0.41 | 5.30 |
| 500 | 0.58 | 7.43 |
| 400 | 0.74 | 9.55 |
| 300 | 0.90 | 11.66 |

## 3. Testing of theory with Alberta observations

To test the relationship of maximum snowfall amounts with cloud base temperature for Alberta conditions we need experimental data. Our analysis covers a total of 259 snowfall events within Alberta encompassing three cold periods: October 1990 – April 1991, October 1991 – April 1992, and October 1992 – April 1993. These do not include snowfall cases in the Rocky Mountains. Steep topography tends to locally enhance the snowfall due to forced orographic lifting. These orographic effects are beyond the scope of our investigation. Figure 1 shows the locations of the 21 Environment Canada weather reporting stations used in our analysis (YOJ, YSM, YPY, YPE, YMM, YQU, YZH, YZU, YOD, YET, YXD, YLL, WRM, YQF, WCT, YYC, YBW, ZPC, YQL, YXH and WGM). At each location the snowfall accumulation is measured manually once per day. These measurements are included in the weather (SA) reports for snowfall amounts exceeding 1 cm. The measurements are given to the nearest cm. The time duration of snowfall amounts was chosen to be the 24 hour period to cover the entire duration of the snow event. In most cases, the duration of snowfalls lasted less than 12 hours, and there were no cases of snowfall continuing without interruption for more than 24 hours. Only cases of snowfall events were chosen for this study. Mixed precipitation (rain and/or snow) cases were excluded. The choice of selecting the analysis period from 1990 to 1993 was based to coincide with a special forecasting project conducted by Max Dupilka at the Alberta Weather Centre. The project involved correlating snowfall measurements with other observations. There was enhanced quality control over the snowfall measurements from remote sites. The period also coincides with the studies of precipitation organization by slantwise convection (Reuter and Aktary, 1995). They showed that the winters of 1990-91 and 1992-93 were close to the 30 year climatology in terms of the number of days with snowfall and the daily snowfall amounts for central Alberta. For specific case studies of snowfall events within this period we refer to Aktary and Reuter (1993) and Reuter and Beaubien (1996).

For each of the 259 cases of snowfall we identified the upper air station upwind of the snow reporting site. Specifically, the 850 mb weather charts were used to backtrack the airmass with maximum snowfall. The distance of transport on the 850 mb isobaric surface was estimated to be consistent with a 12 hour time interval. For example, if the 850 mb map suggested southerly flow, we used the upper air sounding from Great Falls, Montana (47$^0$N, 111$^0$W). Other upper air stations used were Stony Plain from Alberta; Port Hardy, Prince George and Vernon from British Columbia; Quillayute and Spokane from Washington; Salem and Medford from Oregon; Great Falls and Glasgow from Montana; Whitehorse from Yukon, and Fort Smith from the Northwest Territories. The backtracking of moisture sources along 850 isobaric surfaces has some uncertainties and there were cases where it was difficult to identify uniquely the "optimal" upwind sounding. For those cases, satellite images were consulted to identify suitable air mass trajectories. Having identified the appropriate upper sounding site we used the observed 850 mb temperature to the nearest °C.

It is debatable whether one should back track air samples at the 850 mb level for the cases where the air originated from the Pacific coast. The Continental Divide extends above the 850 mb level, and thus the sounding characteristics are modified when the air crosses over the mountain range. As an alternative to using the upwind soundings from the coastal sites, one might choose to restrict use of soundings to those located east of the Continental Divide (i.e. Stony Plain, Great Falls, Glasgow and Fort Smith). Even if the trajectories would be less-than-perfect matches, the 850 mb temperature observed at Stony Plain might be more representative of the true conditions than those taken from a coastal site with a "perfect" trajectory. An alternative would be to take the NWP model output and select the warmest model-predicted temperature at 850 mb as the input in Eq. (8).

Figure 2 summarizes the measurements for the three Alberta winters. Fig. 2a depicts the scatter diagram of 24-hourly maximum snowfall (S, in cm) plotted against 850 mb temperature ($T_0$, in °C), which was measured by the balloon sounding upwind from the snowfall. Alberta snowfall occurred in air masses with $T_0$ values ranging from -18 °C to +8 °C. There were no cases of heavy snowfall (i.e. $S \geq 10$ cm) for $T_0 \leq -8$ °C. For a given $T_0$ value there was a fair spread of S values, but there was a clear tendency of higher snowfall associated with warmer $T_0$. The dashed straight line denotes the optimal linear regression expression calculated as

$$S = 0.9\, T_0 + 9.7 \tag{9}$$

The correlation coefficient based on all data points was calculated to be 0.62. Based on statistics tables, a linear regression with 200 values must have a correlation coefficient ≥ 0.14 for the regression to be considered significant. This suggests that $T_0$ affects the snowfall and the linear dependence of $S$ on $T_0$ (derived by conserving water mass) fits the observations. The solid straight line in Figure 2a represents the theoretical prediction of

$$S = 0.74\, T_0 + 9.6 \tag{10}$$

based on $\rho_{snow} = 1$ kg m$^{-2}$ cm$^{-1}$, $p_1 = 400$ mb, $q_{s1} = 0.0002$ kg/kg. The coefficients in Eq. (10) could be changed if different assumptions would have been made about snow densities and cloud top conditions. In addition, of course, the cloud base pressure of $p_0 = 850$ mb could differ in the observed events. Despite all these uncertainties, the prediction line given by Eq. (10) provides a basis for describing the observed $(S, T_0)$ data points scatter.

The data shown in Fig. 2b are the average and maximum of the 24-hour accumulated $S$ values versus $T_0$. Comparing the averaged $S$ bars with the best regression line (solid) and the theoretical predicted line (dashed) suggests that, on average, the observed snowfall depends linearly on the upwind temperature. The discrepancy at $T_0 = 5$ °C comes from the extreme maximum snowfall of 56 cm. This extreme event occurred on 25 November 1990. Interestingly, for that day only two stations recorded snowfall: Medicine Hat (YXH) had 56 cm, and Lethbridge (YQL) had 24 cm. Clearly, the precipitation was localized. The Stony Plain sounding (Fig. 3) suggested the potential for convective instability in two layers: 850 to 650 mb and 580 to 450 mb. The dry sounding above the boundary layer would further suggest that the snowfall event would likely be isolated since the entire airmass was not moist. Thus, this case did not fit the assumption of synoptic-scale lifting, and we could have eliminated this outlier point. Nevertheless we considered it useful to keep this extreme convectively forced snowfall case as these cases can (and do) occur.

As pointed out before, a mandate for the public weather service is to provide heavy snowfall warnings, defined as events when the 24-hour accumulated snowfall is 10 cm or more. With this in mind, we tallied the number of cases with $S \geq 10$ cm for a given $T_0$ value. Fig. 2c shows that for $T_0 \leq -1$ °C the frequency of heavy snow is less than 0.3; for 0 °C $\leq T_0 \leq 1$ °C the frequency is about 0.4, and for $T_0 \geq 2$ °C the frequency exceeds 0.5. We infer from these historic data points that the conditional probability of heavy snowfall (i.e. $S \geq 10$ cm ) exceeds 50% provided the upwind 850 mb temperature is $\geq 2$ °C. The condition to be satisfied is, of course, that only cases of actual snowfall are considered. The decision of whether it will snow has to be determined a priori, for example by examining the prognostic weather charts.

We thought it would be interesting to test whether the snowfall measurements S showed good correlation with other thermodynamic variables from the upwind soundings. In particular, we examined the dependence of $S$ on thermodynamic variables observed at 700 mb, as this level is above the depth of the cold arctic air that at times obscures the 850 mb data. Fig. 4 shows the results for $S$ plotted against the wet-bulb potential temperature taken at the 700 mb level at the upwind sounding. The best regression equation for wet-bulb potential temperature ($\Theta_w$) at 700 mb was computed as

$$S = 1.4\ \Theta_w - 2.7 \tag{11}$$

with $\Theta_w$ in units of °C. The correlation coefficient for $\Theta_w$ is 0.7 which is slightly higher than that found for $T_0$. This may be due in part to large portions of the mountain range in British Columbia that extend above the 850 mb level and thus some of the moisture may be depleted due to orographic forcing. Fig. 4c shows that the historic frequency of heavy snowfall ($S \geq 10$ cm) exceeds about 0.5 whenever the $\Theta_w \geq 9\ ^{\circ}\mathrm{C}$ at 700 mb. This could be utilized as a criterion for issuing a heavy snowfall warning, conditioned to the fact that there is snowfall. For all cases of heavy snowfall the relative humidity at 700 mb was quite high, with little differences between the values of temperature, wet-bulb temperature, and dewpoint temperature. The $\Theta_w$ at 700 mb has been tested here as it is readily available to the operational forecaster as part of the sounding information.

## 4. Comparison with ECMWF model QPF

In the previous section, we found a positive correlation between the 850 mb temperature value and the maximum 24-hour accumulated snowfall amount. In order to justify the development of a new technique, it must add value above and beyond what is available from Numerical Weather Prediction (NWP) output that is currently available to the forecaster. In other words, we must compare the snowfall- temperature with the model Quantitative Precipitation Forecasts (QPF). We could not obtain archived QPF fields produced by the Canadian Regional Finite Element (RFE) Model that was operational during 1990 to 1993. However, the QPF values were available for the European Centre for Medium-Range Weather Forecasting (ECMWF) model, which is widely considered one of the best NWP models for mid-latitude forecasting of winter weather (Djuric, 1994). In recent years, data assimilation techniques of four dimensional atmospherics have been improved, which have been incorporated in the ECMWF Re-Analysis (ERA) output (Gibson et al., 1999). This model used spectral triangular truncation at wave number 106. This gives an effective horizontal resolution of ~1.6° (~125 km). It is likely that the coarse horizontal resolution could account for the low instance of >10 cm snowfall forecasts (discussed later). Today's higher resolution models may show significant improvements for the spatial pattern of QPF. In the vertical the flow is divided into 31 layers with the highest resolution in the boundary layer (where the levels follow the Earth's topography); and with the lowest resolution in the stratosphere (where the levels follow the pressure surfaces). The lead time was 6 hours. A time step of 30 minutes is used for the semi-Lagrangian scheme. The ECMWF model provides 6 hour accumulated precipitation in millimeters of melted water substance. Assuming the density of snow to rain to be 1 to 10 (consistent with our previous analysis), and accumulating the snowfall over 24 hours, we obtained model predicted 24 hour snowfall in cm. The Grided Binary (GRIB) output was contoured using the Grid Analysis and Display System (GrADS) package which allowed us to identify the

ECMWF predicted maximum 24-hourly snowfall for Alberta.

Figure 5a compares the 24 hour maximum observed snowfall (*S*) with the predicted snowfall (*P*) based on the 850 mb temperature using Eq. (10). The temperature based prediction misses several heavy snowfall cases. However, its skill is superior to that of the ECMWF (Figure 5b). The ECMWF 24 hour maximum snowfall amounts tended to be much lower than the observed snowfall amounts, with few exceptions.

To better quantify the forecasting skills for snowfall warnings we have computed several forecasting skill scores based on 2 × 2 contingency tables for the two forecasting methods. A hit was noted when 24 hour snowfall ≥ 10 cm was both observed and forecasted. A fail was recorded when 24 hour snowfall was forecast but the observed snowfall < 10 cm. And finally a miss was recorded when the forecast snowfall < 10 cm, but the observed snowfall ≥ 10 cm. Following Brimelow et al. (2002), from the 2 × 2 contingency tables we computed the Probability of Detection (POD, number of hits divided by hits plus misses), the False-Alarm Ratio (FAR, number of fails divided by number of hits plus fails) and the Critical Success Index (CSI, number of hits divided by the number of hits plus misses plus fails).

Table 2 compares the skill scores for three forecasting methods: *P* based on the 850 mb temperature using Eq. (10), snowfall amounts based on the 700 mb wet-bulb potential temperature (WBPT) using Eq. (11), and the ECMWF model predicted QPF. The POD value for snowfall ≥ 10 cm was 88% for *P*, 85% for WBPT, and 7% for the model QPF. Essentially, the ECMWF seldom predicted snowfall amounts exceeding 10 cm. The 850 mb temperature method had a high FAR of 41%, about 50% more than the WBPT method.

In terms of the CSI values, which quantify the overall skill of a forecasting method, the WBPT method was highest at 64%.

Table 2 also lists the Root-Mean Square Error (RMSE) and the Bias for the cases with $S \geq 10$ cm. The RMSE values for the 850 mb temperature method (8.2 cm) and the 700 mb WBPT method (7.5 cm) are smaller than the ECMWF model values (14.4 cm).

Table 2. Comparison of statistical skill scores of three methods to forecast 24 hour maximum snowfall amounts ≥ 10 cm. The techniques are: the predicted snowfall (TT) based on the snowfall-temperature relationship Eq. (10), the wet-bulb potential temperature (WBPT) method using Eq. (11), and the 24 hour maximum snowfall accumulation snowfall using the ECMWF model.

| | TT | WBPT | ECMWF |
|---|---|---|---|
| Probability of Detection (POD) | 88% | 85% | 7% |
| False Alarms Ratio (FAR) | 41% | 27% | 17% |
| Critical Success Index (CSI) | 54% | 64% | 7% |
| Root-Mean-Square Error (cm) | 8.2 | 7.5 | 14.4 |
| Bias (cm) | -4.4 | -2.7 | -12.0 |

The ECMWF exhibits a strong negative bias (of -12 cm) and thus severely under forecasts heavy snowfall amounts. The 850 mb temperature method and $\Theta_w$ method show much smaller negative bias values. Clearly, the ECMWF based QPF values could have improved statistics if one would simply multiply the forecasted snow amounts by constant factor. However, that would be without any physical basis as the model physics should provide the most reliable QPF value.

## 5. Discussion

The comparison with the ECMWF model output suggests that the simple snowfall-temperature method can compliment the use of NWP model guidance for deciding whether to issue a snowfall warning for Alberta, i.e. predicting the likelihood of 24-hourly maximum snowfall ≥ 10 cm. Models have come a long way since the study period, and skill scores are likely to be higher today. McBride and Ebert (2000) verified model QPF over Australia. They found that model skill degraded dramatically for 24 hour precipitation thresholds greater than 10 mm. Mullen and Buizza (2001) found the same for the ECMWF ensemble prediction system over North America. QPF forecasts skill scores were high for 24 hour precipitation thresholds of 1 mm. However, the skill scores for a 24 hour precipitation threshold of 50 mm were very poor. There is anecdotal evidence that the current Canadian operational GEM model has difficulty providing useful guidance for heavy snowfall warnings in Alberta. It is beyond the scope of this paper to make a detailed analysis of why the operational NWP models tend to under predict heavy snowfall. However, we would like to take the liberty of offering a speculation as to the short-coming. of the model. The GEM model, similar to the ECMWF model, has an explicit microphysical scheme based on bulk-water parameterization. The GEM model uses the Kong-Yau (1997) scheme which includes prognostic equations for the conservation of cloud water, rain particles, and ice particles/snow. The important microphysical processes related to ice phase in wintertime precipitation weather systems include nucleation, deposition and sublimation, freezing and melting, riming, accretion, and aggregation. The Kong-Yau scheme has explicit parameterization for the first seven of the eight microphysical processes. However, the Kong-Yau scheme does not explicitly parameterize ice crystal- ice crystal aggregation, which is the primary process of forming large snowflakes. The implicit parameterization of aggregation via assuming a fixed ice particle size distribution cannot adequately handle the situation of heavy snowfall. We speculate that a microphysical scheme is required that explicitly models the aggregation process.

Closely related to the aggregation of ice particles to form snowflakes is the issue of collection efficiency of ice - ice particle interactions. Ice collection efficiency is defined as the probability of a collision and coagulation with an ice particle located at random within the sweep out volume of a collector crystal. The collection efficiency of crystal aggregation is not well understood because it depends on the crystal shape and structures (Rogers and Yau, 1989, pp. 165). Indications are that open structures like dendrites are more likely to stick, given a collision, than closed structures like plates or needles. What is well-established, however, is the fact that sticking is more likely at relatively warm temperatures. Specifically, there is a monotonic relationship between temperature and ice-ice collection efficiency (Khain and Sednev, 1995): As temperature decreases, so does the collection efficiency of ice particles. Khain and Sednev propose that a relatively warm temperature is needed for the occurrence of heavy snowfall. This is consistent with our snowfall-temperature relationship which has been derived from water budget considerations rather than from cloud microphysical considerations.

## 6. Conclusions

Operational forecasters are faced with two major issues when predicting snowfall for Alberta. Firstly, they must predict where it will snow; and secondly, they must predict whether the 24 hour snowfall for a given location will meet or exceed 10 cm (i.e. decide to issue a warning for heavy snowfall).

Numerical weather prediction models offer reliable guidance for point 1. However, the model accumulation often underestimates the observed amount of snowfall and the forecaster benefits from additional tools to determine if the snowfall accumulation will reach the warning criterion of 10 cm or more in a 24 hour period. We analysed 259 snowfall events in Alberta from three winter seasons to examine the correlation between the maximum 24 hour snowfall accumulation ($S$) and the temperature at 850 mb recorded at an upwind sounding ($T_0$). The observed data suggest that the $S$ values increase with increasing $T_0$ values and that their dependence is a roughly linear relationship. The best regression line is $S = 0.9\ T_0 + 9.7$ with a correlation coefficient of 0.62. This empirical relationship agrees well with our theory based on conserving water substance. Assuming that the 850 mb air of the upwind sounding represents the cloud base conditions of the snow event, the water balance yields a linear relationship. The coefficients (listed in Table 1) for different cloud top levels are consistent with the observations. It is intriguing that the amount of maximum snowfall is correlated to the 850 mb temperature of the upwind air mass in a simple linear fashion. Specifically, our analysis suggests that for $T_0 \leq -1\ ^{\circ}\mathrm{C}$ the frequency of heavy snow is less than 0.3; for $0\ ^{\circ}\mathrm{C} \leq T_0 \leq 1\ ^{\circ}\mathrm{C}$ the frequency is about 0.4, and for $T_0 \geq 2\ ^{\circ}\mathrm{C}$ the frequency exceeds 0.5. The data also showed that using the wet-bulb potential temperature $\Theta_w$ at 700 mb (instead of the 850 mb temperature) improved the statistical significance of the linear correlation. The theory, however, is based on cloud base temperature and not $\Theta_w$ at 700 mb.

Many of the synoptic-scale weather systems that produce heavy snowfall pass over the Continental Divide of the Rocky Mountains with altitudes exceeding the 850 mb pressure level. There tends to be significant orographic moisture removal when the moist air is forced upslope, resulting in precipitation over British Columbia. Therefore, the 850 mb temperature value recorded at a Pacific coast sounding may not quantify adequately the moisture available for sublimation in central Alberta. Thus, the 700 mb wet-bulb potential temperature may be a better measure for the available moisture for the snowstorm than the 850 mb temperature. This is consistent with our finding that Eq. (11) gives a better correlation with the observed maximum snowfall amount than Eq. (10).

The ECMWF model predictions of 24 hour maximum snowfall amounts were compared with the observations, and with the snowfall-temperature relationship. It was found that the snowfall-temperature relationship offers value beyond the model QPF output in deciding whether to issue a heavy snowfall warning. Even so, we emphasize that the snowfall-temperature relationship should not be used as a "stand-alone" method, but rather, be used as a tool to compliment model guidance for cases of large-scale snow events over Alberta.

In the analysis presented here, the value of $T_0$ was obtained by identifying the upwind sounding. Instead, one could use the predicted 850 mb temperature from the NWP model prognostic chart. As long as the model-predicted temperature field at 850 mb is accurate, the criterion for issuing heavy snowfall could be easily implemented. A further refinement might entail actually examining forecasted soundings at model grid points. Based on the prognostic sounding one might compute the appropriate cloud base level and estimates of the maximum snowfall based on predicted cloud base level rather than the assumed 850 mb cloud base conditions. It not obvious that these suggested refinements would necessarily result in a better estimation of the snowfall accumulation because of the inherent uncertainties of the factors such as snow density and cloud base height. Also entrainment into the cloud would affect the water budget in the clouds and this cannot be easily included. In some ways the simplest approach of identifying critical thermodynamic conditions necessary for heavy snowfall may be the most useful in an operational setting having severe time constraints. The results presented here are based on three winters for Alberta. It would be useful to expand this dataset to cover more winter seasons and other geographical regions such as the Canadian Arctic.

## Acknowledgements

We appreciated the thoughtful comments of anonymous reviewers that helped to clarify our analysis. This research was supported by the Natural Sciences and Engineering Research Council (NSERC) of Canada through a GEWEX Collaborative Research Network Grant.

## References

Aktary, N., and G. W. Reuter, 1993: Observations of a snowband in a symmetrically unstable flow over Alberta. *Contrib. Atmos. Phys.*, **66**, 25-282.

Auer, A. H., 1987: An aid to forecasting heavy snowfall episodes. *Natl. Wea. Dig.*, **12**, 11-14.

Brimelow, J. C., G. W. Reuter, and E. R. Poolman, 2002: Modelling maximum hail size in Alberta thunderstorms. *Wea. Forecasting*, **17**, 1048-1062.

Carlson, T. N., 1980: Airflow through midlatitude cyclones and the comma cloud pattern. *Mon. Wea. Rev.*, **108**, 1498-1509.

Chung, Y. S., K. D. Hage, and E. R. Reinelt, 1976: On lee cyclogenesis and airflow in the Canadian Rocky Mountains and East Asian mountains. *Mon. Wea. Rev.*, **104**, 879-891.

Djurić, D. 1994: *Weather Analysis*. Prentice Hall Inc., 304 pp.

Gibson, J. K., P. Kållberg, S. Uppala, A. Hernandez, A. Nomura, and E. Serrano, 1999: ERA-15 Description – Version 2 - January 1999, 84 pp. [Available from European Centre for Medium-Range Weather Forecasts; see also at http://badc.nerc.ac.uk/data/ecmwf-era/era-15_doc.pdf]

Khain, A. P., and I. L. Sednev, 1995: Simulation of hydrometeor size spectra evolution by water-water, ice-water and ice-ice interactions. *Atmos. Res.*, **36**, 107-138.

Kocin, P. J., and L. W. Uccellini, 1990: Snowstorms along the northeastern coast of the United States:1995 to 1985. *Meteor. Monographs*, **22**, Amer. Meteor. Soc., Boston, MA., 280 pp.

Kong, F. Y., and M. K. Yau, 1997: An explicit approach to microphysics in MC2. *Atmos. Ocean*, **35**, 257-291.

McBride, J. L. and E. E. Ebert, 2000: Verification of quantitative precipitation forecasts from operational numerical weather prediction models over Australia. *Wea. Forecasting*, **15**, 103-121.

Mullen, S. L., and R. Buizza, 2001: Quantitative precipitation forecasts over the United States by the ECMWF ensemble prediction system. *Mon. Wea. Rev.*, **129**, 638-663.

Reuter, G. W., and N. Aktary, 1995: Convective and symmetric instabilities and their effect on precipitation: Seasonal variations in Central Alberta during 1990 and 1991. *Mon. Wea. Rev.*, **123**, 153-162.

_________, and R. Beaubien, 1996: Radar observations of snow formation in a warm pre-frontal snowband. *Atmos. Ocean*, **34**, 605-626.

Roebber, P. J., S. L. Bruening, D. M. Schultz, and J. V. Cortinas Jr., 2003: Improving snowfall forecasting by diagnosing snow density. *Wea. Forecasting*, **18**, 264-287.

Rogers, R. R., and M. K. Yau, 1989: *A Short Course in Cloud Physics*: Third edition, Pergamon Press, 293 pp.

Rouse, W. R., and co-authors, 2003: Energy and water cycles in a high-latitude, north-flowing river system: Summary of Results from the Mackenzie GEWEX Study – Phase 1. *Bull. Amer. Meteor. Soc.* **84**, 73-87.

Stewart, and co-authors, 1998: The Mackenzie GEWEX study: The water and energy cycles of a major North American river system. *Bull. Amer. Meteor. Soc.*, **79**, 2665-2683.

Szeto, K. K., R. E. Stewart, and J. M. Hansiak, 1997: High latitude cold season frontal cloud systems and their precipitation efficiency. *Tellus*, **49**, 439-454.

Szeto, K. K., 2002: Moisture recycling over the Mackenzie basin. *Atmos. Ocean*, **40**, 181-197.

Xin, L., and G. W. Reuter, 1996: Numerical simulation of the effects of mesoscale convergence on convective rain showers. *Mon. Wea. Rev.*, **124**, 2828-2842.

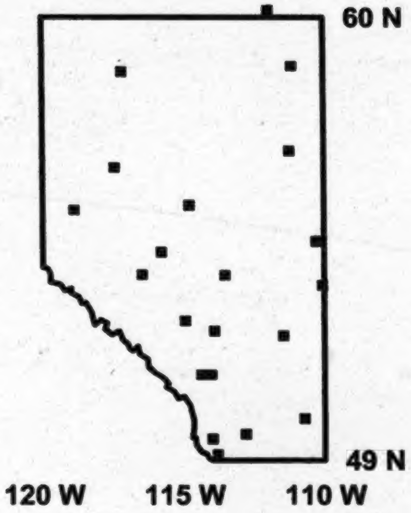
60 N
49 N
120 W
115 W
110 W

Fig. 1. Outline of Alberta with the locations of the snowfall reporting sites used in this study.

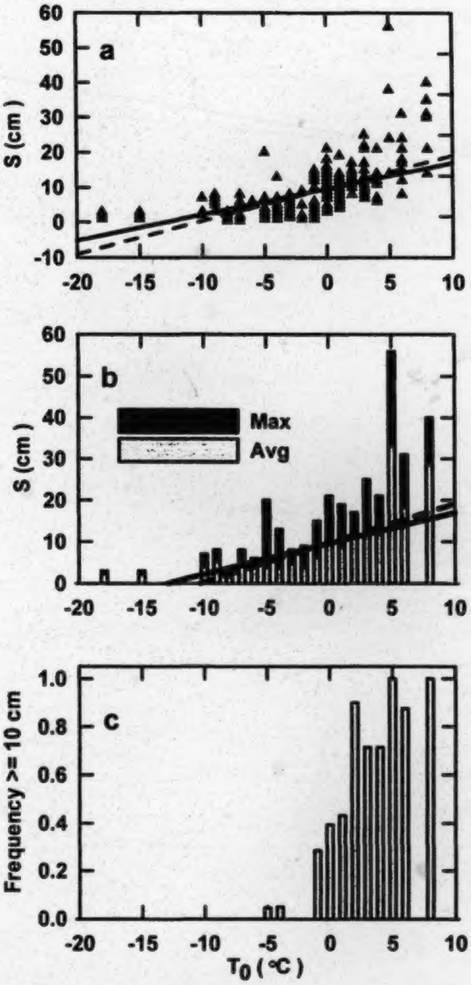

Fig. 2. Snowfall observations compared with 850 mb temperature values from upwind site. a) Measurements of maximum 24 hour snowfall *S* plotted versus temperature $T_0$ at 850 mb. The triangles denote the observations and the dashed line shows the optimal regression line. The solid line shows the theoretical prediction based on Eq. (10); b) Average and maximum *S* values plotted against $T_0$ at 850 mb; c) Percentage frequency of cases when $S \geq 10$ cm plotted against $T_0$ at 850 mb.

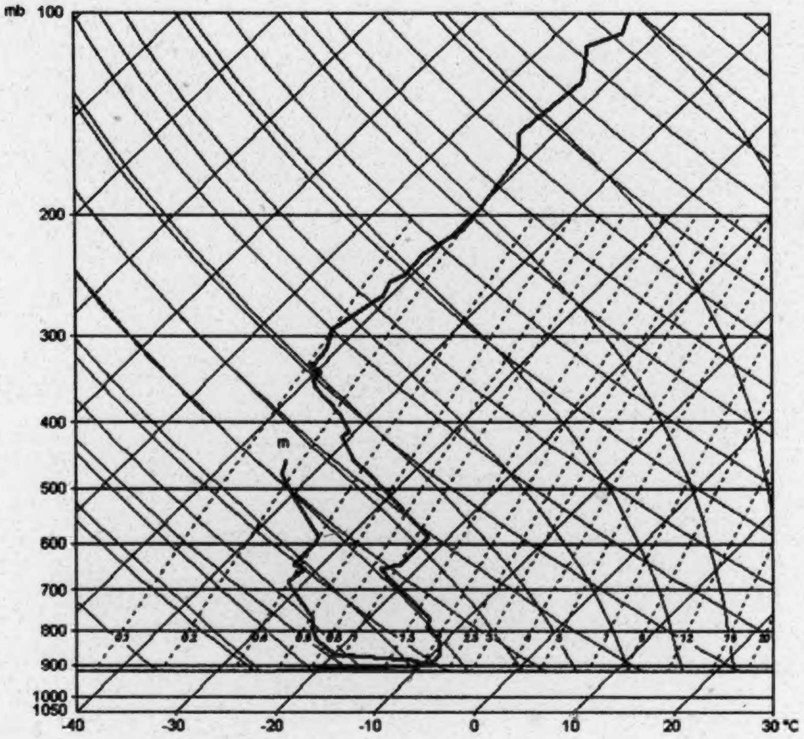

Fig. 3. Skew-T sounding observed at Stony Plain (50 km west of Edmonton, Alberta) at 1200 UTC, November 25, 1990, depicting temperature and dewpoint profiles. Horizontal lines are isobars (mb), straight lines skewed to the right are isotherms (°C), thin curved lines skewed to the left are dry adiabats (°C), thicker curved lines are moist adiabats (°C), and dashed lines are mixing ratio (g $kg^{-1}$).

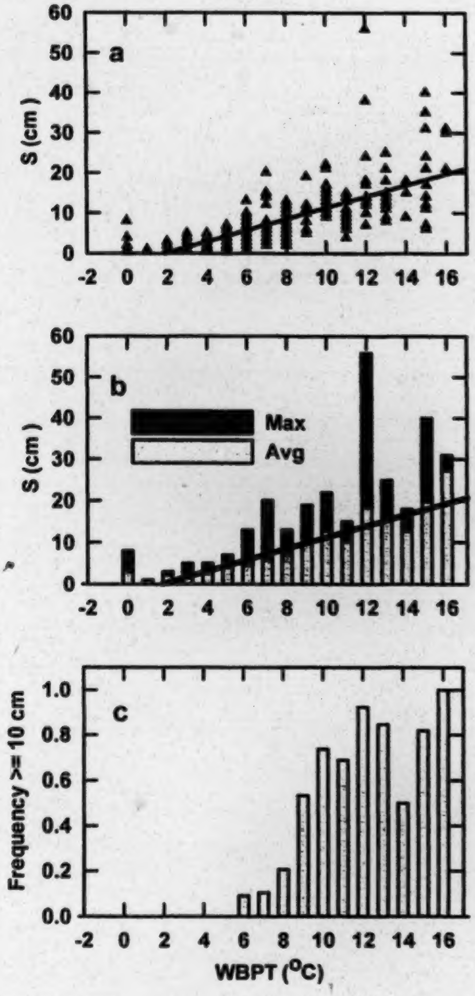

Fig. 4. Snowfall observations compared with 700 wet-bulb potential temperature values from upwind site. a) *S* plotted versus 700 mb wet-bulb potential temperature (WBPT) at 700 mb in °C. The triangles denote the observations and the solid line shows the optimal regression line Eq. (11); b) Average and maximum *S* plotted against WBPT at 700 mb; c) Percentage frequency of cases when $S \geq 10$ cm plotted against WBPT at 700 mb.

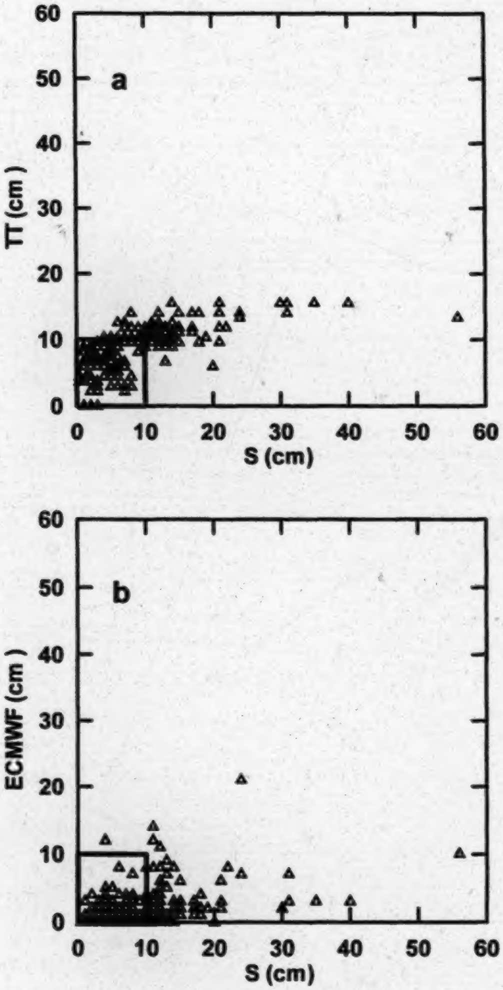

Fig. 5. Comparison of forecasting techniques for Alberta snowfall. a) Predicted snowfall amounts (TT) based on snowfall-temperature relationship Eq. (10) plotted against observed maximum 24 hour snowfall (*S*); b) Predicted 24 hour snowfall amount from the ECMWF model plotted against observed maximum 24 hour snowfall (*S*).

# Chapter VII

# Conclusion and Discussion

## 1. Summary

This thesis investigated the use of rawinsonde data to assist in forecasting severe weather for Alberta. Specifically, it addressed the issue of whether environmental sounding parameters could provide probabilistic guidance for discriminating between Significant Tornadoes (F2 to F4), Weak Tornadoes (F0 and F1) and Non-Tornado severe thunderstorms (i.e. thunderstorms with 3 cm or greater diameter hail and no reported tornado). The dataset consisted of 74 tornadic storms and 13 Non-Tornadic severe thunderstorms in central Alberta. Parameters investigated included bulk shear for different layers, Convective Available Potential Energy (CAPE), normalized CAPE, storm-relative helicity, lifted condensation level, precipitable water, and tropospheric humidity. In addition, a new sounding parameter referred to as "storm convergence" (introduced in Chapter IV) was examined. The use of sounding parameters to predict tornadoes has been a significant focus of tornado research in the U.S. However, similar research has been lacking for Alberta, even though that region has one of the highest frequencies of tornadoes in Canada. The paucity of tornado research in Alberta is due, in large part, to the scarcity of recorded data or tornado occurrences. The tornado climatology, dating back to 1879, compiled by Hage (2003) was the first comprehensive documentation of Alberta tornadoes. The research in this thesis is the first to exploit Hage's tornado climatology data.

Values of bulk shear (through the 900-500 mb layer) associated with each of the three storm classes (Non-Tornado, Weak Tornado and Significant Tornado) were statistically distinct. As well, low-level shear in the 900-800 mb layer showed skill in discriminating Severe Tornado events from Weak Tornado events. These results suggested that shear threshold pairs could be useful to define threat regions for Severe Tornadoes in a probabilistic manner. For example the threshold pair of 900-500 mb shear = 3 m $s^{-1}$ $km^{-1}$ and 900-800 mb shear = 6 m $s^{-1}$ $km^{-1}$ would have captured about 75% of the Significant Tornado cases.

Storm-relative helicity, especially in the 0-3 km layer, showed skill in distinguishing Significant Tornado cases from Weak Tornado and Non-Tornado cases. However, storm-relative helicity added little information beyond that available from bulk shear for discriminating the Significant Tornadoes. Additionally, bulk shear can be computed more directly from a sounding wind profile since, unlike storm-relative helicity, it does not depend on methods for estimating the storm motion vector.

Sounding parameters closely related to thermal buoyant energy (such as CAPE, normalized CAPE, lifted condensation level, and storm convergence) did not offer any help in distinguishing between the three storm classes. The Bulk Richardson Number showed limited skill in distinguishing between Significant Tornado and Weak Tornado events, related to the finding that buoyant energy was not well correlated with different storm categories.

Precipitable water provided discrimination of Significant Tornadoes from both Weak Tornadoes and Non-Tornadoes cases. All Significant Tornadoes developed in environments which had precipitable water ≥ 21 mm. This is considerably greater that the mean value of 15 mm during the summer months in Alberta (Taylor 1999). In fact, most of the storms in entire data set (Non-Tornadoes, Weak Tornadoes, Significant Tornadoes) had precipitable water values greater than about 20 mm. This suggests that, for Alberta, precipitable water values greater than 20 mm indicate an unusually moist environment which is likely to be associated with thunderstorm development. Tropospheric humidity, the ratio of precipitable water to saturation precipitable water, was also examined. There was a tendency for larger precipitable water values to be correlated with higher tropospheric humidity values, especially for the Significant Tornado cases. A combination of tropospheric humidity and precipitable water provides additional information about the vertical moisture structure of the atmosphere which may be critical in the formation of tornadoes.

This thesis also provided a comparison of the three most severe tornadoes in Alberta in the past 28 years: the F4 Edmonton tornado of 31 July 1987, the F3 Holden tornado of 29 July 1993, and the F3 Pine Lake tornado of 14 July 2000. This was the first peer reviewed examination of the Edmonton tornado (the only F4 tornado recorded in Alberta). Results suggested that the build-up of CAPE was caused, in large part, by differential temperature changes at various altitudes. In two cases (Edmonton and Holden) the temperature lapse rate increased by strong low-level warming (>4 °C below 850 mb) likely due to diabatic heating. In contrast, for the Pine Lake storm strong cooling at low and mid-levels (above 850 mb) intensified the potential instability with only a shallow layer near the surface experiencing warming. The Holden and Pine Lake storms showed cooling above about 850-800 mb, compatible with the Smith-Yau (1993a,b) model, while the Edmonton storm showed warming throughout most all of the column. The Holden and Pine Lake cases showed the greatest cooling near the 800 mb level. It can be speculated that, while upper-level cooling serves to increase the thermal buoyancy potential, low-level cooling (850-700 mb) is a major component for breaking the capping inversion to release the latent instability. The Edmonton storm environment did not feature a surface dewpoint gradient (dryline), rather the entire boundary layer was very humid with spatial uniformity. The presence of a surface dryline may not be a necessary feature for the formation of thunderstorms. A comparison of the tracks of the Edmonton, Holden and Pine Lake thunderstorms showed the Pine Lake and Holden storms moved with constant direction and speed. The Edmonton storm, however, made an abrupt change in direction and speed. Thus, extrapolation of thunderstorm movement would not have been a viable nowcasting technique in that case.

Finally, this thesis introduced a snowfall accumulation theory which related the snowfall amount (specifically snowfall > 10 cm) in Alberta to the 850 mb temperatures from an upwind sounding site. The theory was based upon conservation of total water substance. An analysis of snowfall events in Alberta from three winter seasons suggested that snowfall amounts increased monotonically and roughly linearly with increasing 850 mb temperature. The best regression line was $S = 0.9\ T_0 + 9.7$ (where $S$ is the observed snowfall amount in cm and $T_0$ is the 850 mb temperature in $^{\circ}$C). This empirical relationship agreed well with theory.

## 2. Implications for forecasting

Forecasting of severe weather and issuing timely warnings is a mandate of the

Canadian weather service. In the summer months in Alberta, severe weather most often occurs in the form of thunderstorms producing large hail (≥ 2 cm diameter) and occasionally tornadoes. In the winter months Alberta's severe weather often takes the form of heavy snowfalls (≥ 10 cm in 24 hours). As the population of Alberta continues to rapidly increase and expand into presently rural areas, the need for timely weather warnings of tornadoes and snowstorms will become increasingly important. There is anecdotal evidence to suggest reports of tornadoes have increased as people occupy once unpopulated areas. It is likely that the number of tornadoes has not significantly increased rather there are now more people to observe and report them. The concern for safety of the general public is certainly a priority for the weather service. However, it is additionally important for a number of private enterprise sectors to have the most accurate weather warnings possible. For example, the aviation sector is critically dependent upon accurate forecasts of thunderstorms and potential tornadoes in the vicinity of airports. Air traffic must abide by strict regulations in regards to maintaining a safe distance from severe thunderstorm activity. In the winter, snowfall forecasting is important for economical maintenance of highways as road crews must be put on alert when heavy snowfalls are expected. With an increasing population, highway traffic will also increase resulting in a greater demand for additional tools to aid in forecasting snowfall amounts. Forecasting aids, specific to the geographical location and complexities of the terrain in Alberta, are needed in order to help maintain and improve prediction of severe weather in this region.

At present, warnings of severe thunderstorms in Alberta take the form of a special warning statement which describes the motion and expected development of the storm in relation to one or more of the following conditions: heavy rainfall (≥ 30 mm per hour), damaging winds (≥ 90 km $h^{-1}$), large hail (≥ 2 cm in diameter), or intense lightning. In addition the warning may include a statement indicating the some severe thunderstorms may also produce tornadoes. Only once a tornado is seen and reported is a tornado warning issued describing the expected motion, development and duration. The following is an example of a severe thunderstorm warning:

> **Severe thunderstorm warning for**
> City of Edmonton - St. Albert - Fort Saskatchewan issued.
>
> Radar is showing a severe thunderstorm southwest of the City of Edmonton moving northeastward at 60 km/h. Large hail and damaging winds are possible with this storm. This is a warning that severe thunderstorms are imminent or occurring in these regions. Remember some severe thunderstorms produce Tornadoes. Listen for updated warnings.

The tornado warning process could be improved by having longer lead times and also by issuing a "probabilistic assessment" of the likelihood for tornado development and the potential for a Significant (F2-F5) Tornado. Under this scenario a forecaster could assess the potential for tornadic activity within a given area several hours in advance of storm development. Once a severe storm had developed, the thunderstorm warning could include a probability forecast for potential tornado development. In order to move toward this enhanced tornado warning system a forecaster requires additional information and tools specific to their region, in this case Alberta.

This research suggests that some threshold values for tornado potential developed in the United States may not apply to tornadic development in Alberta. In particular the range of storm-relative helicity values for Alberta tornadoes was found to be lower that in the U. S. Also precipitable water, which may not be a discriminating parameter in the some very moist regions of the southern U. S., appeared to be associated with the probability for formation of Significant Tornado storms in Alberta. To aid the forecaster in making an assessment for the potential of Significant Tornadoes in Alberta, threshold values are suggested for parameters which provided a statistically significant separation of Significant Tornadoes from both Weak Tornadoes and Non-Tornado storms. Thresholds of bulk shear, 0-3 km storm-relative helicity, and precipitable water were chosen as the 25th percentile value (from box and whisker plots in Chapters III and IV) for the Significant Tornado cases. Table 1 shows the threshold values a forecaster might associate with Significant Tornado development for Alberta. Bulk shear thresholds are generally consistent with those from modeling and observations in the U.S. (e.g. Rasmussen and Blanchard 1998; Thompson et al.2003). Precipitable water ranges correspond to those found by Djurić (1994, pp. 86) for the U. S. However, as previously noted precipitable water values above 20 mm are rare in Alberta. Ranges of 0-3 km storm-relative helicity are lower than found in the U.S. (e.g. Thompson et al. 2003)

During the winter months the forecasting of heavy snowfall potential in Alberta becomes extremely important, as previously outlined. Results from Chapter VI show that numerical weather prediction models often greatly underestimate the amount of precipitation for a given region. Just as with severe thunderstorms in the summer, forecasters need additional tools to aid in predicting the potential for heavy snowfall in winter. This thesis provided an original method for estimating maximum snowfall amounts based on values of 850 mb temperature and 700 mb wet-bulb potential temperature. This technique could be used to augment numerical model Quantitative Precipitation Forecast (QPF) of snowfall. In addition to the snowfall equations developed in Chapter VI, threshold values are suggested to aid the forecaster in making an assessment for the potential of heavy snowfall in Alberta. The threshold values of 850 mb temperature and 700 mb wet-bulb potential temperature for heavy snowfall were chosen such that there was at least a 0.50 probability of snowfall ≥ 10 cm. Threshold values of 850 mb temperature ≥ 2 °C or 700 mb web-bulb potential temperature ≥ 9 °C (Table 1) might be associated with the potential for heavy snowfall for Alberta. The snowfall equations developed in Chapter VI and the suggested threshold values for heavy snowfall were first introduced at a Canadian Meteorological and Oceanographic Society (CMOS) conference in June 2003. Since then, these methods have been adopted by operational forecasters for Alberta as an aid in predicting snowfall amounts.

Table 1. Suggested thresholds associated with severe weather events in Alberta.

| Parameter | Value |
|---|---|
| Significant Tornadoes (F2 to F4) | |
| 900 – 800 mb Bulk Shear ($m\ s^{-1}\ km^{-1}$) | ≥ 6 |
| 900 – 500 mb Bulk Shear ($m\ s^{-1}\ km^{-1}$) | ≥ 4 |
| 0-3 km Storm-Relative Helicity ($m^2\ s^{-2}$) | ≥ 140 |
| Precipitable Water (mm) | ≥ 23 |
| Heavy Snowfall (≥10 cm in 24 hr) | |
| 850 mb Temperature ( °C ) | ≥ 2 |
| 700 mb Wet Bulb Potential Temperature ( °C ) | ≥ 9 |

It is important to emphasize that these thresholds are probably necessary ingredients but they are not sufficient. Thresholds should only be applied once the forecaster has determined, *a priori*, that convection or snow is likely and are not meant to be used as a type of "black box" to determine the whether or not thunderstorms or snow storms will occur. In particular, for thunderstorms it is likely the interplay of several environmental variables in sufficient amounts that leads to tornadogenesis (Rasmussen and Blanchard 1998) and isolating any one variable as a type of "magic parameter" is strongly discouraged. For example, strong shears may exist without the atmosphere being unstable and capable of thunderstorm development. This can occur when a westerly jet stream lies over Alberta, resulting in strong mid and upper-level winds coupled with light boundary layer winds. As an extreme example of this, consider a common winter synoptic pattern for Alberta in which a strong westerly flow overrides a shallow low-level layer of arctic air. In this case, boundary layer winds in the arctic airmass are often very light while 500 mb winds can be on the order of 30 m $s^{-1}$. This situation could result in 900-500 mb bulk shear of about 7.5 m $s^{-1}$ $km^{-1}$, greater than the shear associated with storm development in this study. This winter pattern results in a very stable atmosphere and convection is certainly not expected.

An emerging trend throughout many forecast communities suggests a move toward *probabilistic* rather than *deterministic* forecasting. In a probabilistic forecast regime a forecaster would provide an estimate of the likelihood of an event rather than indicating specifically whether that event will occur or not. An example in use today is the Probability of Precipitation forecast in which the probability of rain for a given day is forecast, rather than categorically stating "rain today". When assessing the probability of an event the forecaster is guided by baseline probabilities which can come from climatological frequencies or from objective forecasting systems (such as numerical model output statistics). By using these objective baseline probabilities, a forecaster assesses the relative threat associated with his/her estimate. For example, if the event in question occurs under a relatively confined set of environmental conditions and these conditions are realized, the forecast probability is likely much greater than the mere climatological frequency would suggest. In contrast, if the event occurs over a very broad range of environmental conditions this would suggest the forecaster is unable to distinguish the likelihood of the event on this day compared with any other randomly chosen day in the historical record. The results presented in Chapters III and IV indicate that in some regions of a parameter space it is more likely that Significant Tornadoes will occur than in other regions. For example, Significant Tornadoes tended to occur with a combination of large values of low-level shear and deep-layer shear. They were also more likely when greater deep-layer shear was combined with greater values of precipitable water. Heavy snowfalls in the winter months were more prevalent when the upwind 850 mb temperature was greater than 2 °C. The thresholds given in Table 1 define conditions under which severe weather events may be more likely to occur.

### 3. Recommendations for further research

The Storm Prediction Center (SPC) of NOAA has assembled a huge archive of severe storm data for the continental United States encompassing the period from 1950 to 2002. The data of thunderstorms and tornadoes are freely available on-line at http://www.spc.noaa.gov. At present there is no similar national tornado database in

Canada. The Meteorological Service of Canada is in the process of developing a tornado database for Ontario. This should be expanded to all of Canada, with a national standard in place for classifying and recording tornadoes. This thesis research could then be expanded to examine tornadoes throughout Canada.

Values of precipitable water in conjunction with tropospheric humidity appear useful for providing information about the vertical moisture structure of the atmosphere. Since the temperature characteristics of a rear-flank downdraft appear to be critical to the development (or non-development) of a tornado, more research is needed to clarify whether precipitable water values are indeed correlated with the air temperature in a rear-flank downdraft.

There is an issue of whether tornado research using sounding parameters to predict tornadoes is actually isolating parameters which distinguish between non-tornadic and tornadic storms or if, in fact, some of these parameters are merely discriminating based upon geographical differences of storms (Rasmussen 2003). To this end it would be useful to divide the large U.S. database of severe storms into several sections based upon geographical location. For example, one subset of storms may be for areas east of the Mississippi River, another subset for storms on the high plains of the southwest, and another subset for storms between the plains and the Mississippi River.

The snowfall method developed in this thesis could be expanded to all areas of Canada. Using model predicted sounding data at grid points corresponding to the location of the expected event, rather than upwind soundings, could be explored. Precipitable water instead of (or in addition to) the 850 mb temperature or 700 mb wet-bulb potential temperature could be used to estimate the amount of total moisture available for snowfall A regression equation may relate precipitable water to snowfall amounts. However, it is not obvious that these suggestions would necessarily result in a better estimation of the snowfall accumulation due to the inherent uncertainties of factors such as snow density and cloud base height.

# References

Djuric, D. 1994: *Weather Analysis*. Prentice Hall Inc., 304 pp.

Hage, K. D., 2003: On destructive Canadian prairie windstorms and severe winters. *Natural Hazards*, **29**, 207-228.

Rasmussen, E. N., 2003: Refined supercell and tornado forecast parameters. *Wea. Forecasting,* **18**, 530–535.

_______, and D. O. Blanchard, 1998: A baseline climatology of sounding-derived supercell and tornado forecast parameters. *Wea. Forecasting*, **13**, 1148-1164.

Smith, S. B., and M. K. Yau, 1993a: The causes of severe convective outbreaks in Alberta. Part I: A comparison of a severe outbreak with two nonsevere events. *Mon. Wea. Rev.*, **121**, 1099-1125.

_______, and _______, 1993b: The causes of severe convective outbreaks in Alberta. Part II: Conceptual and statistical analysis. *Mon. Wea. Rev.*, **121**, 1126-1133.

Taylor, N. M., 1999: Climatology of sounding parameters identifying the potential for convective storm development over Central Alberta. M. S. thesis, Dept. of Earth and Atmospheric Sciences, University of Alberta, 121 pp. [Available from the University of Alberta, 114 St. – 89 Ave., Edmonton, AB, Canada, T6G 2E21]

Thompson, R. L., R. Edwards, J. A. Hart, K. L. Elmore, and P. Markowski, 2003: Close proximity soundings within supercell environments obtained from the Rapid Update Cycle. *Wea. Forecasting*. **18**, 1243-1261.

## APPENDIX A Defining a Tornado

During the past 30 years or so much research has been devoted to both understanding and predicting the formation of tornadoes. In the early years, a tornado was defined as a meteorological phenomenon. The *Glossary of Meteorology* (Glickman 2000) provides the following definition:

*Tornado* -- 1. A violently rotating column of air, in contact with the ground, either pendant from a cumuliform cloud or underneath a cumuliform cloud, and often (but not always) visible as a funnel cloud.

In recent years however, there has been a shift in thinking concerning tornadoes and tornadogenesis. Since there still is not a complete understanding of all the relevant physical processes of tornado formation, we are caught in somewhat of a "Catch-22" situation: in order to understand tornadoes, we need proper clarification and classification, but to develop a proper classification we need to understand tornadoes. To date, there has never been a formal definition of a tornado that has been extensively peer-reviewed (Doswell 2001). According to Doswell, a tornado, regardless of which definition one may choose, is not an *object*; it is a *process*. That is, the rotational wind field that we define to be the "tornado" is continually evolving and changing in response to other processes. There does not exist a uniformly formed object which is carried along by a thunderstorm to leave extensive damage in its wake. Observationally, it seems that vortices of tornadic intensity are produced virtually exclusively in association with deep moist convection. There surely are dust devils (dry convective vortices) that attain damaging proportions but are not classified as tornadoes. Since dust devils are generally not destructive, they are given little attention. In addition, dust devils tend to occur in arid regions of extremely sparse population (e.g. open fields), furthering our ignorance of these events. Within the range of vortices associated with deep moist convection there are likely many different processes which can produce vortices from convective clouds that do not affect the surface. For example, the discussion of "cold air funnels" by Cooley (1978) is about the only paper dealing with this topic in the refereed journals. At times forecasters have issued tornado watches based on observations of these cold air funnels. Classifying such vortices in this manner may be prompted by a perceived need to "explain" observations of *all* funnels, but it probably does more harm than good to provide a misconception that these funnels are "embryonic tornadoes". Science can offer little more than speculation about the origins of these non-tornadic vortices (e.g. Bluestein 1994). It is conceivable that some small percentage of these minor events could produce damaging winds at the surface but we have no way of knowing what that percentage might be. Waterspouts are often used as special names for funnels moving over the water. However, there does not appear to be any special physical processes which separate waterspouts from tornadoes. A waterspout is merely a tornado moving over a body of water.

In light of the confusion over what exactly constitutes a tornado, Doswell (2001) proposed the following definition:

*Tornado* -- A vortex extending upward from the surface at least as far as cloud base (with that cloud base associated with deep moist convection), that is intense enough at the surface to do damage, should be considered a tornado.

This is without regard to

- the underlying surface
- the existence/non-existence of a condensation cloud from cloud base to the surface
- the depth of the moist convective cloud
- the presence/absence of ice in the upper reaches of the convective cloud
- the occurrence/non-occurrence of lightning within the convective cloud
- the intensity of the phenomenon beyond some lower threshold

This broadened definition is designed to ignore what Doswell terms to be "incidental aspects of the situation". That is, the physical process giving rise to an intense vortex (tornado) is not associated with the formation of minor vortices. This definition excludes any phenomena not associated with deep moist convection, such as dust devils or cold air funnels and avoids making artificial and scientifically unjustified distinctions between "spouts" and tornadoes. It is important to emphasize this definition does not mean that the physical processes giving rise to tornadoes are all the same. It appears that tornadoes develop through a variety of mechanisms and perhaps different physical processes are even associated with a given tornado at different phases in its life cycle. It is likely that not all tornadoes associated with a given moist convective cloud arise via the same processes. At present, we have assumed most tornadoes develop from severe or supercell thunderstorms. However, there is increasing evidence that not all tornadoes are spawned by such supercell storms (Wakimoto and Wilson 1989). In the future, it may become scientifically useful to sub-classify tornadoes even further, as we learn more about the physical processes of tornadogenesis.

The previous mention of a supercell also implies a definition of this phenomenon is necessary. Unfortunately, much like tornadoes, there does not seem to be a consensus on a clear definition of a supercell. The definition most often accepted is: "*a supercell is a convective storm that possesses a deep, persistent meso-cyclone*" (Doswell 1996). The meaning of "deep" is taken to be that the circulation meeting meso-cyclone criteria is present and vertically connected through a significant fraction (about 1/3) of the depth of the convective storm. Persistent is measured with comparison to a convective time scale defined by the time it takes a parcel to rise from the base of the updraft to the top of the cloud (about 10-20 min). A "meso-cyclone" can be defined in many ways. Doswell (1996) suggests using the vorticity magnitude, where a "meso-cyclonic vorticity unit" is $10^{-2}$ $s^{-1}$. This definition of a meso-cyclone (and hence a supercell) requires some way to obtain a reasonably accurate measurement of the wind field associated with a thunderstorm. Doppler radar is about the only means of providing these measurements of the wind field. However, the resolution of the Doppler radar in Alberta (1.1° beamwidth) makes the detection of most meso-cyclones a very challenging task. Authors have classified supercells using environmental parameters such as wind shear and Convective Available Potential Energy (CAPE). The Bulk

Richardson Number (BRN), defined as BRN = CAPE / (½ $U^2$), (where U represents the difference between the density weighted mean winds in the 0-6 km and 0-500 m layers) quantifies the ratio of the vertical component relative to the horizontal component of the kinetic energy. As the BRN decreases, multicell convection becomes better organized, and at small enough values, quasi-steady supercell convection may occur. A storm environment with a high CAPE value and a BRN value less than about 50 increases the likelihood of a supercell storm (Weisman and Klemp 1982, 1986; Thompson et al. 2003). Rasmussen and Wilhelmson (1983) proposed that non-rotating thunderstorms could be found in environments of low shear and low CAPE while tornadic supercell storms occurred with moderate-strong shear ($> 3.5 \times 10^{-3}$ $s^{-1}$ ) and high CAPE ( > 2500 J $kg^{-1}$).

In conclusion, Doswell (2001) sums up the situation by stating that, in practice, the definition of a supercell matters to an operational forecaster only to the extent that the probability of a given severe weather event changes when those events are related to supercell and non-supercell storms.

## References

Bluestein, H., 1994: Funnel clouds pendant from high-based cumulus clouds. *Weather*, **43**, 220-221.

Cooley, J.R., 1978: Cold air funnel clouds. *Mon. Wea. Rev.*, **106**, 1368-1372.

Doswell, C. A. III, 1996: What is a supercell? Preprints, *18 th Conf. Severe Local Storms,* San Francisco, CA, *Amer. Meteor. Soc.*, 641.

_______, cited 2001: What is a tornado? Cooperative Institute for Mesoscale Meteorological Studies. [Available online at http://www.cimms.ou.edu/~doswell/a_tornado/atornado.html.]

Glickman, T. S., 2000: *Glossary of Meteorology. 2nd Ed.*, Amer. Meteor. Soc., 855 pp. [Also available online at http://amsglossary.allenpress.com/glossary.]

Lemon, L. R., and C. A. Doswell III, 1979: Severe thunderstorm evolution and mesocyclone structure as related to tornadogenesis. *Mon. Wea. Rev.*, **107**, 1184-1197.

Rasmussen, E. N., and R. B. Wilhelmson, 1983: Relationships between storm characteristics and 1200 GMT hodographs, low level shear and stability. Preprints, *13th Conference on Severe Local Storms*, Tulsa, OK, Amer. Meteor. Soc., 55-58.

Thompson, R. L., R. Edwards, J. A. Hart, K. L. Elmore, and P. Markowski, 2003: Close proximity soundings within supercell environments obtained from the Rapid Update Cycle. *Wea. and Forecasting*, **18**, 1243–1261.

Wakimoto, R. M., and J. W. Wilson, 1989: Non-supercell tornadoes. *Mon. Wea. Rev.*, **117**, 1113-1140.

Weisman, M. L., and J. B. Klemp, 1982: The dependence of numerically simulated convective storms on vertical wind shear and buoyancy. *Mon. Wea. Rev.*, **110**, 504-520.

_______, and _______, 1986: Characteristics of isolated storms. *Mesoscale Meteorology and Forecasting*. P. S. Ray, Ed., Amer. Meteor. Soc., 331-357.

## APPENDIX B Tornado Classification Scale

The intensity or wind speed of a tornado is related to the type of damage it produces. The Fujita damage scale (Fujita 1973, 1981) is widely accepted as a means of rating tornadoes according to the type of *damage* they do, not the *appearance* of the funnel (Table 1). Storm spotters, storm chasers and other weather observers often try to estimate the intensity of a tornado when they are in the field, basing their judgment on criteria such as the estimated rotational speed, amount of debris being generated, and width of the tornado funnel. However, the official damage estimate is made *after* the tornado has passed, when personnel from a weather office survey the site to determine the F-Scale rating. The things they look for are: attachment of the walls and floor to the foundation of the building, attachment of the roof to the rafters and walls, whether or not there are steel reinforcing rods in concrete or cinder block walls, and whether there is mortar between the cinder blocks A key point to remember is that the size of a tornado is not necessarily an indication of its intensity. Large tornadoes may sometimes be weak, and small tornadoes can be violent. The Fujita scale (F-scale) is certainly not a perfect system for linking damage to wind speed but it has distinct advantages over what had gone on before its inception and it was fairly simple to use in daily practice.

Table 1. The Fujita Tornado Damage Scale, referred to as the F-Scale, classifies tornadoes based on the resulting damage. The relation between wind speed $v$ and F-value is given as:

$$v = 22.68(F+2)^{\frac{3}{2}} \qquad \text{where } v \text{ is in km h}^{-1}.$$

| F-scale | Intensity Phrase | Wind Speed (km $h^{-1}$) | Type of Damage |
|---|---|---|---|
| F0 | Gale tornado | 64-116 | Some damage to chimneys, TV antennas, roof shingles, trees, and windows. |
| F1 | Moderate tornado | 117-180 | Automobiles overturned, carports destroyed, trees uprooted. |
| F2 | Significant tornado | 181-253 | Roofs blown off homes, sheds and outbuildings demolished, mobile homes overturned. |
| F3 | Severe tornado | 254-332 | Exterior walls and roofs blown off homes. Metal buildings collapsed or severely damaged. Forests and farmland flattened. |
| F4 | Devastating tornado | 333-418 | Few walls, if any, standing in well-built homes. Large steel and concrete missiles thrown far distances. |
| F5 | Incredible tornado | 319-512 | Homes leveled with all debris removed. Schools, motels, and other larger structures have considerable damage with exterior walls and roofs gone. Top stories demolished. |
| F6 | Inconceivable tornado | 513-606 | Very unlikely. The small area of damage they might produce would probably not be recognizable along with the mess produced by F4 and F5 wind that would surround the F6 winds. |

## References

Fujita, T. T., 1973: Tornadoes around the world. *Weatherwise*, **26**, 56-62.

_______, 1981: Tornadoes and downbursts in the context of generalized planetary scales. *J. Atmos. Sci.*, **38**, 1511-1534.

## APPENDIX C Storm Convergence Method

The evolution of vorticity on the convective scale is given by (e.g. Holton 1979):

$$\frac{d}{dt}(\zeta + f) = -(\zeta + f)\left(\frac{\partial u}{\partial x} + \frac{\partial v}{\partial y}\right) - \left(\frac{\partial w}{\partial x}\frac{\partial v}{\partial z} - \frac{\partial w}{\partial y}\frac{\partial u}{\partial z}\right) + \frac{1}{\rho^2}\left(\frac{\partial \rho}{\partial x}\frac{\partial p}{\partial y} - \frac{\partial \rho}{\partial y}\frac{\partial p}{\partial x}\right) \quad (1)$$

(convergence) (tilting) (baroclinic)

where ($u$, $v$, $w$) denote the wind components in ($x$, $y$, $z$) coordinates, $\zeta = \partial v/\partial x - \partial u/\partial y$ is the vertical component of relative vorticity, $f$ is the Coriolis factor, $p$ is the perturbation pressure, and $\rho$ is the air density. On the convective time scale appropriate for tornadogenesis, $f$ is small compared to $\zeta$ and can be neglected (Lemon and Doswell 1979). Equation (1) states that the rate of change of vorticity following the motion is given by the sum of the convergence term, the tilting term, and the baroclinic term. Lemon and Doswell (1979) estimated the magnitudes of the vortex tilting and the vortex stretching terms in supercells. They concluded that the tilting term is likely the dominant factor, but that the convergence term is a close rival, especially in the low levels. It is not obvious whether the baroclinic term in Eq. (1) makes a significant contribution towards vortex spin-up. Heymsfield (1978) argued that it can be typically neglected based on scale analysis. In contrast, Lemon and Doswell (1979) noted that within certain regions of supercells the baroclinic term can be significant and should not be disregarded. Specifically, supercells often develop a cold rear-flank downdraft in close spatial proximity to an intense warm updraft. The cold downdraft/warm updraft couplet causes strong local gradients in air density, and thereby a significant solenoidal effect.

The convergence term can be estimated from the continuity equation (e.g. Holton 1979):

$$\frac{1}{\rho}\frac{d\rho}{dt}+\frac{\partial u}{\partial x}+\frac{\partial v}{\partial y}+\frac{\partial w}{\partial z}=0 \tag{2}$$

A scale analysis of deep and shallow convection by Ogura and Phillips (1962) showed the continuity equation can be simplified. Using the so-called Exner function $\pi = (p/P)^{\kappa}$ as the non-dimensional pressure variable where $P$ is a reference pressure, and $\kappa$ is the ratio $R/c_p$ ($R$ [= 287 J kg$^{-1}$ K$^{-1}$] is the gas constant for dry air and $c_p$ [= 1004 J kg$^{-1}$ K$^{-1}$] is the specific heat at constant pressure) they approximated $\pi$ as:

$$\pi = 1-\frac{d}{H}z \tag{3}$$

where $H$ is a characteristic depth of the atmosphere (~ 30 km), $d$ is the depth of the convective layer, and $z$ is a non-dimensional height unit. The density is given as:

$$\rho = (P/R\Theta)\pi^{(1/\kappa)-1} \tag{4}$$

where $\Theta$ is a constant characteristic potential temperature of the atmosphere. For shallow convection ($d \sim 3$ km) $d \ll H$ and Eq. (3) reduces to $\pi = 1$. This in turn implies that $\rho$ in Eq. (4) is a constant since $P$, $R$, and $\Theta$ are all constants. Therefore the first term containing $\rho$ in Eq. (2) vanishes and the continuity equation for shallow convection becomes:

$$\frac{\partial u}{\partial x}+\frac{\partial v}{\partial y}=-\frac{\partial w}{\partial z} \tag{5}$$

Even though the above results by Ogura and Phillips (1962) show that, for shallow convection, the density term in the continuity equation is negligible it is nevertheless instructive to estimate the magnitude of the density term compared to the convergence term. In a typical thunderstorm the vertical velocity can be approximated as $w \approx 0$ at the Level of Free Convection (LFC) which is near the cloud base, and $w \approx 10$ m s$^{-1}$ at 100 mb above the LFC. Pressure and height are related by the hydrostatic approximation $dp = -\rho g dz$ which gives 100 mb ≈ 1 km in the lower levels. An estimate of the gradient of vertical velocity from the LFC to 1 km above the LFC is calculated as $\partial w/\partial z \approx 10^{-2}$ s$^{-1}$. The change in density can be estimated using the equation of state $p = \rho RT$ for $p_0$, $T_0$, $\rho_0$ at the LFC and $p_1$, $T_1$, $\rho_1$ at 100 mb (~ 1 km) above the LFC. Typical values for LFC pressure and temperature are $p_0 = 800$ mb and $T_0 = 285$ °K. The vertical change in temperature is estimated using the saturated adiabatic lapse rate of ~ -4 °K km$^{-1}$. The resulting change in density is $\Delta\rho = (\rho_1 - \rho_0) = -0.1$ kg m$^{-3}$. Choosing an average vertical velocity of ~ 5 m s$^{-1}$ over the 1 km vertical depth results in a time for the parcel to rise of $\Delta t = 200$ s. With $\rho \approx 1$ kg m$^{-3}$ results in $1/\rho(\Delta\rho/\Delta t) = -5 \times 10^{-4}$ s$^{-1}$. Thus the density term is about two orders of magnitude less than the convergence term which supports the results given by Ogura and Phillips.

The convergence term is the product of vorticity times convergence. Initially the vorticity is small, but as the tornado develops, $\zeta$ increases in magnitude. Consider the case where the vortex stretching effect is so dominant that the tilting and baroclinic effects can be neglected:

$$\frac{d\zeta}{dt} = \zeta \frac{\partial w}{\partial z} = \zeta\, C \tag{6}$$

where $C = \partial w/\partial z = -(\partial u/\partial x + \partial v/\partial y)$ is the convergence. As an interesting application of Eq. (6), we can examine a so-called "doubling time" for vorticity generation by vortex stretching. Assuming that the Storm Convergence, $C$, remains constant for the time interval $t_0$ to $t$, Eq. (6) can be integrated over the time interval $t_0$ to $t$:

$$\zeta(t) = \zeta_0\, e^{Ct} \tag{7}$$

where $\zeta_0 = \zeta(t_0)$. Therefore, the vertical vorticity increases at an exponential rate with a vorticity doubling time, $\tau$, given by

$$\tau = \frac{\ln 2}{|C|} \tag{8}$$

For $C = 0.01\ \mathrm{s}^{-1}$, the vorticity doubling time is 69 s or about 1 minute. It is obvious from Eq. (8) that vorticity doubling time is minimized when the convergence is a maximum. Dynamically, strong storm convergence is associated with a rapid increase of storm rotation as quantified by the vorticity doubling equation above.

Storm Convergence ($C$) can be estimated in a layer between $z$ and $z + \delta z$ as:

$$C = \frac{\partial w}{\partial z} \approx \frac{w(z+\delta z) - w(z)}{\delta z} \tag{9}$$

where $w(z)$ was assumed to be the adiabatic storm updraft as a function of height $z$. The adiabatic storm updraft can be approximated by (e.g. Rogers and Yau 1996):

$$w(z+\delta z)^2 = w(z)^2 + 2g\int_z^{z+\delta z} \frac{T - T'}{T'}\,dz \qquad (10)$$

where $T'$ and $T$ denote the ambient and parcel temperatures respectively. Eq. (10) can be written in terms of CAPE as:

$$w(z+\delta z)^2 = w(z)^2 + 2\times\text{CAPE} \qquad (11)$$

where the thermal buoyancy or CAPE between levels $z$ and $z + \delta z$ is defined as

$$\text{CAPE} \equiv g\int_z^{z+\delta z} \frac{T - T'}{T'}\,dz \qquad (12)$$

Combining Eqs. (9) and (11) gives the maximum storm convergence ($C_{layer}$) for the layer $z$ to $z + \delta z$ as:

$$C_{layer} \approx \frac{\sqrt{w(z)^2 + 2\times\text{CAPE}} - w(z)}{\delta z} \qquad (13)$$

The average Storm Convergence through a height from $z_0$ to $z_0 + N\,\delta z$ where $z_0$ is taken at the Level of Free Convection (LFC), N = number of intervals and it is noted that $w(z_0) \approx 0$ is:

$$\bar{C} = \frac{1}{N}\sum_{z=z_0}^{z_0+N\delta z} \frac{\sqrt{w(z)^2 + 2\times\text{CAPE}} - w(z)}{\delta z} \qquad (14)$$

Storm Convergence can be calculated for a height interval of $\delta z$ or, using the hydrostatic relation $\delta p = -\rho g\ \delta z$, for a pressure interval $\delta p$. The calculations of $w$ and CAPE are based upon simple parcel theory which neglects potential contributions from aerodynamic drag, mixing with ambient air, compensating forces of the surrounding air such as non-hydrostatic pressure perturbations, and the weight of condensed water (water drag) which is carried along with the rising parcel. Including these contributions would likely result in lower values for $w$ than suggested by simple parcel theory. Therefore Eq. (14) can be taken as an estimate of the *maximum* average Storm Convergence in a layer. According to Doswell and Markowski (2004) even though simple parcel theory neglects the above noted contributions, parcel theory–based parameters such as CAPE can still be valid predictors of convection and vertical velocity. However, they should *not* be understood as representing a complete description of the contribution due to buoyancy in convective storms. Considering thermal buoyancy alone typically overestimates the magnitude of the total buoyancy and the resulting vertical velocity. The use of cloud models which include some or all of the neglected parameters may provide better estimates of vertical velocity.

## References

Doswell, C. A. III, and P. M. Markowski. 2004: Is buoyancy a relative quantity? *Mon. Wea. Rev.*, **132**, 853–863.

Heymsfield, G. M., 1978: Kinematic and dynamic aspects of the Harrah tornadic storm analyzed from dual-Doppler radar data. *Mon. Wea. Rev.,* **106,** 233–254.

Holton, J. R., 1979: *An Introduction to Dynamic Meteorology.* 2nd ed. Academic. Press, New York, 300 pp.

Lemon, L. R., and C. A. Doswell III, 1979: Severe thunderstorm evolution and mesocyclone structure as related to tornadogenisis. *Mon. Wea. Rev.*, **107**, 1184-1197.

Ogura, Y., and N. A. Phillips: 1962: Scale analysis of deep and shallow convection in the atmosphere. *J. Atmos. Sci.,* **19,** 173–179.

Rogers, R. R., and M. K. Yau, 1996: A Short Course in Cloud Physics. 3rd ed. Butterworth-Heinemann, Massachusetts, 290 pp.

## APPENDIX D A Day in the Life of a Severe Weather Forecaster

In this section I would like to give a personal account of the procedures involved in operational forecasting of thunderstorms and tornadoes. I was a forecast meteorologist with Environment Canada for about 19 years, much of that time spent in the Alberta weather office. I spent many hectic days, as well as some relaxing days, attempting to predict the formation and movement of convective weather in Alberta. As is the case with all forecasters, I had successful forecasts and some which I would rather not remember (but make for good coffee room banter). To the person not familiar with the functions of a weather office, the processes involved with forming and disseminating a forecast are largely unknown. Many outsiders may not have an appreciation for the work load and stresses involved, even during a moderate convective situation, let alone a severe outbreak of thunderstorms. To illustrate forecast procedures I have used the Holden tornado event of 29 July 1993. The methods have remained much the same right to the present.

A typical day for a severe weather forecaster in the Alberta weather office begins at 1300 UTC (0700 MDT). To start the day off, most forecasters begin with the very necessary cup of coffee, since they often know a long day lay ahead. The first duty of the forecaster is to attend the morning briefing given by the previous night shift. The briefing consists of a discussion of synoptic and meso-scale patterns, both past and present, and how these patterns are expected to evolve during the day. Standard charts discussed include fields at the surface, 850 mb, 700 mb 500 mb and 250 mb. Any other charts the briefer deems relevant to the upcoming weather can also be summarized. A discussion of the various numerical weather prognosis charts is also included, noting how the models are handling important features and whether different models (e. g. Canadian GEM, U.S. ETA) are presenting differing solutions. The briefing also highlights any weather watches or warnings in effect or expected. The briefing normally takes about 15 minutes after which the forecasters for the day separate into their defined stations. The severe weather forecaster gathers up the necessary weather charts and data to construct a prediction of the expected threat area for this day's convective activity. The *Miller Diagram* (hand drawn by the severe weather forecaster) is still an essential aid to determine potential convective threat regions. This diagram is either drawn up by the severe weather forecaster or an assistant.

The Miller diagram (see Fig. 1 example) is a tool to assess the potential for convection by analyzing synoptic features associated with severe weather outbreaks. The diagram was developed in 1948 by Robert Miller and Ernest Fawbush who noticed similarities in the synoptic patterns associated with tornado outbreaks. A cartoon-style analysis is performed for the surface, 850 mb, 700 mb, 500 mb, and 250 mb levels. The results are plotted on a single chart. The area(s) over which most of the features convergence is deemed to have the greatest potential for convective development. The features commonly plotted on a Miller diagram are:

- **Surface** fields including low pressure centers, fronts, and dryline(s)
- **850 mb** fields including dryline(s), general flow, low-level jet(s), thermal ridge, moisture axis, moisture tongue, and confluent zones.

- **700 mb** fields including a dry tongue, general flow, wind maximum axis/axes, moisture, and confluent/diffluent zones.
- **500 mb** fields including trough/ridge axes, baroclinic zone, thermal trough/ridge axes, jet flow, diffluent zone(s), horizontal speed shear zones.
- **Jet-level** (generally 250 mb) fields including jet flow, jet maximum, speed shear zones, diffluent zones
- **Stability** fields such as the lifted index and Showalter index.

These fields provide the forecaster with a "checklist" of parameters to examine which are related to convective development. However, it is important to point out there is no provision within the diagram for assessing the severity of the convection which may develop. For this the forecaster must use other tools, such as strength of the wind shear, helicity values, amount of moisture available, etc. The fields analyzed on the Miller diagram are usually obtained from numerical model predictions valid for the time in question (e.g. 0000 UTC) using the most recent model output. In most cases, not all of these parameters are evident at the same time. An example of a Miller diagram (Fig. 1) is shown for the severe Holden tornado event which occurred in central Alberta on the evening of 29 July 1993. The shaded area outlines a high threat for thunderstorm development. Once this area is determined, the forecaster then estimates the severity potential of a storm which may develop in this region. The severity includes hail size, maximum wind gust, and possible tornado development. To do this, the forecaster will examine the values of various parameters associated with thunderstorm development, including wind shear, helicity, available moisture, buoyancy, etc. Once the potential area for development and the severity of any expected storms has been assessed the forecaster must decide whether a severe thunderstorm watch/warning is necessary. The Meteorological Service of Canada criteria for issuing watches and warnings are:

**Severe thunderstorm watch**

Conditions are favorable for the development of severe thunderstorms with large hail, heavy rain, intense lightning or damaging winds.

**Severe thunderstorm warning**

A severe thunderstorm has developed, producing one or more of the following conditions: heavy rain (≥ 30 mm in one hour), damaging winds (≥ 90 km $h^{-1}$), large hail (≥ 2 cm in diameter) or intense lightning.

**Tornado watch**

Conditions are favorable for the development of tornadoes.

**Tornado warning**

One or more tornadoes are occurring in the area specified.

Once the potential area and intensity of convective activity has been assessed, the forecaster waits until convective development begins. In most cases convection in Alberta does not develop until the afternoon. During this time the forecaster reanalyzes many of the fields to confirm the predictions and ensure (as well as possible) that something was not overlooked. New data may arrive (e.g. regular surface observations of temperature, dewpoint, and wind) which may or may not confirm that the synoptic pattern is evolving as the numerical models have predicted. In cases where the observational data differ from model predictions, adjustments may have to be made to the spatial, temporal, and intensity of predicted areas of convection. Since severe thunderstorms generally occur in the afternoon and evening the forecaster may find that noon is a good time to take a lunch break because, in many cases, once thunderstorms begin developing there is little time for breaks. During the afternoon, convection generally begins along the foothills in Alberta and progresses eastward as outlined by the Smith and Yau (1993a,b) conceptual model of severe thunderstorm outbreaks in Alberta. Radar is the main nowcasting tool for the forecaster. The radar site in Alberta is located at Carvel (about 40 km west of Edmonton). The Carvel Doppler radar is a Constant Altitude Plan Position Indicator (CAPPI). Small isolated reflectivity echoes begin to show up on the CAPPI radar. As the afternoon progresses some of these echoes may intensify while others dissipate. The job of the forecaster is to predict which of the cells may form into severe thunderstorms. For example, cells which form west of the threat area on the Miller diagram (Fig.1) and move east toward the threat region should have the greatest chance form developing into severe storms whereas cells well away from the threat area are more likely to dissipate. The forecaster must decide which cells have the potential to become severe and which direction these cells will move. Radar is an invaluable aid for short-range forecasting (about one-half to one hour). Figure 2 shows an example of a CAPPI radar image at 2030 UTC (1430 MDT) 29 July 1993 (several hours prior to the Holden tornado). Several cells are evident in the western (left) half of the radar. The forecaster must decide (often within tens of minutes) the potential for continued development of each of these cells to determine whether (and where) severe thunderstorm watches or warnings need to be issued. If the potential for tornadic development is subjectively deemed high, a tornado watch may be issued. For the Holden storm, the circled cell in Fig. 2 will eventually develop into the thunderstorm complex which spawns a tornado. This storm, along with other cells, developed to severe category in the early afternoon. Several severe thunderstorms continued into the evening. At 0230 UTC (1830 MDT) there was a significant line of severe thunderstorms west of Holden (storm complex on Fig. 3) and also numerous other storms in the northern section of the radar. The forecaster has to track and assess the development potential for each of these cells. Several thunderstorm watches and warnings for different regions may be in effect at the same time, all requiring updates as the storms evolve. In some cases the work load may be too much for one person and the forecaster will call for additional help (usually on overtime). In addition to issuing watches and warnings the forecaster handles frequent inquires from various media (radio, television) needing updates on storm locations, movements, and intensities for dissemination to the public. In the case of the Holden tornado, the thunderstorms persisted through the evening with the tornado eventually forming near 2200 MDT. Even after the tornado had dissipated, an area of severe storms kept moving east well into the night. The day does not end for the forecaster until all severe thunderstorms have either dissipated or moved east of Alberta and all watches and warnings are ended.

## References

Smith, S. B., and M. K. Yau, 1993a: The causes of severe convective outbreaks in Alberta. Part I: A comparison of a severe outbreak with two nonsevere events. *Mon. Wea. Rev.*, **121**, 1099-1125.

_______, and _______, 1993b: The causes of severe convective outbreaks in Alberta. Part II: Conceptual and statistical analysis. *Mon. Wea. Rev.*, **121**, 1126-1133.

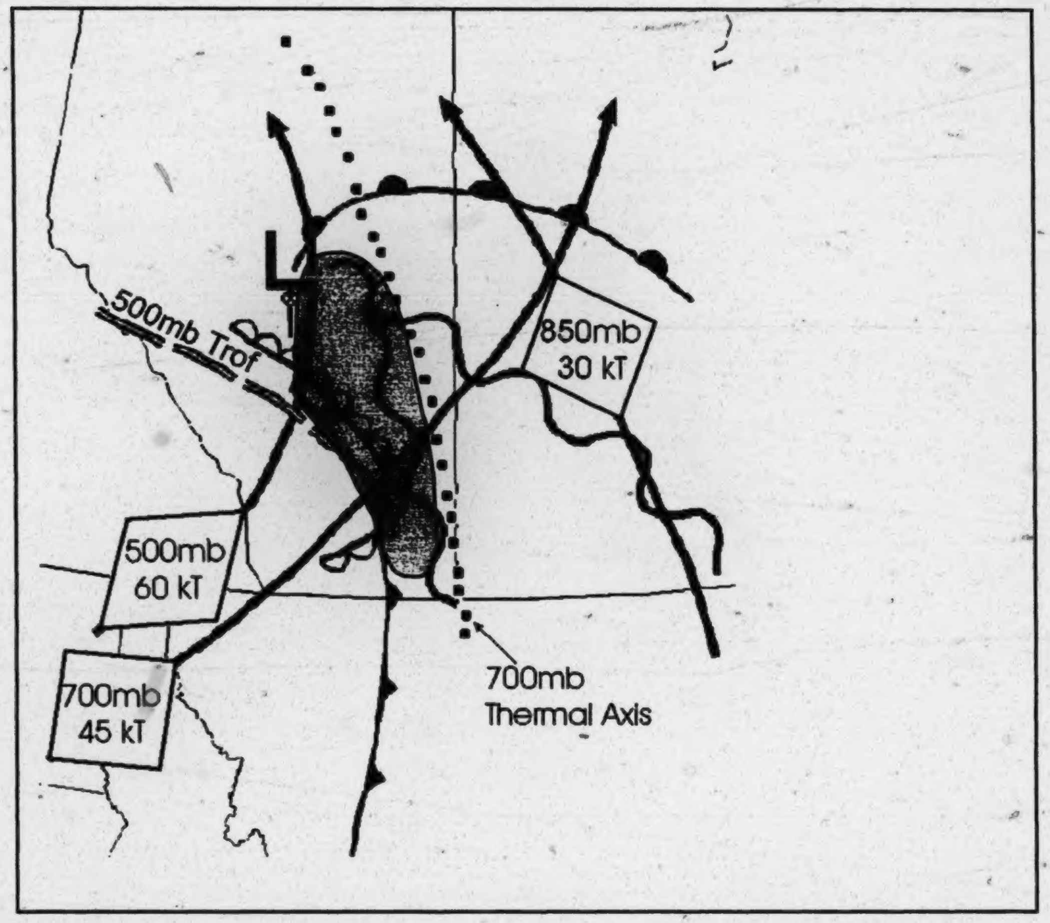
500mb Trof
850mb
30 kT
500mb
60 kT
700mb
45 kT
700mb
Thermal Axis

Fig. 1. Miller diagram at 0000 UTC 30 July 1993 showing the jet cores at 500mb, 700mb,and 850mb (arrows), the 500mb trough (double dashed line), the 700mb thermal axis (dotted line), the surface dryline (open semi-circle front), and 500 mb ridge axes (wavy lines). The shaded area denotes a greater potential for severe convective development.

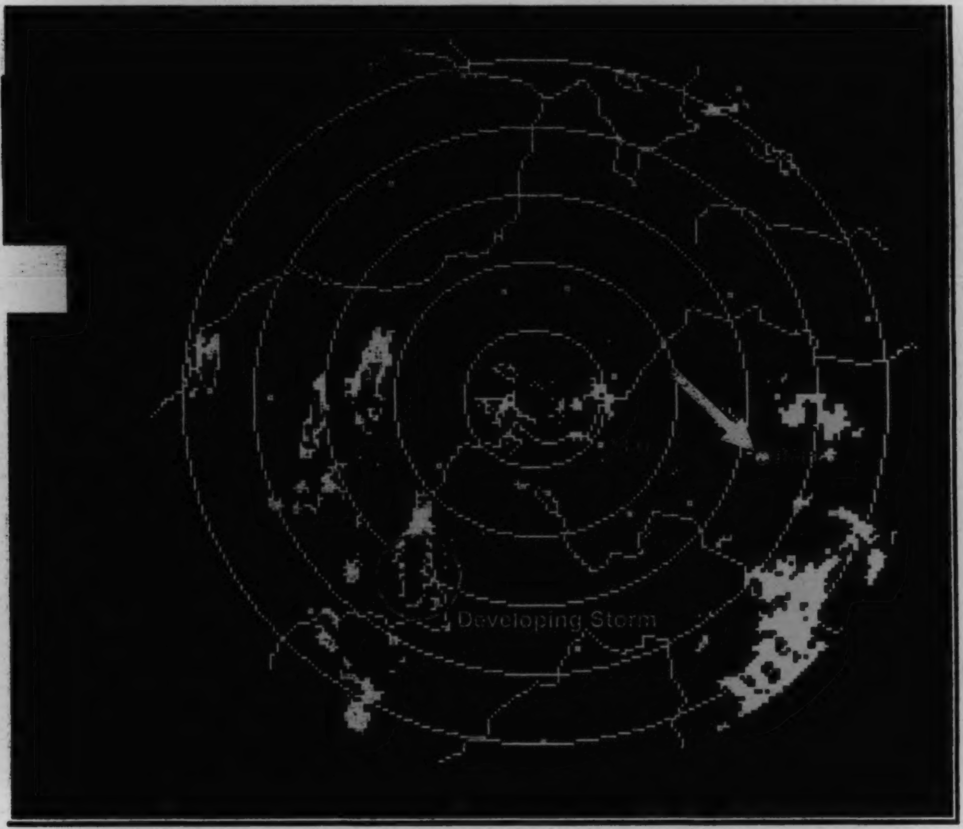

Fig. 2. 1.5 km CAPPI image from the Stony Plain (WSE) radar at 2030 UTC 29 July 1993 (the afternoon of the Holden tornado event) The range rings are spaced every 40 km. The colors represent either rainfall rates (mm/hr) or reflectivity (dBZ). The arrow points to the Holden site. The storm which may develop into the tornadic storm is circled.

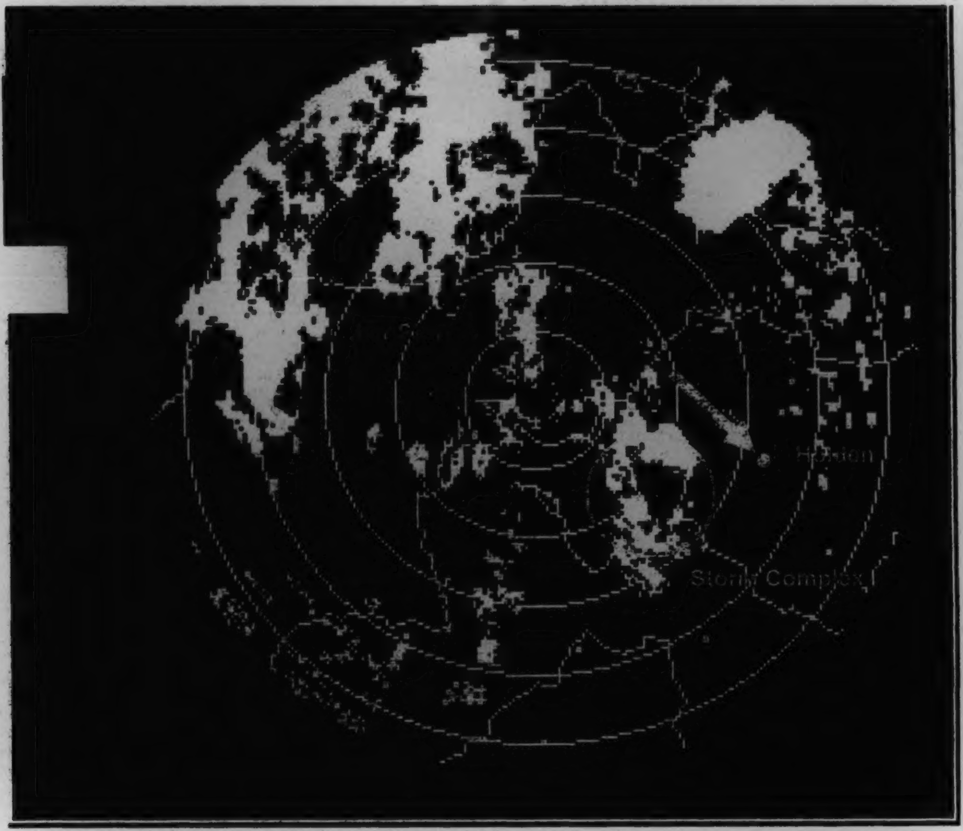
Holden
Stony Complex

Fig. 3. 1.5 km CAPPI image from the Stony Plain (WSE) radar at 0230 UTC 30 July 1993 (about 2 hours before the Holden tornado event)